Estimate vessel emissions in ports using AIS data

A study to identify emission distribution patterns in ports and evaluate emission reduction strategies

R. van den Berg

TU Delft

Estimate vessel emissions in ports using AIS data

A study to identify emission distribution patterns in ports and evaluate emission reduction strategies

by

R. van den Berg

to obtain the degree of Master of Science

at the Delft University of Technology,

to be defended publicly on Tuesday August 30, 2022 at 08:30 AM.

Student number:	4394100	
Project duration:	September 15, 2021 – August 30, 2022	
Thesis committee:	Prof. dr. ir. M. van Koningsveld,	TU Delft
	Dr. ir. J. F. J. Pruijn,	TU Delft
	Ir. S. E. van der Werff,	TU Delft
	Ir. P. A. L. de Vries,	Royal HaskoningDHV
	Ir. T. M. de Boer,	TU Delft & Royal HaskoningDHV
	Dr. ir. J. Á. A. Antolínez,	TU Delft

An electronic version of this thesis is available at `http://repository.tudelft.nl/`.

TU Delft

Preface

This thesis marks the end of my study at the Delft University of Technology. It is the final step towards obtaining the Mater of Science degree in Civil Engineering, with the master track Hydraulic Engineering. This thesis has been carried out in collaboration with Royal HaskoningDHV, which gave me the opportunity to work with even more people specialised in the hydraulic engineering field. Ports and sustainability were always of special interest to me and combining them in a research around green ports could not have been a better way to finalize my studies. I was eager to start of with this subject and I am happy that I could contribute to a more sustainable shipping industry.

I would like to acknowledge all the members of my graduation committee for their supervision and guidance throughout the process. I am grateful that everybody always wanted to help me and I could not have completed this thesis without them. First, I would like to thank Solange van der Werff for her great involvement throughout my thesis and for always making time for me to think along with the difficulties which I needed to overcome. I would always leave our weekly meetings with new energy and motivation. I would like to thank Peter de Vries for always keeping me focused on the goal of the research, the practical tips on how to approach certain things, for making me feel welcome at Royal HaskoningDHV and the random Team-calls for checking in. I would like to thank Mark van Koningsveld for his great enthusiasm around the subject and the much appreciated feedback. I would like to thank Jeroen Pruijn for his critical eye, his help during the practical problems and for keeping me sharp during the process. I would like to thank Thijs de Boer for always being interested, enthusiastic and involved with the project and spontaneously joining the meetings at the TU Delft and even spontaneously joining the thesis committee. Last, I would like to thank José Antolínez for sharing his fresh perspective on the research.

Finally I would like to thank my family and friends for giving me their unconditional support throughout my studies and my graduation process. I am very grateful for the joyful moments and endless coffee breaks, but also for the brainstorming and the help during serious times.

R. van den Berg
Delft, August 2022

Abstract

The shipping industry is responsible for almost 3% of the world's greenhouse gas emissions and is looking for possibilities to reduce their share. The demand for lowering the emissions of the maritime industry creates the need for insight in the emissions. Currently a generic method to specify emissions in space and time, as a function of vessel and waterway properties is not available.

Although most of the emissions of vessels take place at sea, the most noticeable part takes place in ports since they are located close to urbanized areas. Therefore, this research focuses specifically on emissions in ports. The study investigates the impact of sea-going vessels. By gaining insight in the emissions of sea-going vessels, the big polluters can be tackled. Due to the scope of the research, not all vessel types and emission types are taken into account. Ten vessel types are selected and only CO_2, NOx, SOx and PM_{10} emissions are estimated. These are the most relevant polluters in the shipping industry since they cause health and environmental related issues, both locally as more widely.

To provide insight in the emissions, the objective of this study is to develop a generalized method to calculate and map the emission of a single vessel in space and time in ports based on reliable data. To reduce these emissions, emission reduction strategies have to be drawn up, targeting the largest emission sources and the most crucial locations. Therefore, the developed method must not only quantify the emission sources, but must also provide insight in emission patterns in ports and indicate emission hotspots.

A bottom-up method is developed to estimate the emission of a single vessel in space and time. To derive the emission rate of a vessel, the fuel and energy consumption of the vessel is multiplied by a vessel-specific emission factor. The CO_2 and SOx emissions follow a fuel-based approach, in which the emissions produced are directly proportional to the fuel consumption and therefore depend on the engine load. The energy-based approach is used for estimating NOx and PM_{10} emissions, which can not be directly related to the fuel consumption but depend on engine characteristics. The fuel consumption is determined by multiplying the energy consumption of the engine with a fuel consumption factor specific to each vessel, meaning the fuel consumption is related to the energy consumption.

The amount of energy the main engines of a vessel consume, is the energy needed to overcome the resistance a ship experiences from sailing through the water and is therefore related to the vessel's speed. This speed is derived from AIS data. AIS data represents real-life vessel tracking data and is gathered automatically, which makes it a reliable and realistic data source. It also provides the ability to make the emission estimations time dependent. Due to the global coverage, AIS data is a good data source to develop a generic method applicable to ports all around the world.

However, in ports the vessel's speed alone is not a good indicator of the energy consumption, since this neglects the amount of energy the auxiliary engines consume. Their energy consumption is dependent on how much energy the electrical systems of a vessel require at that moment, which can be high when a vessel is for example at berth or manoeuvring. The energy consumption is therefore related to the operations a vessel performs. This leads to an approach which takes into account the vessel's resistance and operational modes.

Four operational modes are important to distinguish in ports: 'sailing', 'manoeuvring', 'anchoring' and 'berthing'. According to the operational mode, the main engine power is either estimated with the resistance calculation from Holtrop and Mennen (1982) when the vessel is sailing or manoeuvring, or assumed zero when laying still at anchor or berth. According to the operational mode, the auxiliary engine power can be derived from values of the International Maritime Organization (2021) research. Depending on the emission type and vessel characteristics, the emission factor is determined.

The algorithm to determine the emission of a single vessel in space and time is implemented in a model. The model's input consists of Automatic Identification System (AIS) data providing the speed and position of the vessel, a vessel database containing vessel characteristics based on information from the Sea-web Ships database, and a Fairway Information System (FIS) graph of the port network. This graph contains the fairway

characteristics needed to calculate the resistance. The calculated emissions will also be displayed on the FIS graph for a detailed insight in the emission distribution in space.

The model provides an insight in the emissions patterns in a port. The fairway sections which are subjected to high emissions can be identified immediately and so the emission hotspots are determined. The source of the emissions can be identified by down-drilling of the emissions. The model can drill down to vessel types, operational modes and all the way down to a single vessel in space and time.

The model is illustrated by means of two case studies concerning the Port of Rotterdam and the Port of Constanța. These case studies indicate that the port basins hosting the largest vessels have the highest estimated emissions. These basins are indicated as an emission hotspot by the model when the emissions are projected on the FIS graph. In ports generally, high emissions are observed at places with a high traffic intensity, such as the port entrance. Junctions of fairway sections or port basin entrances also show locally higher emissions. The rise in emissions, is probably due to the fact that vessels are slowing down when approaching a junction. This increases the emission rate of a vessel due to more inefficient engine use, but also since they spend a larger amount of time at this fairway section.

By indicating the location and source of the emission hotspots, targeted emission reduction measures can be taken. Three of these measures are demonstrated on one of the case studies. The first strategy concerns installing shore power. The model is able to simulate vessels connected to shore power, by setting their emission rate at berth to zero. This simulation is compared to the original situation without using shore power. Out of the evaluated reduction measures, this seems the best strategy to reduce emissions since it shows the largest reduction of the total emissions. Besides that, it is an effective measure especially for ports, since the largest emissions reduction takes place at berth. The second evaluated strategy shows also good results and is about switching from a normal tugboat fleet to a zero-emission tugboat fleet. The model simulates this switch by eliminating all the tugboats from the fleet since their emissions will be zero. This new case is compared to the original situation with normal tugboats. The third option to reduce emissions is applying Emission Control Area (ECA) limits which do not seem to have a lot of effect on reducing emissions except for the SO_x emissions. This is derived from comparing the original situation without ECA limits, to a new case study where a situation with ECA limits is simulated. This means that the fuel types of the vessels are changed from the most economical fuel type to the lightest fuel type on board and that the sulphur content in the fuel is altered.

However, the model has some limitations. The method does not take into account the effect of currents or variations in time of the water depth. The accuracy of the resistance calculation can be improved by adding these. Furthermore, the emission pattern of tugboats needs further examination as it could not be demonstrated that the split of emissions into operational modes is correctly. The research has also shown that the method to estimate the energy consumption is not suitable for tankers at berth, since their energy consumption pattern is different. The quantity of emissions in the case study of the Port of Rotterdam is far from the expected amount of emissions. The quantification of emissions is assumed to be unreliable and further research should focus on validating these results.

Concluding, the developed model makes use of AIS data, local waterway properties, empirical emission factors and operational modes. This data is used in a physics-based method to estimate the resistance and the energy consumption. If this information is available, all this combined makes the approach in principle applicable to any port. The developed model provides an insight in the emission distribution patterns and provides the ability for down-drilling to find the source of the emission hotspots. A targeted emission reduction strategy can be proposed as a result of this and the model has the ability to evaluate specific emission reduction strategies. The strategies can be simulated with the developed model and the effect of these measures can be quantified by comparing the emission reduction strategy to a situation without these measures.

Contents

1 Introduction 1
1.1 Background on shipping in ports . . . 1
1.2 Research gap . . . 3
1.3 Research objective and scope . . . 5
1.4 Research questions . . . 5

I Literature, methods and models 7

2 Literature 9
2.1 Research method . . . 9
2.2 Energy consumption . . . 9
2.3 Emission factors . . . 12
2.4 Considered fleet. . . . 15

3 Method 17
3.1 Estimate emissions . . . 18
3.2 Estimate energy consumption . . . 18
3.3 Total emission factor . . . 22

4 Model 25
4.1 Model input. . . . 25
4.2 Model . . . 27
4.3 Model output . . . 31
4.4 Implementation of emission reduction strategies . . . 31

II Results 33

5 Case study Port of Rotterdam 35
5.1 The case . . . 35
5.2 Model input for case study - Port of Rotterdam . . . 35
5.3 The case study model - Port of Rotterdam. . . . 36
5.4 Model output - Port of Rotterdam . . . 37

6 Case study Port of Constanța 43
6.1 The case . . . 43
6.2 Model input for case study - Port of Constanța . . . 43
6.3 The case study model - Port of Constanța . . . 44
6.4 Model output - Port of Constanța . . . 45

7 Emission reduction strategies 51
7.1 Shore power. . . . 51
7.2 Zero-emission tugboats . . . 52
7.3 Applying ECA limits . . . 55

III Discussion, conclusions and recommendations 57

8 Discussion 59
8.1 method . . . 59
8.2 Model . . . 61
8.3 Results . . . 62

9 Conclusions 63

10 Recommendations 67
10.1 Recommendations for emission reduction strategies . . . 67
10.2 Recommendations for future research . . . 67

Appendices 69

A Energy consumption of the main engine 71
A.1 Resistance calculation . . . 71
A.2 Efficiency components . . . 81

B Energy consumption of the auxiliary engine 83

C Base emission factors 85
C.1 Base emission factor CO_2 . . . 85
C.2 Base emission factor SO_x . . . 86
C.3 Base emission factor NO_x . . . 87
C.4 Base emission factor PM_{10} . . . 89

D Missing entries vessel database 91
D.1 Deadweight tonnage . . . 91
D.2 Number of screws . . . 92
D.3 Build year . . . 92
D.4 Installed engine power . . . 93
D.5 Fuel type . . . 94
D.6 Engine type . . . 94
D.7 Tables with characteristic values . . . 94

E Results from case study Port of Rotterdam 107
E.1 Model input . . . 107
E.2 Emission split in vessel types . . . 111
E.3 Emission distribution - January 2022 . . . 111

F Results from case study Port of Constanța 115
F.1 Python code for constructing the FIS graph from a shape-file . . . 116
F.2 Twelve randomly selected vessel trajectories . . . 116
F.3 Emission split in vessel types . . . 117
F.4 Emission distributions - June 2021 . . . 118

List of Figures 125

List of Tables 127

Bibliography 129

1 Introduction

Nowadays, we are all working towards a more sustainable world. Climate change is a worldwide problem of which global warming is one of the most well-known aspects. For many, the greenhouse effect is a familiar topic: greenhouse gasses trapped close to the earth's surface like a blanket to keep the earth temperature stable. Humankind has been interfering with the natural process by using fossil fuels which (mainly) produce carbon dioxide (CO_2), the greenhouse gas which is the largest driver of global warming. The carbon dioxide level is rising throughout the years and this rise must be brought to a standstill to reduce the rate at which global warming is taking place. For this reason, in 2015 the Paris agreement is set up by the United Nations Framework Convention on Climate Change (UNFCCC). This is a global and legally binding agreement to limit global warming to a maximum of two degrees Celsius in the upcoming century.

In 2018, the largest producer of CO_2 emissions was the energy sector (76%), and within that energy sector 'Transportation' was the second largest contributor of emissions after 'Heat and Electricity' (Ge et al., 2020). Even though emissions from road transport take up the largest share, the shipping sector still has a considerable share in the world's greenhouse gas emissions of almost 3%. But, where other sectors took action earlier on, the share of emissions of the maritime sector is still growing (International Maritime Organization, 2021). This means the shipping industry has a significant impact on the environment and therefore it is important to gain insight in the emissions this industry produces.

1.1. Background on shipping in ports

1.1.1. Emissions from the shipping sector

As for all other transport sectors, measures and goals are set up specifically for the maritime sector. During the latest gathering of the United Nations in 2021 in Glasgow, the COP26 (26th Conference of the Parties), some takeaways of the strategy were stated:

1. **Zero emissions by 2050**
   The previous standards stated a 50% reduction compared to 2008 values for 2050. During the COP26 a tighter standard was determined, aiming towards zero greenhouse gas emissions by 2050.
2. **The future of fuels**
   The takeaway from this topic is to accelerate the phase-down of coal power and inefficient fossil fuel subsides. Over 100 countries also announced to cut the emissions of methane by 2030, which will impact the LNG sector. Alternative energy sources must be used such as hydrogen, batteries, wind and methanol. Over 20 countries pledged to create emission-free corridors to accelerate the development of alternative energy sources.
3. **Supporting seafarers**
   To guide seafarers throughout the energy transition the 'Just Transition Maritime Task Force' was set up. The taskforce represents shipowners, seafarers, port workers and other important organisations like the International Labour Organization (ILO) and the International Maritime Organisation (IMO).
4. **Financing the transition**
   Startups about innovative technology must possess the financial resources to grow. The Poseidon Prin-

ciples, developed by a number of banks, provide a framework for financing alternative solutions for a green industry.

The IMO is the United Nations' specialized agency responsible for the safety and security of shipping and the reduction of emissions from ships. Therefore they are one of the leading parties in guiding the process to live up to the emission reduction targets. To provide guidelines, the IMO has developed a global 'Greenhouse Gas strategy'. Although the IMO leads the global strategy to reduce emissions, the European Union has also set up guidelines to speed up the process. This includes monitoring, reporting and verification of CO_2 emissions from large ships using EU ports and again greenhouse gas reduction targets.

Measures to achieve the goal of a climate neutral industry by 2050, are mostly focused on reducing CO_2 emissions. However other environmental polluters are also of importance and the pressure to reduce these is also growing. When looking into shipping emissions the most frequently occurring pollutants are: $PM_{2.5}$, PM_{10}, CO_2, NO_x, SO_x, CO, metals and black carbon (Merk, 2014; Olmer et al., 2017; International Maritime Organization, 2021). Due to the scope of this research, not all emissions are taken into account but (besides CO_2) the focus will be on nitrogen oxides (NO_x), sulfur dioxides (SO_x) and particulate matter (PM_{10}) since these are the most relevant polluters in the shipping industry. Of the total global SO_x and NO_x emissions, 5-10% and 17-31% respectively come from shipping, for PM_{10} this is around 2.3%. All three can have harmful effects on the environment and on human health, and ports are the places where the impact of these emissions is most noticeable (Merk, 2014). For this reason, stricter regulations in ports around these emissions are being drawn up. The two most concrete ways in which these polluters are regulated are the "IMO 2020" rule and the so-called engine certificate. The new "IMO 2020" rule limits the sulphur in the fuel oil used on board ships to 0.50% m/m (previous limit of 3.5%), and within defined Emission Control Areas (ECAs) the limits are even stricter (0.10%). This rule is used to limit the SO_x and the particulate matter emissions (International Maritime Organization, 2019b). The nitrogen oxides level is regulated through an Engine International Air Pollution Prevention Certificate, which has different levels (Tiers) of control based on the ship construction date. Within those Tiers a limit value is determined from the engine's rated speed. All marine diesel engines installed on ships must have this Tier I, II or III certificate. The regulations mentioned here are applied globally, but many more measures have been taken on a smaller scale (International Maritime Organization, 2019a).

To achieve all the previously named goals, it is important to gain insight in emissions of ships. To support a strategy to reduce the emissions it is key to know who are the largest polluters, what are their emissions patterns and types and where do the emissions occur exactly. Therefore, this research focuses on the emissions of a single vessel in time and space. By doing this the emission-'bottlenecks' can be identified and the impact of certain reduction measures can be identified in a more detailed manner. We expect to provide new insights for working together towards a more sustainable marine industry.

1.1.2. Ports

Although most of the emissions of vessels take place at sea, the most noticeable part takes place in ports. Ports are places where many vessels come together, which creates a sort of 'emissions hotspot'. This hotspot is located close to urbanized areas, since most ports are connected to cities. This makes ports interesting fields of study and also the focus of this research.

Research shows that shipping emissions in ports are approximately ten times larger than the emissions coming from port activities on land (Winnes et al., 2015). Several studies have tried to identify the air pollution-related health effects coming from shipping in ports. Most studies show worrying results stating air pollution from international shipping causes 50,000 to 60,000 premature deaths per year, with most deaths occurring near coastlines in Europe, East Asia, and South Asia (Corbett et al., 2007). Emissions in ports therefore have a large impact on the environment and on the health of the population. The emission types responsible and the way in which they are responsible for these health problems will be explained in Section 2.3.1.

Another important aspect of emissions in ports is that vessels in ports perform various operations besides the actual sailing, for example manoeuvring. These operations have an influence on whether the main engine is running in its most efficient design operating range. If the engine is operating outside this range, the engine system is not performing in optimal conditions, thus causing higher emission rates. In this research four main operations are distinguished in ports: sailing, manoeuvring, berthing and anchoring, which will be explained in Section 2.2.2. In this research, these operations will be referred to as 'operational modes'. The operational modes have a large influence on the power consumption and emission distribution of the vessel.

Nowadays, ports base their emission reduction strategies on generalized emissions patterns. Currently, four main indices are widely used to reduce air pollution in port areas: the Environmental Ship Index (ESI), the Green Award, Clean Shipping Index (CSI) and the GHG Emissions Rating of RightShip. For example, the Port of Rotterdam bases the port tariff for vessels on their ESI score and Green Award certificate. Besides ship safety, these indexes look at their ship efficiency and CO_2, NO_x, SO_x and PM_{10} emissions. These emissions are based on the engine characteristics of the vessel (International Transport Forum, 2018). This leads to a general emission profile, which is a good estimation for when a vessel is for example sailing at sea. However, the emission profile is different when a vessel is sailing inside a port area (think of the operational modes). It would be of added value to be able to develop new port-specific indices based on emission patterns specifically inside ports. This is however not yet possible since methods to obtain a detailed breakdown of emission patterns in ports is lacking. Insight in these distribution patterns is of great value in order to reduce emissions.

1.1.3. Sea-going vessels

This research will focus on estimating the impact of sea-going vessels in ports. In absolute sense, sea-going vessels typically emit more per vessel than for example inland vessels or service vessels, since they are larger and therefore have more powerful engines installed. Therefore, by gaining insight in the emissions of sea-going vessels, the big polluters can be tackled.

When looking into the emissions on Dutch territorial waters, approximately 70% of the emissions from shipping comes from sea-going shipping and only 30% from inland shipping, see Figure 1.1. For other ports around the world, the sea-going share of emissions is presumably even higher. The estimated spread between sea-going shipping and inland shipping in the Netherlands is somewhat conservative when compared to other countries since the Netherlands hold a very large market share of inland waterway transport (the Netherlands makes up approximately 35% of the global inland waterway transport market (Kriedel et al., 2021)).

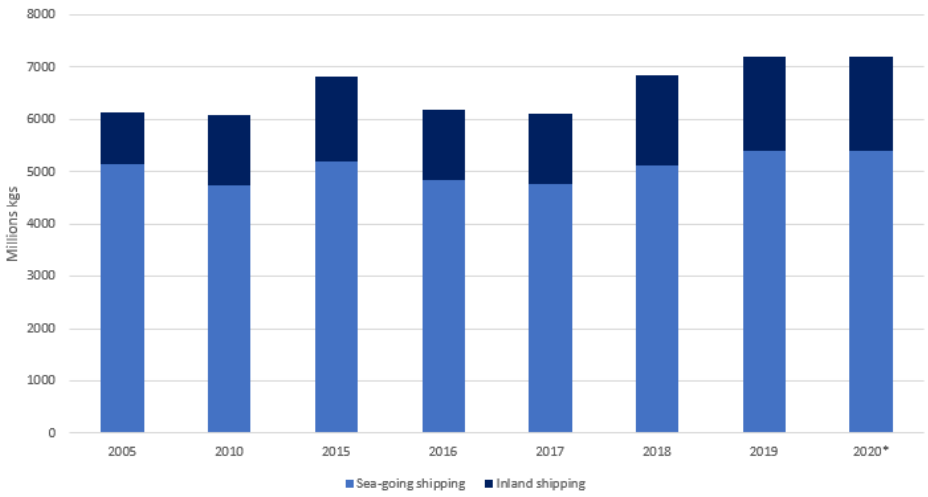

Figure 1.1: CO_2 emissions from shipping in the Netherlands, based on data from CBS (2021)

1.2. Research gap

The demand for lowering the emissions of the maritime industry creates the need for insight in the emissions of vessels in ports. To lower the emissions, it is important to identify the components which have the largest impact. So not only the total emissions in a port are of importance, but also a detailed insight in the distribution of the emissions is needed. Therefore, this research focuses on developing a method to estimate the emissions of a single vessel in space and time. This will provide the ability to down-drill the total emissions completely to identify the emission hotspots and the emission sources which have the largest impact. When these are identified, emission reduction strategies can be drawn up. It would be of added value if these emission reduction strategies can be evaluated with the developed model as well.

Several studies have been performed around this subject. When looking into previous research, typically two types of methods are used to estimate emissions from vessels: a bottom-up approach and a top-down ap-

proach. A top-down approach means that the total emissions are calculated without considering the vessels' characteristics, and subsequently the emissions are assigned to a specific ship or group of ships. Most of the time this means that fleet or vessel types-based assumptions are made in their methods. Researches based on a top-down method are for example Corbett and Fischbeck (1997); Corbett et al. (1999); Skjølsvik et al. (2000); Endresen et al. (2007). These methods base their calculation on maritime fuel sales, which makes it hard to break the emissions down into specific locations and the outcome is not as accurate as bottom-up methods. Top-down studies provide a good first quantification of the total emissions on national or global level.

A bottom-up approach works the other way around: the emission of a ship at a specific location is estimated and the emissions of all vessels summed up gives the total emissions. This type of approach requires a lot of data about vessel characteristics and geographical information of the study area, which has become more widely available in recent years. This enables more detailed approaches with the possibility to evaluate emissions on a smaller scale, for example in a port (Miola and Ciuffo, 2011). Another advantage of this type of approach is that local real-time data can be used, which makes it possible to evaluate emissions in space and time. A bottom-up approach therefore aligns better with the goal of this research.

The leading and one of the most detailed bottom-up method to estimate emissions from shipping is the one from International Maritime Organization (2021) and the results derived with this method are considered to be a 'consensus estimate' (Miola and Ciuffo, 2011; Moreno-Gutiérrez et al., 2015). However, this research is not specifically focused on ports. It provides a more generalized method, estimating emissions of the whole route of a vessel (also at sea and in inland waterways). This makes the approach not directly applicable for ports, since different operations are performed in ports which are not of large influence on the total route of the vessel but are of great influence on the emissions in a port. Besides that, the research of the IMO does not take in the fairway network, leading to room for improvement as well. It makes it harder to evaluate the distribution of the emissions over space and to indicate the exact hotspots. Additionally, the emissions can be estimated more accurately when taking in external influences on the vessel from the fairway.

Segers (2020) has developed a model to estimate shipping emissions of a single vessel as well, however, it is built around inland navigation considering different fleet characteristics than the ocean-going vessels in ports. Another important note when comparing the inland navigation model to models applicable for ports, is that the operations performed in ports are more complex. Vessels can no longer be categorized as sailing or laying still (as done in this research), but in ports manoeuvre actions also play an important role.

Another problem with applying generalized methods to ports, is that some methods (for example the one from Olmer et al. (2017) from the International Council on Clean Transportation (ICCT)) use data which only covers vessel types larger than a specific tonnage. Most of the time this means they exclude tugboats. This might not be of great influence when investigating sea areas, but in port areas they are likely to contribute considerably to the emission profile. The share of CO_2 emission of tugboats in ports varies from 7% to 22 % of the total CO_2 emission in the port (Khan et al., 2008; Leong et al., 2015). Excluding tugboats can therefore be a great unreliability when researching emissions in ports.

Some research does focus on ports specifically. Here, the problem is that many methods are mostly country-specific or focus on one specific port. For example, the research of MARIN covers only Dutch ports (Kauffman and Hulskotte, 2021), and the reports like the 'Port of London Emissions Inventory' (Williamson et al., 2016), 'Port of Los Angeles inventory of air emissions' (Starcrest consulting group LLC, 2020a) and many others, cover just one specific port. In their research method assumptions are made, based on specific conditions applying at that exact location and/or data sets are used only available at this location. For example the research of Starcrest consulting group LLC (2020a) uses auxiliary engine data from the tankers and cruise vessels which visited the port of Los Angeles in 2020. This makes their applied methods not generic for ports around the world. This is inconvenient if ports around the world need to be compared to each other and makes evaluating ports by for example international companies and institutions very labour intensive.

None of the previously named research has the ability to evaluate emission reduction measures, although they are very important for the ultimate goal of reducing emissions. If the developed method can identify emission hotspots and can identify the components which have the largest impact, more targeted emission reduction measures can be drawn up. It would be an addition to previous research, it the developed method can provide insight in the effect of these measures on the emission distribution in ports in space and time.

In summary, it is of increasing value to develop a generalized method to estimate and map the emissions of a single vessel in space and time in ports. Parts of the research are in existing methods, but they are not

integrated into one general method to estimate emissions in ports all over the world.

1.3. Research objective and scope

This study will focus on developing a bottom-up method to estimate the emission of a single vessel in time and space. In this way the total emission of ships in a specific port can be estimated, and these emissions can also be drilled down into components, making it possible to investigate the impact of a specific vessel or vessel type, and the influence of time and space.

The developed model will assign an emission distribution to an individual vessel and the model must be able to differentiate between ship types and individual vessels, as well as between port-specific operational modes to describe the emission pattern of a single vessel more accurately.

To make it possible to break down the emission distribution of a vessel in space and time, this research will be based on Automatic Identification System (AIS) data. AIS was in first instance developed for maritime authorities to track and monitor vessel movements. Nowadays it is a widely used automatic tracking system providing detailed information on vessel properties and vessel locations. AIS data represents real-life data and is gathered automatically, which makes it a reliable and realistic data source. This provides also the ability to make the emission estimations time dependent. Due to the global coverage, AIS data is a good data source to develop a generic method applicable to ports all around the world. More information on AIS data is provided in Section 4.1.1. Besides AIS data, the input will consist of a Fairway Information System (FIS) containing characteristics of the waterways, which are necessary to estimate the emissions. To map the estimated emissions, the results will be projected on the FIS graph. This makes it possible to single out fairway components and to compare port areas and fairway channels with each other. More information on the FIS is provided in Section 4.1.2.

The goal is to establish a model which can be applied to all ports around the world. To illustrate this, two case studies will be discussed: one on the Port of Rotterdam located in the Netherlands and one on the Port of Constanța located in Romania. Two very different ports are chosen, to indicate if the model can be applied to all types of ports around the world rather than only a specific type of port. The Port of Rotterdam is an interesting port to look into. This is the largest port of Europe and therefore a large source of emissions and thus a great deal is to be gained in terms of emission reduction (Transport & Environment, 2022). Furthermore it is a well known international port about which a lot of information is available. The Port of Constanța is of a much smaller scale. Also the location of the port differs greatly from the location of the Port of Rotterdam. Firstly, it is located outside an emission control area whereas the Port of Rotterdam is located inside an emission control area. This means different emission regulations apply, influencing the fleet composition and vessel behaviour (for example fuel consumption) and with that the emission patterns. Secondly, the Port of Constanța is located on the coast of Romania, meaning it is connected to the Black Sea, whereas the Port of Rotterdam is connected to the North Sea. This provides different environmental circumstances influencing the emission patterns (for example in the Black Sea there will be less influence of currents). By performing two different case studies, the influence of these factors on the developed model can be identified.

1.4. Research questions

The problem is defined and the research objective and scope are known. This has led to the following question to which this research must provide an answer to:

How to estimate vessel emissions in ports using AIS data in order to identify emission distribution patterns and evaluate emission reduction strategies?

To answer this question, the following sub questions are drawn up:

1. How can we develop a method for estimating emissions in ports in space and time?
2. What aspects of a vessel movement in a port should be distinguished when evaluating emissions of a vessel in a port?
3. What data is needed for developing a model to estimate emissions?
4. How can emissions patterns in a port be estimated and how can important emission sources be identified with the developed method?
5. How can the effects of emission reduction measures be quantified with this method?

6. How does the method perform when applied on AIS data of global ports?

These questions will determine the structure of the report. The steps corresponding to these questions are visualized in the figure below.

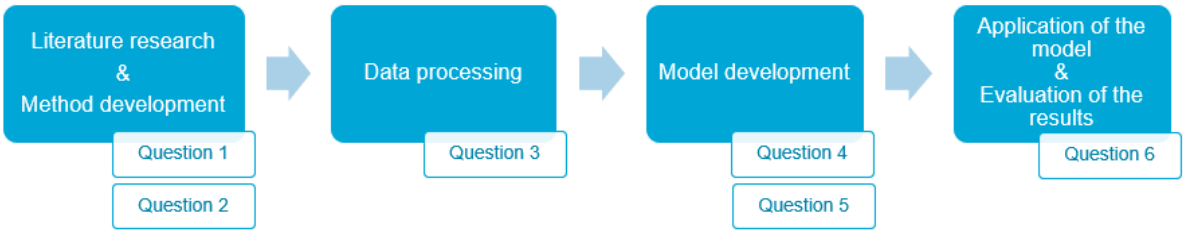

Figure 1.2: Report structure

I

Literature, methods and models

2

Literature

The theoretical framework of the research is presented in this chapter. To define the study parameters, the research method is briefly discussed first and from that the study parameters are derived and some background information around these subjects is provided. The relevant fleet in ports is also elaborated in the last section of this chapter.

2.1. Research method

The leading and one of the most detailed bottom-up method to estimate emissions from shipping is the one from International Maritime Organization (2021). Therefore, this research will be used as a base when developing a method to estimate emissions in ports.

The IMO approach is like many other bottom-up researches, based on the energy and fuel consumption of the vessel's engines times a vessel-specific emission factor (Cofala et al., 2007; Olmer et al., 2017; Kauffman and Hulskotte, 2021). The IMO approach, calculates the energy an engine has to deliver for estimating the NO_x and PM_{10} emissions, and calculates the fuel consumption of the engine for estimating the CO_2 and SO_x emissions. The fuel consumption is determined by multiplying the energy consumption of the engine by a specific fuel consumption factor differing for each vessel, meaning the fuel consumption is dependent on the energy consumption. More generally speaking, to estimate the emissions an approach to estimate the energy consumption of a single vessel, specific fuel consumption factors and emission factors are needed.

However the IMO approach is not port-specific and their approach to estimate the energy consumption of the vessel does not depend on the fairway characteristics. Therefore, some adjustments will be made to the method of the IMO. The most important components influencing these alterations are described in the following sections.

2.2. Energy consumption

The energy and with that the fuel consumption of a vessel depend on many characteristics. They are depending on the vessel characteristics and the movement of the vessel, but also on external influences such as the fairway characteristics and the weather. Background information on the most important characteristics will be provided in this section and their relation to this research will be addressed.

2.2.1. Engine types

The vessel's engines are the emission sources of a vessel. On board a ship typically several type of engines can be found: main engines responsible for driving the propeller of a ship to move the ship through the water, auxiliary engines needed to power the ship's electrical systems, boilers which are responsible for running various ship's machineries and lastly, a very small group (4% of the emission sources): gas turbines and inert gas generators responsible for additional services such as heat and steam production and ignition (European Commission, 2020). For all engines, except the main engines, there is a shortage of data on the engine specifications. Due to the scope of this research, the gas turbines and inert gas generators are therefore neglected.

The number of boilers installed on ships is significant, however their contribution to the amount of emissions is much smaller then of the main and auxiliary engines. This means that a method which only accounts for emissions coming from the main and auxiliary engines, is likely to give a reliable estimation of the emissions. However it will somewhat underestimate the total emissions. A special note should be made regarding tankers. Tankers use their boilers intensively to heat the cargo and drive the unloading pumps. Neglecting this will lead to an underestimation of emissions.

It is important to make a distinction between the emissions coming from the main engine or from the auxiliary engine. This way the method will provide a better emission estimation for vessels of which the magnitude of the two engine loads are far apart. Furthermore, the emission reduction measures further on in the research can also be addressed more specifically. For example, when a vessel is connected to shore power, only the auxiliary engine emissions will change. By applying a method which differentiates between these two engines, the reduction measure can be investigated more precisely.

A more detailed insight in engine-specific characteristics and their influence on the method, are elaborated on later on in the report in Chapter 3.

2.2.2. Operational modes

When focusing on the main engine, the amount of energy the engine consumes, is the energy needed to overcome the resistance a ship experiences from sailing through the water. In traditional energy estimations this resistance is related to the vessel's speed. Meaning that when a vessel is sailing at high speed, this requires more energy than when a vessel is sailing at a lower speed. However in ports the vessel's speed alone is not a good indicator of the energy consumption, since slow sailing does not necessarily mean that a vessel is consuming less energy. A low vessel speed could also mean that a vessel is manoeuvring through a port basin with the auxiliary engines driving the bow thrusters causing higher emissions, or that a vessel is at a berth or anchorage with its main engines off but still emitting considerably due to the fact that the auxiliary engines are on powering the electrical systems. Relating the total energy consumption of a vessel only to speed, neglects the fact that the amount of energy an auxiliary engine consumes, is dependent on how much energy the electrical systems of a vessel require at that moment. During sailing the energy consumption is generally low, but when a vessel is manoeuvring or loading/unloading this increases. The energy consumption of the auxiliary is therefore related to the operations a vessel performs.

To determine the energy consumption of a vessel, a distinction is necessary between all vessel operations that have their own energy consumption characteristics. Since the energy consumption of the main engine is related to the speed of the vessel, it make sense to divide these operations into categories which have the same speed characteristics.

When looking into other researches, different categorizations of operational modes based on speed occur. Generally, they all have the same scope where they contain a mode for normal sailing, manoeuvring and hotelling, but some make a distinction between different speeds in 'sailing' and some make a distinction in 'hotelling' between berthing and anchoring. For example Ng et al. (2013) uses 'cruise, fairway cruise, slow cruise, manoeuvring and hotelling' and Starcrest consulting group LLC (2020b) uses 'transit, manoeuvring, berth-hotelling, anchorage-hotelling'. On a smaller scale, such as in ports, it is important to make a distinction between berthing and anchoring since this influences the auxiliary engine's power consumption (International Maritime Organization, 2021). This influences the spatial distribution of the emissions, as berths and anchorages are located elsewhere in ports.

For tankers a distinction in the operational mode 'berthing' between loading and unloading would be advisable, since their power consumption at berth during loading is almost zero while their power consumption at berth during unloading is extremely high to power their pumps. However, the distinction between those two operations can not be made based on speed and requires a lot of extra data and research. Due to the scope of the research, the operational mode 'berthing' for tankers is not split up in loading and unloading.

Since the contribution of the auxiliary engine will be small in the 'sailing' mode, differentiating between different speeds in this mode is not of added value in this approach. Determining the energy consumption of the main engine with a method based on vessel speed will take into account these differences in energy consumption at different speeds. This leaves us with four relevant operational modes in ports: 'berthing', 'anchoring', 'manoeuvring' and 'sailing'. The contribution of the main and auxiliary engines is different in each of the modes and the method must take that into account. The four modes will be explained in short:

- **Berthing** means the vessel is laying still at berth for loading and unloading operations. Generally the main engines are turned off and the auxiliary engine load is high to support the vessels' electrical systems needed for loading and unloading.
- **Anchoring** is similar to berthing, however anchorages are mostly located outside a port or in front of a berth to accommodate vessels waiting to enter the port or waiting for open berths.
- **Manoeuvring** occurs when a vessel enters a port and is proceeding towards its berth/anchor or the other way around when leaving the berth/anchor. It can also occur when a vessel is sailing in high intensity traffic zones and for example is passing another ship or is approaching a fairway intersection. This operation normally requires low speeds (between 0-8 knots) with moments of instant acceleration and deceleration. The main engines are operating at low loads and the auxiliary engine loads are high to supply energy to the additional onboard equipment such as thrusters (Bacalja et al., 2020). Manoeuvring operations are sometimes accompanied by tug assistance. Expert opinion states that vessels keep their main engines running when assisted by tugs. The rate at which they are running, differs per captain (Man Jiang (TU Delft), personal communication, October 17, 2021). This makes it more difficult to estimate the energy consumption of the main engine. For the scope of this research, energy fluctuations due to tug assistance are neglected.
- **Sailing** means the vessel is traveling at medium to high speed and not performing any specific operations. This requires high main engine loads to propel the ship and relatively low auxiliary engine loads since few electrical systems are used in this mode.

2.2.3. Fairway characteristics

Energy is provided by the main engines, which is needed to overcome the resistance a ship experiences from sailing through the water. This resistance depends on the fairway characteristics. Think of the dimensions of the fairway, but also external influences on the fairway such as wind and waves. The dimensions of the fairway have a big influence on the resistance. Lateral waterway restrictions are generally of less influence in ports (Segers, 2020). However, the limited water depth in ports have a big influence and can therefore not be neglected. A limited depth in combination with the displacement of a vessel, causes flow acceleration underneath the vessels bottom. The physical explanation of this is that when water gets shallower, the boundary layer decreases. With the decrease of the boundary layer, the velocity gradient normal to the bottom of the ship increases (acceleration). When the flow velocity increases, the local friction increases as well. For this reason, it is important to take into account shallow water effects in ports. This falls within the scope of this research, as information about the water depth is widely available for ports around the world.

External influences on the fairway play a role in ports when determining resistance of a vessel. The first two external influences which will be discussed are wind and waves. When sailing against the wind, the vessel will experience additional resistance than when compared to sailing along with the wind. The same rationale goes for waves. Quantification of this change in resistance requires detailed information of vessel characteristics such as the hull-shape, loading conditions and speed, and detailed time-dependent information of the wind and waves, such as the fortitude and direction. Ports are typically aerodynamically complex environments with complicated wave patterns. Wind and wave forces vary strongly and it is hard to obtain detailed time- and space-dependent data. Since most ports are located inland and are relatively sheltered by for example breakwaters, the effect of wind and waves on the vessel resistance is considered to be minor. The research of Seo et al. (2017) supports this; In harbour basins, typically long waves are observed, and this research states that the added resistance of ships for long wavelengths is between 2 and 5 %. This also gives an indication for the wind resistance, as for ocean-going vessels this is generally significantly lower than the wave resistance (MAN Energy Solutions, 2018). Due to their small contribution, these external influences are neglected in this research.

A third external component influencing the resistance is the current of the fairway. Generally two terms are used to describe vessel speed: 'speed through water' and 'speed over ground'. The velocity available in the AIS data is the 'speed over ground'. This is the speed with respect to the land. However, the velocity of the vessel relative to the water, the so called 'speed through water', is used in resistance calculations. This takes into account the current of the fairway. If a vessel is moving against the current the speed through water is higher than when a vessel is sailing along with the current. The representation of this is:

- along the current: speed over ground + speed of the current = speed through water
- against the current: speed over ground - speed of the current = speed through water

A higher speed through water means a higher frictional resistance. The speed is quadratically related to the resistance, so small changes to the vessel speed will have a large influence on the resistance. To take into account the currents, time- and space-dependent data about the magnitude and the direction of the currents is necessary. Obtaining this data is difficult and not available for ports all around the world. For the scope of this research, the effect of currents is therefore neglected. This will lead to higher uncertainty in the estimation of emissions.

2.3. Emission factors

Several companies and institutions have derived emission factors. The most extensive researches are performed by Nederlandse Organisatie voor toegepast-natuurwetenschappelijk onderzoek (TNO) and IMO. The emission factors of TNO consider only three operational modes: 'sailing at sea', 'sailing inland' and 'hotelling' (Hulskotte, 2019). They are based on certification-measurements commissioned by engine suppliers and validated by performing tests on exhaust gas plumes from vessels sailing on Dutch territory (J.H.J. Hulskotte (TNO), personal communication, July 24, 2021). The IMO emission factors are based on literature and extensive testing on multiple engine types of vessels sailing all around the world and therefore apply in global setting. Another advantage is that they cover the same four operational modes as the ones which will be used in this report. Therefore, the emission factors of the IMO align better with this research.

The IMO differentiates between energy-based and fuel-based emission factors depending on the emission product. The energy-based emission factor is stated in terms of gram pollutant per kWh and the fuel-based emission factor is stated in terms of gram pollutant per gram fuel. The reason for this division is that fuel-based emissions are directly proportional to the fuel consumption and therefore dependent of the engine load; the fuel consumption is higher if the engine does not operate at it's optimum engine range. Once the fuel consumption is known, the emissions can be derived directly from the emission type content in the fuel (United States environmental protection agency, 2016). The energy-based emission types are not engine load dependent. They can not be derived directly from the fuel content, but they need to take in engine characteristics such as the age and engine speed.

Besides the engine load, the emission factors differentiate between many other characteristics. These different characteristics are explained in more detail in Appendix C.

2.3.1. Emission types

Due to the scope of this research, not all greenhouse gasses are taken into account but the focus will be on CO_2, NO_x, SO_x and PM_{10}. These are, as mentioned before, the four most noticeable polluters in the shipping industry, but become even more important when zooming in on ports.

Most current regulations applicable in ports, cover these four aforementioned polluters. The reason these specific emission types are highlighted, is because they have the largest impact on many levels. For starters, CO_2, NO_x, SO_x and PM_{10} are the four largest contributors to the total emissions in ports (Merk, 2014). These three considered gasses and PM_{10} are harmful for people's health and the environment. NO_x, CO_2 and PM_{10} emissions in ports have been linked to health issues such as bronchitic symptoms, respiratory issues, high blood pressure, heart problems, strokes and premature deaths and cause environmental acidification and nutrient pollution in coastal waters (EPA, United States Environmental Protection Agency, August 16, 2021). CO_2 and SO_x are of global environmental importance, whereas NO_x and PM_{10} effect the environment more locally, which is important when considering ports and port-cities.

The fuel type and quality, the engine type and the combustion process influence the amount of these emissions. To get more insight in this process, more detailed information is provided about the four considered emission types.

Carbon dioxide (CO_2)

Around 97% of emissions in ports consists of CO_2, which is by far the largest share (Merk, 2014). Due to its large presence and its ability to remain in the atmosphere for over 300 years, CO_2 is an important pollutant contributing to global warming and climate change (NASA, 2022).

The formation of CO_2 depends on the carbon present in the fuel. The carbon reacts with the oxygen in the air and forms CO_2. The emission is directly proportional to the amount of fuel used and thus with the efficiency of the engine (Witkowski and Kazimierz, 2020). Therefore this emission type follows a fuel-based approach,

which allows for variation in engine load and carbon content of the fuel. The load dependency is captured in the fuel consumption (International Maritime Organization, 2021).

Nitrogen oxides (NO_x)
NO_x contributes to the formation of photochemical smog and acid rain and promotes the formation of ozone (Jun et al., 2001). Besides this, NO_x has a harmful effect on the health of the local population. NO_x is highly reactive and decays in the atmosphere in a few days, for this reason it is not subjected to long-range transport away from the source (Haga et al., 2021). However, this increases the importance of the local effects of NO_x. Many legislative initiatives are being drawn up to reduce NO_x emissions locally, such as in ports.

The air consist of approximately 21% oxygen and 79% nitrogen. When an engine burns fuel, the oxygen reacts with the nitrogen present in the fuel, but also with the nitrogen already present in the air. This way mostly NO and NO_2 are formed, together summarized as NO_x (ANWB, 2022). This formation only happens at high temperatures and the amount of NO_x produced depends on the combustion temperature and the time the nitrogen and oxygen are subjected to these high temperatures (Witkowski and Kazimierz, 2020). Therefore, the engine type and engine speed play a dominant role in determining NO_x emissions. NO_x emissions are independent of the engine load and will follow an energy-based approach.

Sulfur dioxides (SO_x)
The shipping sector's contribution to the total SO_x emission is large and approximately 70% of these emissions occur within 400 km of land, such as ports (Endresen et al., 2003). Here, SO_x emissions have a large impact. It contributes to the formation of photochemical smog and acid rain and causes health related issues like respiratory problems. This leads to many initiatives to limit the SO_x emissions, like the IMO sulphur regulation.

The SO_x emission is directly related to the level of sulfur in the fuel being used. When sulfur content is lowered, the emitted SO_x is less. During combustion approximately 98% of sulfur in the fuel is oxidized to SO_2 and the remaining part to SO_3. These two components are together referred to as SO_x.

The emission is directly proportional to the sulfur content of the fuel. Therefore this emission type follows a fuel-based approach, which allows for variation in engine load and sulfur content of the fuel.

Particulate matter (PM_{10})
PM stands for particulate matter, and PM_{10} covers the particles with a diameter of less than 10 micrometer. These small particles can penetrate deep into the respiratory system and are therefore related to many acute or chronic health effects. The most prominent sources of PM_{10} emissions are local sources (Haga et al., 2021). Therefore the measures to reduce these emissions are drawn up locally, such as in ports, which makes it important to consider this emission type in this research.

The sulfur that is not converted to SO_x is assumed to be converted to PM_{10} (International Maritime Organization, 2021). This means that when the SO_x emissions decrease, the PM_{10} emissions increase. This also means that the PM_{10} emissions are directly related to the sulfur content of the fuel and the fuel consumption. However the amount of emission is related to the engine combustion processes. Determining PM_{10} emissions, follows an energy-based approach and is dependent on respectively the fuel type and the engine type.

2.3.2. Fuel types
For a better understanding of emission factors, the fuel consumption but also the fuel type must be known. A little background on the types of fuel used in the marine industry is provided in this section.

The world fleet is mainly powered by diesel engines running on marine fuels. Marine fuel is obtained from the distillation of crude oil and includes distillates (the lighter fractions) and residues (the heavier fractions). The most common fuel types used in the marine industry can be divided into distillate fuels and residual fuels (Vermeire, 2021).

Residual fuel, also called Heavy Fuel Oil (HFO), was until recently the most widely used fuel as it is very cheap (around 30% cheaper than distillate fuels). The downside of this fuel is that it has a high sulfur content (Fritt-Rasmussen et al., 2018). To comply with the current regulations (IMO 2020 rule), so-called exhaust gas cleaning systems (EGCS) are installed which clean the exhaust gasses and limit the sulphur oxide emission. The most widely used EGCS are scrubbers. From the Clarkson vessel database, is inferred that approximately

4.700 ships were fitted with scrubbers in June 2022. This is around 4.5 % of the world fleet in terms of the number of vessels. Due to Covid-19 the fuel prices dropped and the expected increase in scrubbers did not increase as much as was expected. On top of that the effect of scrubbers is currently being questioned by several environmental organizations. This in combination with economic considerations makes it uncertain whether the number of vessels with scrubbers will increase strongly in the future. Besides the sulphur oxide and particulate matter emissions, scrubbers do not heavily affect the emission pattern of other evaluated emission types and therefore, the use of scrubbers is not taken into account in this research (Johnson, 2013). It is important for future research to keep evaluating this trend, since the neglect of scrubbers will cause an over-estimation of the actual amount sulphur-related emissions.

When the sulfur regulation tightened on 1 January 2020, a small part of the world fleet installed scrubbers, but most vessels switched to a different fuel type with lower sulphur content (Wagenborg, 2020). They switched to distillate fuel of which the most widely used ones are marine diesel oil (MDO) and marine gas oil (MGO). The common distillate fuels can comply with the current regulations (without scrubbers), as MDO has a maximum sulphur emission of 0.50% and MGO a maximum sulphur emission of 0.10%. The higher quality distillate fuels are primarily used in emission control areas (ECAs) (European Technology and Innovation Platform, 2017).

The shipping industry is, like any other transport industry, focusing on cleaner fuel solutions. This leads to an increased use of alternative fuels. An increasing group of vessels uses liquid natural gas (LNG) to power their engine. It is often referred to as 'the fuel of the future' since it has a low sulphur content, consists of clean burning properties and is cheap. However, it is difficult for existing vessels to adapt their engines to run on LNG. Furthermore the storage of LNG aboard a vessel might lead to difficulties (Al-Enazi et al., 2021). Recently another drawback arose from research done by Ushakov et al. (2019), namely: methane slip produced at lower engine loads. Methane is considered to have a 86 times higher 20-year global warming potential than CO_2. For these reasons, a world wide switch to LNG might take years.

Other groups of alternative fuels often named to reduce greenhouse gas emissions, are the biofuels and blends with biofuels. Biofuels currently available are Straight Vegetable Oils (SVO), biodiesel (FAME), renewable diesel (HVO), ethanol and butanol from sugar and starch, and tall oil renewable diesel. Although the interest for these biofuels has increased over the last decades, it is not likely to be widely used soon. Most biofuels are short in supply and expensive, the handling of some biofuels is difficult and the volumes needed to supply the power are large. Biofuels are therefore more applicable for smaller vessels or for auxiliary ultra-low sulphur fuel in ports (Hsieh and Felby, 2017).

Methanol is the exception and is considered to be an important fuel to achieve the emission targets. It can be a carbon neutral fuel when made from biomass or green electrical power and the emissions are very low and sulfur-free (Siemens Energy, 2020). Only minor engine modifications are needed for diesel engines to switch to methanol, however a drawback is that the storage of methanol takes in more space then the storage of current diesel fuels, since the energy density is low (Andersson and Salazar, 2015). Nowadays, except for Stena which has one ferry operating on methanol, Methanex is the only company operating tankers using methanol diesel engines (de Jong, 2020).

Besides alternative fuels, also use is made of renewable energy. There are ships utilizing batteries, hydrogen, solar power, wind and wind energy. A few electric ferries using electric energy from batteries are in operation, but this energy source still has limited applications since the capacity of the batteries is limited to short voyages. Furthermore, the energy to power the batteries is still mainly generated by onshore power plants. Hydrogen fuel is a relatively new technology, which is garnering interest because of its applicability for long voyages. However, in the future the use of batteries is more likely to grow since it is cheaper, the technology is more mature and not many logistical changes are necessary for implementing this technology compared to hydrogen fuel (Horton et al., 2022).

Some naval ships use gas turbines or steam power, the latter mostly in combination with nuclear installations. There is also a sizeable number of mostly older LNG carriers operating on steam power, using boil-off methane gas from the cargo as fuel for their boilers. Gas turbines have a poor efficiency and cannot compete successfully with diesel engines for most applications (de Jong, 2020).

2.4. Considered fleet

For the scope of the project, not all vessel types will be included. To determine which vessel types are the most relevant, a literature study is performed on vessel data from 2019 since this represents the fleet most realistically due to Covid-19. The vessel categories which are responsible for the largest share of emissions in ports are considered most relevant (for this research). However, the biggest polluters in ports are difficult to identify due to the lack of insight in emissions in ports. Therefore, first the world fleet will be observed and subsequently additions will be made to this fleet specifically focusing on polluters in ports.

Most climate change goals are focused on reducing CO_2 emissions, as they have the largest contribution to the total emissions (98%) (Kauffman and Hulskotte, 2021). Therefore, data about CO_2 emissions is the most widely available from previous studies. According the International Maritime Organization (2021), considering the commercial world fleet, there are seven vessel types which together account for approximately 90% of the CO_2 emission of the world total. By including these vessel types in this research, the biggest polluters are tackled. Figure 2.1 shows the contribution of the commercial fleet to the total CO_2 emissions. The pie chart on the left covers the seven vessel types which are responsible for 90% of the total emissions. The figure on the right covers the vessel types excluded from this 90%.

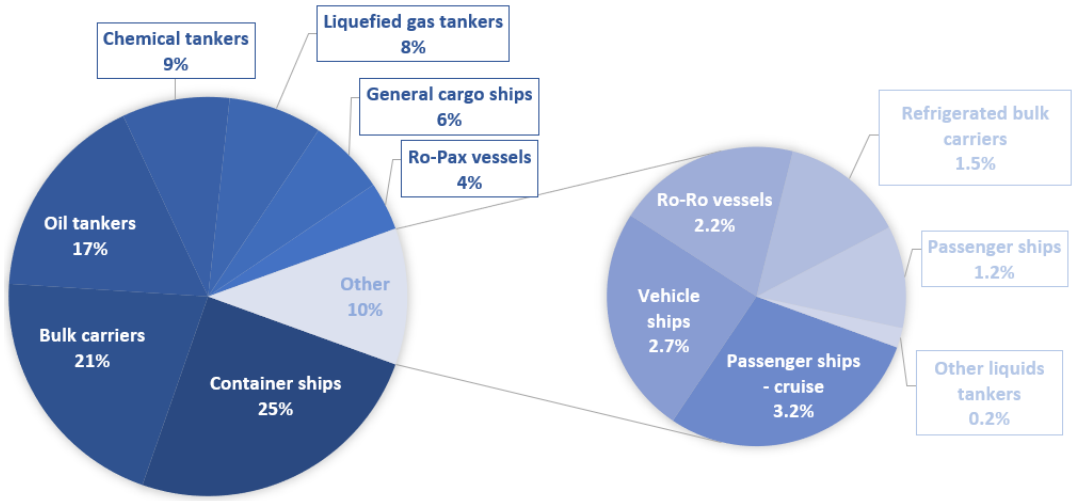

Figure 2.1: Percentage CO_2 emission per vessel type of total CO_2 emissions of the commercial world fleet

When looking at the pie chart on the right, the eight-largest vessel type is the 'Cruise ship'. When looking on a European scale like the researches of Olmer et al. (2017); European Commission (2020) and Bullock (2020), compared to the world fleet the category 'Passenger ships' or 'Cruise ships' is also part of the 90%. It would be of added value to include a passenger ships category in the research. Not only because this way all large polluters are taken into account, but also since their energy demand in ports is generally considerable and therefore they emit large amounts of CO_2, NO_x and SO_x (Celic et al., 2014).

A division is made between passenger ships since the energy consumption patterns of cruise vessels differ significantly from other passenger vessels. Their characteristics and other vessel-specific values vary throughout the research, so therefore they are considered as two different categories: the cruise ships category 'Passenger ships - cruise' and the rest of the passenger vessels summarized as category 'Passenger ships'.

Another often-named vessel type is the refrigerated cargo vessel. Although their emissions are significant, this vessel type is not part of the eight largest emitters and the number of refrigerated cargo vessels is decreasing (News, 2019). Furthermore, the emission pattern of this vessel type is complicated since the cargo of the vessel also demands energy. The method followed in this research will lead to emission rates with a high uncertainty. For the scope of this research this category is therefore left out.

When comparing the world fleet to the fleet in a port, it must be noted that not only the number of vessels is important, but also their time spend in port. The cargo vessels will generally spend the same amount of time in ports (hours to days) and will therefore contribute to the emissions in ports as described above. However

a group of vessels spending significantly more time in port than cargo vessels are the service vessels. They do not emit as much per vessel, but since they are always present in the port, they can still be responsible for a large share of emissions. The largest part of the port service fleet consist of tugboats. When looking into other researches the share of CO_2 emissions of tugboats in ports has a large scatter, varying from 7% to 22 % of the total CO_2 emission in the port (Khan et al., 2008; Leong et al., 2015). To investigate the reason for this scatter and to avoid exclusion of a possibly large part of the emissions in ports, tugboats are also considered part of this research.

The complete overview of the vessel types which are taken into account is as follows:

- Container ships
- Bulk carriers
- Oil tankers
- Chemical tankers
- Liquefied gas tankers(LPG/LNG/CNG)
- General cargo ships
- Ro-Pax ships
- Passenger ships
- Passenger ships - cruise
- Tugboats

3

Method

To estimate the emissions from shipping in ports, a bottom up method is developed based on AIS data. The emission of a single ship is estimated and by mapping the components of all single ships along a port network an emission distribution is derived. First the method to estimate the emission of a single vessel in space and time is explained in this chapter. With this method as a basis, a model containing all algorithms to map the emissions can be set up and the necessary input data can be identified.

Figure 3.1 gives a brief overview of the structure of the method used to estimate the emission of a single vessel. With the vessel speed and position from the AIS data, an operational mode is determined. This is necessary because the engine power estimation is operational-mode-specific. According to the operational mode, the main engine power is either estimated with the resistance calculation from Holtrop and Mennen (1982) when the vessel is sailing, or assumed zero when laying still. According to the operational mode, the auxiliary engine power can be estimated with values of the research of International Maritime Organization (2021). Depending on the emission type and vessel characteristics, the emission factor is determined with an energy-based or fuel-based approach. The emission rate for the main engine and auxiliary engine is determined separately and is obtained by multiplying the energy consumption by the specific emission factor. The total estimated emissions of a ship are the sum of the emission from the main engine and the auxiliary engine.

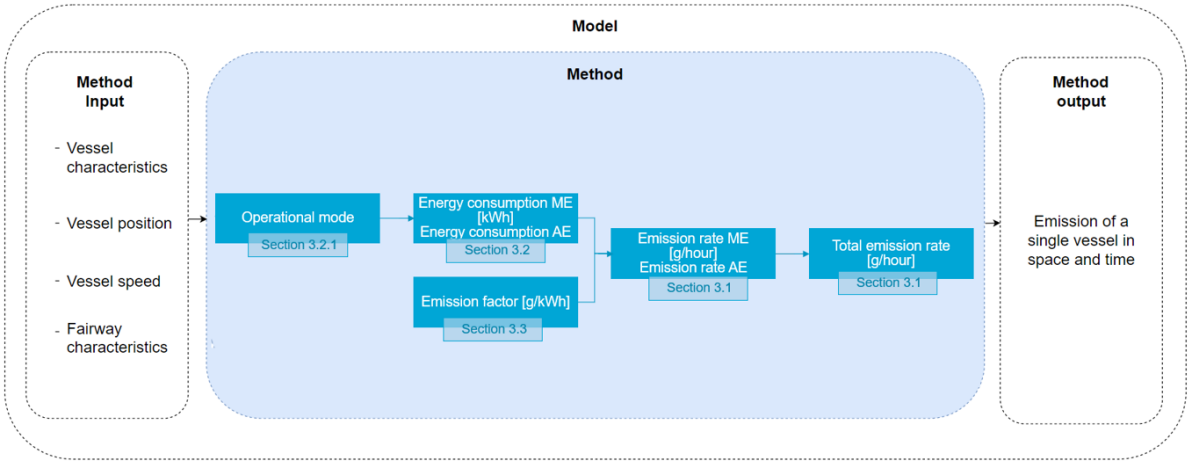

Figure 3.1: Overview of the method to estimate emissions of a single vessel

When the emissions of all individual vessels are known, this can be implemented in the model. The steps on how to implement the method into the model, the input and output of the model and the data processing steps are explained in more detail in Chapter 4. The method used to estimate the emission of a single vessel in space and time is explained in this chapter.

3.1. Estimate emissions

The emission of a vessel per Δt are the sum of the emission from the main engine and the auxiliary engine.

$$EM = EM_{ME} + EM_{AE} \tag{3.1}$$

with:

- EM = total emission of the vessel per Δt
- EM_{ME} = emission of the main engine of the vessel per Δt
- EM_{AE} = emission of the auxiliary engine of the vessel per Δt

The emission of the main and auxiliary engine are calculated apart from each other since they come from different engines with each their own characteristics and fuel type. For all four emission products (CO_2, SO_x, NO_x and PM_{10}), this is done according the following formula:

$$EM_{,i} = E_{,i} * EF_{total} \tag{3.2}$$

with:

- $EM_{,i}$ = emission of the main/auxiliary engine [g / hour]
- $E_{,i}$ = energy consumption of the main/auxiliary engine per Δt [kWh]
- EF_{total} = total emission factor [g / kWh]

3.2. Estimate energy consumption

3.2.1. Determine operational mode

The energy consumption calculation of the main engine and auxiliary engine are operational-mode-specific. Therefore the first step is to determine the operational mode. Four modes are distinguished: sailing, manoeuvring, berthing and anchoring. When a ship is berthing or anchoring, it is assumed that the main engine is turned off and the auxiliary engine is on to power the vessel's electrical systems. When a vessel is manoeuvring or sailing, the power consumption of the main engine is estimated based on the vessel's resistance according the method of Holtrop and Mennen (1982). The auxiliary engine power consumption will have a smaller contribution in these modes.

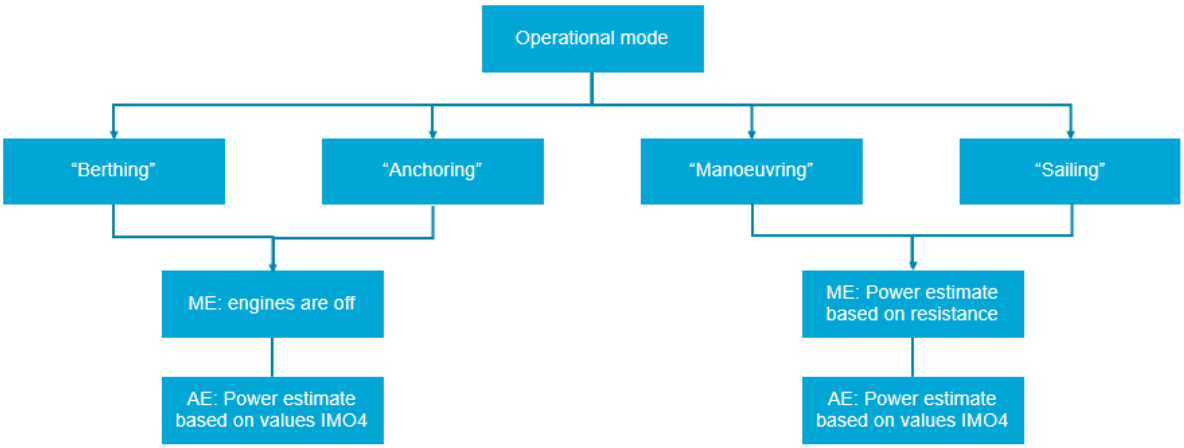

Figure 3.2: Overview of the operational modes and their influence on the engine power consumption

3.2.1.1. Classification of operational modes

The modes are identified based on the speed and position of the ship from the AIS data. Based on previous research from International Maritime Organization (2021), a decision matrix is drawn up for all vessel types with a small alteration for liquid tankers. Liquid tankers operate differently since they can unload offshore. The decision matrix is shown below. The rows represent the speed over ground and the columns the distance of the vessel to it's destination. It is assumed that at the end of each trip, the vessel is berthing to load and unload it's cargo. This point is called the destination point.

	Distance to destination		
Speed over ground	**<1 nm**	**1 - 5 nm**	**> 5 nm**
<0.5 knots	Berthing	Anchoring / Berthing*	Anchoring
0.5 - 3 knots	Anchoring	Anchoring	Anchoring
3 - 5 knots	Manoeuvring	Manoeuvring	Sailing
>5 knots	Manoeuvring	Sailing	Sailing

Table 3.1 Decision matrix to determine operational mode for all vessel types
∗For liquefied tanker only

When reaching the destination of the trip and the speed is close to zero, the operation is categorized as 'berthing'. An exception applies for liquid tankers, which can load and unload within a range of five nautical miles offshore. This generates an uncertainty, since the liquid tankers at anchorage within a range of 1-5 nautical miles from it's destination are now also categorized as berthing. This results in an overestimation of the auxiliary engine load, since the energy demand for unloading of tankers while berthing, is significantly higher than while anchoring.

When the AIS data registers a speed between 0.5 - 3 knots, the vessel is not sailing yet but assumed to be at anchor. This results in speeds close to zero, but never reaching zero since the vessel will be drifting. This generates an uncertainty, since this means that when leaving berth, a vessel is always for a slight period in anchor-mode before manoeuvring. This assumption will cause an underestimation of the emissions since the main and auxiliary engines power demand while manoeuvring is higher than when anchoring.

For both uncertainties stated above, holds that no alterations will be made since the values from the research of International Maritime Organization (2021) are used to estimate the auxiliary engine power. They maintained this categorization of operational modes when they performed tests and measurements to derive the auxiliary engine power, so alterations will influence the auxiliary engine power consumptions.

3.2.2. Energy consumption main engine

The amount of energy the main engine consumes, is dependent on the resistance the ship experiences. This resistance consists of several components which are estimated according the method of Holtrop and Mennen (1982). All components taken in, are explained in Section A.1. To translate the total resistance to total required power, the propulsion characteristics and efficiencies of the system are taken into account. Figure 3.3 shows a schematization of the system.

To overcome the resistance the ship experiences, a certain effective power (P_e) is needed. After some losses in the propeller this power can be expressed as the delivered horsepower (P_d). After again some losses in the gearbox and shaft this can be expressed as the brake horse power (P_b). The brake horse power determines the energy consumption of the main engine.

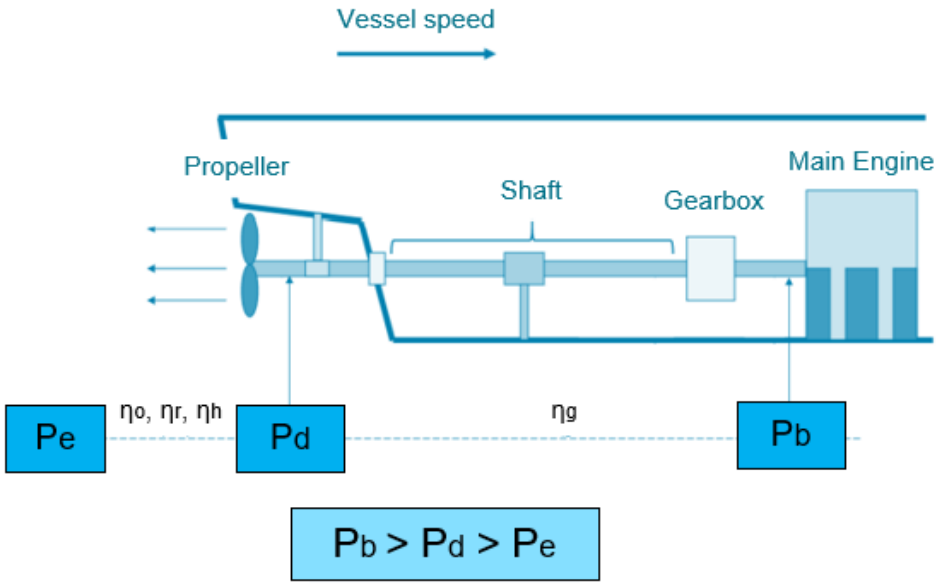

Figure 3.3: Schematization of the main engine system of a ship

The energy consumption of the main engine can be described by the formula below:

$$E_{ME} = P_b * \Delta t \tag{3.3}$$

With:

- E_{ME} = energy consumption of the main engine during Δt [kWh]
- P_b = brake horse power [kW]
- Δt = timestamp [hours]

To determine the required brake horse power, knowledge of engine system is needed. The calculation begins with determining the effective power. With some efficiency factors the effective power can be translated to the brake horse power. In other words: calculating from left to right in the Figure 3.3.

The effective power is the power required to move the ship at a given speed in the absence of propeller action. It can be calculated according:

$$P_e = V_0 * R_{tot} \tag{3.4}$$

With:

- P_e = effective power [kW]
- V_0 = vessel speed [m/s]
- R_{tot} = ships total resistance [kN]

The total resistance the vessel experiences is a sum of multiple resistance components (Holtrop and Mennen, 1982):

$$R_{tot} = R_f(1+k_1) + R_{App} + R_w + R_B + R_{TR} + R_A \tag{3.5}$$

With:

- R_{tot} = total resistance [kN]
- R_f = frictional resistance [kN]
- $1+k_1$ = form factor describing the viscous resistance of the hull form in relation to R_f [-]
- R_{App} = resistance of appendages [kN]
- R_w = wave-making and wave-breaking resistance [kN]
- R_B = additional pressure resistance of bulbous bow [kN]

- R_{TR} = additional pressure resistance of immersed transom stern [kN]
- R_A = model-ship correlation resistance [kN]

All of these resistance components are explained in detail in Section A.1.

The effective power can be expressed as delivered horse power (the power delivered to the propeller) taking in some efficiencies from the propeller. The efficiencies are described in more detail in Section A.2. The delivered horse power becomes:

$$P_d = \frac{P_e}{\eta_0 \eta_r \eta_h} \tag{3.6}$$

With:

- P_d = delivered horse power [kW]
- η_o = open water efficiency of propeller [-]
- η_r = relative rotative efficiency [-]
- η_h = hull efficiency [-]

The delivered horse power can be expressed as brake horse power by taking in the remaining losses from the gearbox and shaft:

$$P_b = \frac{P_d}{\eta_g} \tag{3.7}$$

With:

- η_g = gearing efficiency [-]

The determination of the gearing efficiency can be found in Section A.2.

If the maximum brake horse power exceeds the installed power, the installed power is assumed as this can not be the case.

3.2.3. Energy consumption auxiliary engine

The energy consumption of the auxiliary engine is dependent on the operational mode, vessel type and size category. For each vessel type and operational mode fixed values for the power of the auxiliary engine are determined. These values are based on the most recent study of the International Maritime Organization (2021). The reason for this is that this study maintains the same operational modes as the four operational modes maintained in this report.

The energy consumption can be calculated with the following formula:

$$E_{AE} = P_{AE} * \Delta t \tag{3.8}$$

With:

- E_{AE} = energy consumption of the auxiliary engine per Δt [kWh]
- P_{AE} = power of the auxiliary engine [kW]
- Δt = timestamp [hours]

A table with the fixed values for P_{AE} and how they are derived, can be found in Appendix B.

It must be noted that this research does not take into account boiler emissions. When estimating the emissions at berth from tankers, this can lead to a large underestimation since their machinery to unload the cargo requires a lot of power which is provided by the boiler. To take this into account, in the berthing mode the power consumption of the boiler (stated in the International Maritime Organization (2021)) is added to the power consumption of the auxiliary engine for all three tanker types. This generates an uncertainty in the emission estimation as the boiler is now assumed to have the same engine characteristics as the auxiliary engine. However excluding the share of emission from the boiler leads to even more uncertainty.

3.3. Total emission factor

The IMO has determined some base emission factors based on the emission products and engine characteristics. These base emission factors can be found in Appendix C. The base emission factors need to be translated to the total emission factor. The total emission factor for CO_2 and SO_x is determined differently from the ones for NO_x and PM_{10}. The first two emission types make use of an energy-based approach and the latter two make use of a fuel-based approach.

Method for CO_2 and SO_x - fuel-based
The total emission factors of CO_2 and SO_x are determined following a fuel-based approach. This means that the emissions depend on the engine load and the carbon and sulfur content of the fuel respectively. The base emission factors are stated in terms of [g/kg fuel] instead of [g/kWh]. To obtain the fuel-based total emission factors, the base emission factor (from the fourth IMO greenhouse gas study) must be multiplied with the hourly fuel consumption of the vessel type:

$$EF_{total} = EF_{base} * HFC_{total,i} \tag{3.9}$$

with:

- EF_{total} = total emission factor of CO_2 or SO_x [g / kWh]
- EF_{base} = base emission factor [g / g fuel]
- $HFC_{total,i}$ = total hourly fuel consumption of the ME/AE [g fuel / kWh]

Method for NO_x and PM_{10} - energy-based
The total emission factors for NO_x and PM_{10} are derived following an energy-based approach. This means that it is not necessary to determine the hourly fuel consumption and the base emission factors can directly be used:

$$EF_{total} = EF_{base} \tag{3.10}$$

with:

- EF_{total} = total emission factor of NO_x or PM_{10} [g / kWh]
- EF_{base} = base emission factor [g / kWh]

3.3.1. Hourly fuel consumption HFC

The hourly fuel consumption of the main engine is dependent on the engine load and/or class. It needs a correction since for lower engine loads, the engine is less efficient. This is done by multiplying a base hourly fuel consumption with a correction factor C:

$$HFC_{total,ME} = HFC_{base} * C \tag{3.11}$$

with:

- $HFC_{total,ME}$ = total hourly fuel consumption of the main engine [g fuel / kWh]
- HFC_{base} = base hourly fuel consumption [g fuel / kWh]
- C = correction factor engine load

Gas and steam turbines are not dependent on engine load and therefore their $HFC_{total,ME}$ is the HFC_{base}.

For the auxiliary engine the emission factor is independent of the engine load, because the engine load of auxiliary engines is usually adjusted by switching (multiple) engines on or off. The optimum working range of auxiliary engines is thus maintained and does not have large variability. Therefore the $HFC_{total,AE}$ of the auxiliary engine is the HFC_{base}:

$$HFC_{total,AE} = HFC_{base} \tag{3.12}$$

Base hourly fuel consumption HFC_{base}
The base hourly fuel consumption is dependent on the engine type, fuel type and the year of built of the engine. The vessels are divided in three construction year classes depending on their year of built:

- Built before 1984
- Built between 1984 and 2000

- Built after 2000

Table 3.2 states the HFC_{base} values. These values are derived from the fourth IMO greenhouse gas study.

Engine type	**Fuel type**	**HFCbase**		
		Before 1983	1984-2000	After 2000
SSD	HFO	205	185	175
	MDO	190	175	165
	Methanol			350
MSD	HFO	215	195	185
	MDO	200	185	175
	Methanol			370
HSD	HFO	225	205	195
	MDO	210	190	185
LNG-Otto-SS	LNG			148 LNG + 0.8 MDO
LNG-Otto-MS	LNG		173	156
LNG-Diesel	LNG			135 LNG + 6 MDO
LBSI	LNG		156	156
Gas Turbines	HFO	305	305	305
	MDO	300	300	300
	LNG			203
Steam Turbines	HFO	340	340	340
	MDO	320	320	320
	LNG	285	285	285
Auxiliary Engine	HFO	225	205	195
	MDO	210	190	185
	LNG		173	156

Table 3.2 Base hourly fuel consumption

Correction factor engine load C

The equation for the correction factor is taken from the fourth IMO greenhouse gas study, where several HFC-curves against the main engine load were used to find an empirical equation to estimate $HFC_{total,ME}$ at a specific engine load.

$$C = 0.455 * load_{ME}^2 - 0.710 * load_{ME} + 1.280 \tag{3.13}$$

with:

- C = correction factor engine load [-]
- $load_{ME}$ = main engine load [%]

The main engine load is the ratio between installed engine power and the brake horse power that is used (calculated in Section 3.2.2).

4

Model

A model is set up containing the algorithms to estimate the emissions as described in Chapter 3. The model is based on AIS data. This data provides the vessel speed and position needed as input for the emission estimation. The AIS data in combination with the Sea-web Ships database is used to set up a vessel database containing all vessels occurring in the evaluated AIS data. This provides the vessel characteristics needed in the method. To evaluate the route of each unique vessel, the AIS data is split up in trips. These trips are coupled to the FIS network. This FIS network contains all fairways inside the port and fairway characteristics such as the geometry of the waterway, which are necessary in the emission estimation to determine the vessels resistance. The emission calculation according to the method described in Chapter 3, is performed individually for each trip to determine the emission of a single vessel in time and space. The emission outcomes can be assessed individually or can be projected on the FIS network to derive emission distribution patterns.

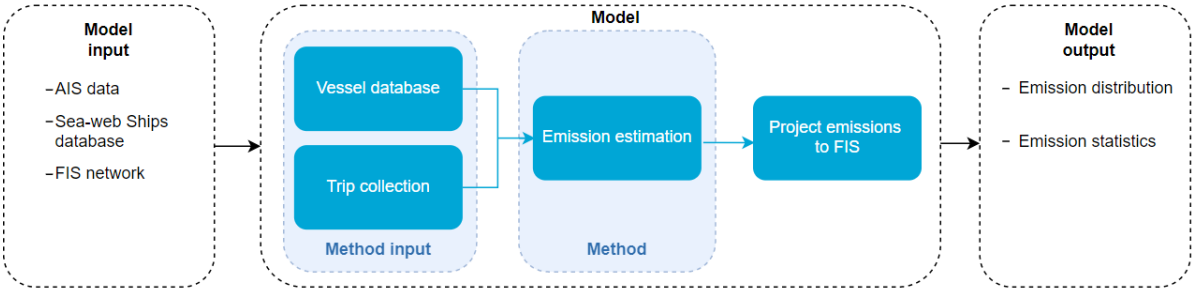

Figure 4.1: Overview of the model

4.1. Model input

4.1.1. AIS data and AIS data processing

Each vessel from 300 GT and larger is obligated to have an AIS transceiver onboard. From this transceiver an AIS message is send to an AIS base station with intervals of several seconds for moving vessel up to intervals of 3 minutes for anchored vessels. This message contains a timestamp, the MMSI-number (a unique identification number) of the vessel, and other information about the vessel and its activities such as heading information, position (latitude and longitude), speed over ground, and rate of turn.

The AIS data used in this research is provided by the engineering company Royal HaskoningDHV (RHDHV) which extracts it from AISHub. AISHub is a platform which gathers and saves AIS data of around 700 base stations and supplies that data freely as long as you submit at least one continuous data feed. Subsequently this raw data is cleaned by rules from AISHub and Vesselfinder. Vesselfinder is also a vessel tracking service provider. Cleaning means erroneous entries are filtered out such as invalid MMSIs, invalid latitudes/longitudes

and improbable speeds or travel distances. The filtered dataset is coupled by MMSI-number to vessel data supplied by Lloyd's List Seasearcher (updated monthly) and the IHS Markit – Sea-web (latest update in 2018).

To extract the AIS data from the RHDHV-platform a polygon must be drawn on a map. The size of the polygon must cover the complete port area of interest. Furthermore a time interval must be chosen in days. The extracted data contains the following fields of which only the 'True heading' will not be used in this research:

- MMSI-number
- Latitude [deg]
- Longitude [deg]
- Course over ground [kn]
- Speed over ground [kn]
- True heading [deg]
- Vessel type
- Sub category
- Main category
- Dead weight tonnage [t]
- Draught [m]
- Length overall [m]
- Breadth [m]
- Received at [YYYY-MM-DD hh:mm:ss.sssssss]

Timestamp, distance and calculated speed
The AIS data is sorted, filtered and enriched before it is used in the model. First the data is sorted by MMSI and timestamp. Next, a column 'Δt' (the time between two succeeding stamps), a column 'distance' (the distance between two succeeding latitude and longitude points) and a column 'calculated speed' (the distance divided by Δt) are added to the AIS dataframe. The calculated speed is necessary since practice shows that the speed over ground (SOG) logged in the AIS data contains some errors. For computations throughout the model the calculated speed is maintained as correct speed. Even though speed outliers are filtered out by the RHDHV AIS platform, a second check on speed outliers is performed based on the calculated speed. Calculated speeds over 40 km/h are filtered out, since these speeds are unrealistically high.

Vessel type
This research takes in many vessel type dependent values based on research of the IMO. However, the vessel type classification of RHDHV does not coincide with the vessel type classification of IMO. Therefore, the next AIS data processing step is translating the vessels classification of RHDHV to the vessel classification of the IMO. Based on the 'vessel type', 'sub category' and 'main category' of RHDHV, a final vessel type is allocated to each vessel. All vessels are divided following the classification from Table 4.1. The vessel types considered in the research are stated in the first column, with their corresponding vessel categories maintained by RHDHV in the other columns. If the main and sub category assigned by RHDHV (and in the case of 'Passenger ships' also the vessel type assigned by RHDHV) match the ones stated in the table, the considered vessel gets assigned the final vessel type stated in the first column. All vessels which do not match with the categories taken into account in this research, are filtered out.

Vessel type IMO	Main category RHDHV	Sub category RHDHV	Vessel type RHDHV
Bulk carriers	Bulk carriers	Bulk dry, Bulk dry/liquid, Other bulk dry, Self discharging bulk dry	
Oil tankers	Tanker	Oil	
Chemical tankers	Tanker	Chemical	
Liquefied gas tankers	Tanker	Gas tankers	
Container ships	Dry cargo/Passenger	Container	
General cargo ships	Dry cargo/Passenger	General cargo	
Passenger ships	Dry cargo/Passenger	Passenger	Ferry, Hydrofoil, Passenger ship, Passenger vessel (unspecified)
Passenger ships - Cruise	Dry cargo/Passenger	Passenger	Passenger (cruise), Passenger/cruise
Ro-Pax ships	Dry cargo/Passenger	Passenger/Ro-Ro cargo	
Tugboats	Miscellaneous	Towing/Pushing	

Table 4.1 Vessel type classification

4.1.2. Fairway Information System (FIS)

A Fairway Information System is a dataset of nodes and edges, with each edge representing a simplification of a fairway section. The edges and nodes can contain information about the fairway section. The characteristics of importance for this study are the depth and length of the fairway section (the edge). The length is known of each edge, the depth however is difficult to derive. The water depth is dependent of time. This means only average water depths are available, which is considered good enough for this study. Neglecting this time dependence means that the results are less reliable.

When working with an existing FIS graph, a processing step is to filter out the unnecessary edges. A polygon is determined around the port area and all edges falling outside this polygon are removed from the graph. The down-scaling of the FIS graph is done to save computational time.

If no existing FIS graph is available, it is also possible to create one by hand. This is a generic procedure and can be done for each port around the world. The edges and nodes can be drawn on the map of the port in for example Google Earth or GIS software, generating a shape-file. In the case study in Chapter 6 an example is presented on how to construct a FIS graph. Due to it's ease of use, Google Earth is used in this example.

4.1.3. Sea-web Ships database

The Sea-web Ships database contains information of over 200,000 vessels of 100 GT and above and the database is updated daily

To create a vessel database, this database is coupled to the AIS data based on matching MMSI-numbers to assign each vessel the following characteristics from the Sea-web Ships database:

- **Deadweight tonnage:** The weight in tonnes of cargo, stores, fuel, passengers and crew carried by the ship when loaded to its maximum draught. This characteristic is only assigned if it is missing in the AIS data.
- **Number of screws:** The number of main engines.
- **Build year:** The year of delivery of the vessel.
- **Installed engine power:** The installed power output of the main engines in kW.
- **Fuel type 1 and Fuel type 2:** The IHS database has two categories for the fuel type of the vessel: 'Fuel Type 1' and 'Fuel Type 2'. The first fuel type is the lightest fuel type registered to the vessel. To illustrate:

Fuel Type 1	Fuel Type 2	Remarks
MDO	HFO	MDO is lighter than HFO
LNG	MDO	LNG fuel is lighter than MDO

  The considered fuel types in the database are: HFO, MDO, LNG, nuclear, coal and methanol.
- **Engine type:** The four possible engine types entries are 'oil', 'gas', 'turbine' and 'reciprocating'. 'Oil' signifies all oil engines. They are internal combustion engines that use compressed air and fuel for combustion. 'Gas' signifies all gas turbines. They use high energy fuel that is burned in the combustion chamber with compressed air. 'Turbine' signifies all steam turbines. They use energy from pressurised steam and not directly from fuel. 'Reciprocating' signifies all steam reciprocating utilises non-combustion heat sources, such as solar and nuclear where water turns to steam in a boiler and reaches a high pressure.
- **Engine stroke type** Ships are fitted with either 2 stroke or 4 stroke engines. Other stroke types are possible but these are exceptional and the database does not cover these.

4.2. Model

When the input of the model is defined, the method to estimate emissions must be implemented in the model. The model contains several algorithms to determine the emissions. To do this, the developed model consists of the following steps:

A) Create a vessel database
This database contains all the vessel characteristics needed to estimate the emission of a vessel.

B) Create a trip collection
This collection contains the sailed routes of all the individual vessels present in the AIS data.

C) For each trip in the trip collection:

1) Project AIS points on edges of FIS network
This couples the fairway characteristics to each AIS message.

2) Retrieve water depths and fairway lengths
The water depth is required in the resistance calculation. The length of the fairway is required to project the emissions in terms of gram per meter fairway.

3) Determine the energy consumption of the auxiliary engine
Here the steps of the method are followed:

i. Determine distance to destination (based on AIS data);
ii. Determine operational mode;
iii. Determine energy consumption of the auxiliary engine based on IMO data.

4) Determine the energy consumption of the main engine
Here the steps of the method are followed:

i. Filter for operational mode “manoeuvering” or “sailing”;
ii. Calculate resistance and main engine power according the method described in Section 3.2.2.

5) Calculate emissions (main engine and auxiliary engine)
The emissions of the main and auxiliary engine are calculated and summed up according the method in Section 3.1

D) Project emissions from trips on FIS network
Each emission is coupled to a fairway section in step C1), these are summed up and divided by the fairway length to provide the total emissions per meter faiway on each fairway section and plotted on a map.

These are the steps which will be maintained throughout the case studies in the next chapter. First, the steps will be described in more detail in the following sections.

4.2.1. Create a vessel database

All vessels present in the filtered AIS data are put in a vessel database. This database holds all the characteristics and parameters for each vessel which are not time-dependent. This database will be connected later on to the AIS data by MMSI-number in the emission calculation.

The vessel database will take the following form: the MMSI-numbers are stated in the first column and behind each specific MMSI-number all the following vessel characteristics are stated:

- Deadweight tonnage [t]
- Draught [m]
- Length overall [m]
- Width [m]
- Vessel type
- Size category [dwt]
- Power auxiliary engine (berth, anchor, manoeuvre, sail) [kW]
- Block coefficient C_b [-]
- *Number of engines [units]*
- *Build year*
- *Installed main engine power [kW]*
- Fuel type main engine
- Fuel type auxiliary engine
- Engine type main engine
- Engine type auxiliary engine
- *Engine speed [RPM]*
- Year category
- Tier
- $S_{app}(1+k_2)$
- Base hourly fuel consumption of the main engine [g fuel / kWh]
- Base hourly fuel consumption of the auxiliary engine [g fuel / kWh]
- Base emission factor for each emission product for the main engine [g / kg fuel] or [g / kWh]
- Base emission factor for each emission product for the auxiliary engine [g / kg fuel] or [g / kWh]

The vessel dimensions, vessel type and size category are present in the AIS data. All italicized characteristics are derived from the Sea-web Ships database based on matching MMSI-numbers. The auxiliary engine power

values while berthing, anchoring, manoeuvring and sailing are derived from the tabel in Appendix B. The remaining characteristics are determined according different methodologies. Their derivations can be found in Section A.1 and Appendix C.

When too little information about the vessel is available, some characteristics are impossible to determine. These are filled in with a statistic approach. Based on the Sea-web Ships database, statistics are derived specific to each size category of each vessel type. This data is used to fill in missing entries in the vessel database from vessels of the same type and size. The results of the statistic analysis and the procedure to fill in the missing entries can be found in Appendix D.

4.2.2. Create a trip collection

The AIS data is split up in trips with the Python package MovingPandas. For each unique vessel the package reads the sailing route based on the AIS geometry, called a trajectory. Trajectories shorter than 1 km are considered unrealistic and are rejected. Subsequently the remaining trajectories are split up in trips. Again trips shorter than 1 km are rejected.

The cutting up in trips is based on the time a vessel is lying still and the engines are turned off. This can be when a vessel is at berth to load or unload, or this can be when a vessel is waiting somewhere for example to enter the port. Practice and research from van Zwieteren (2020) show that when a vessel is waiting less than 30 minutes, the captain keeps the engines idling. The emissions during this idling need to be included. When a vessel is laying still for longer than 30 minutes, the engines are most likely switched off. To not take any emissions into account when the engines are switched off, the trips are split when a vessel is laying still for more than 30 minutes. If the vessel then resumes its route, this is considered a new trip.

This step produces a dataframe for each individual trip containing all timestamps, the vessel's MMSI-number and the draught, speed and location of the vessel.

4.2.3. For each trip in trip collection

When the AIS data is split into trips, the emissions can be estimated. This is done according the method from Chapter 3 which consists of a few steps. Each of the steps will be explained in chronological order.

Project AIS points on edges of FIS network

To add the fairway characteristics to the route of the vessel, the route is coupled to the FIS network. This is done by adding to each timestamp, the closest edge of the FIS network corresponding to the coordinates of the vessel. This creates an extra column with FIS edges for each trip-dataframe in the trip collection.

Retrieve water depths and fairway lengths

Each edge of the FIS network contains characteristics of the fairway. The water depth stated under 'GeneralDepth' is taken as the depth at that current timestamp, the length stated under 'Lenght_m' is used for the length of the fairway section. The depth is necessary for determining the resistance of the vessel. The length is needed later on in the model to express the emission in grams per meter fairway section. These values are added to the trip-dataframe.

Determine the energy consumption of the auxiliary engine

The energy consumption of the auxiliary engine is dependent of the vessel type and size category (derived from the vessel database) and of the operational mode the vessel is operating at. The operational mode is in turn dependent of the speed and the distance to destination. The speed is derived directly from the AIS data. The distance to destination needs to be determined. The following steps are needed to determine the auxiliary engine power consumption:

1. Determine distance to destination (based on AIS data)
   The first step is to determine the location of the destination. This is done by taking the latitude and longitude of the first and last AIS message of the trip. The location at which the vessel speed is smaller than or equals 0.5 knots is considered to be the destination. At this location is is assumed that the vessel is laying still at berth. The other location, at which the speed is larger than 0.5 knots, is the point where the vessel enters the AIS domain. To determine the distance to the destination at a certain timestamp, the distances of all the AIS messages from that timestamp until the destination timestamp are summed up.
2. Determine operational mode

The operational mode depends on the speed and distance to the destination. The speed is derived directly from the AIS data (calculated speed) and the distance to the destination is determined in step one. In this step an operational mode gets assigned based on the criteria from Table 3.1.

3. Determine energy consumption of the auxiliary engine
The energy consumption of the auxiliary engine is based on data from the IMO. These values can be found in Appendix B. Each timestamp is assigned an auxiliary engine power value in kW based on the operational mode of that timestamp.

Determine the energy consumption of the main engine
If at the considered timestamp the operational mode is 'berthing' or 'anchoring' the power estimation of the main engine is set to zero. When the operational mode is 'manoeuvring' or 'sailing' first the resistance is calculated according the method from Holtrop and Mennen subsequently the energy consumption is determined according Section 3.2.2. Summarizing, the following steps are performed:

1. Filter for operational mode "manoeuvering" or "sailing"
2. Calculate resistance and brake horse power

Calculate emissions (main engine and auxiliary engine)
The emissions for all four types of emission products are calculated separately. For the energy based emission products (NO_x and PM_{10}) this is done according in the following steps:

1. Calculate emissions of the main engines
From the vessel database the base emission factor of the main engine of the vessel is derived ($EF_{ME,base}$). This is equal to the total emission factor ($EF_{ME,total}$). Per timestamp the total emission factor is multiplied by the power consumption of the main engine.
2. Calculate emissions of the auxiliary engines
From the vessel database the base emission factor of the auxiliary engine of the vessel is derived ($EF_{AE,base}$). This is equal to the total emission factor ($EF_{AE,total}$). Per timestamp the emission factor is multiplied by the power consumption of the auxiliary engine.
3. Add up the emissions of the main and auxiliary engines
The emissions of the vessel per timestamp are the emissions of the main engine and auxiliary engine summed up. This is added as an extra column to the dataframe of each trip.

For the fuel based emission products (CO_2 and SO_x) this is done according in the following steps:

1. Calculate emission of the main engine
From the vessel database the base emission factor ($EF_{ME,base}$) and the base hourly fuel consumption ($HFC_{ME,base}$) of the main engine of the vessel are derived. Per timestamp the total hourly fuel consumption is determined by multiplying the base hourly fuel consumption by the correction factor for the engine load which differs per timestamp. To determine the correction factor, the main engine load is determined by dividing the calculated horse brake power of every timestamp by the installed engine power of the vessel stated in the vessel database. The main engine load is then filled in in Equation 3.13. With the base emission factor and the total hourly fuel consumption known, the total emission factor ($EF_{ME,total}$) is determined according Equation 3.9. For each timestamp the total emission factor is multiplied by the power consumption of the main engine to calculate the emission of the main engine.
2. Calculate emission of the auxiliary engine
From the vessel database the base emission factor ($EF_{AE,base}$) and the base hourly fuel consumption ($HFC_{AE,base}$) of the auxiliary engine of the vessel are derived. When considering auxiliary engines, the base hourly fuel consumption is equal to the total hourly fuel consumption. With the base emission factor and the total hourly fuel consumption known, the total emission factor ($EF_{AE,total}$) is determined according Equation 3.9. For each timestamp the total emission factor is multiplied by the power consumption of the auxiliary engine to calculate the emission of the auxiliary engine.
3. Add up the emissions of the main and auxiliary engines
The emissions of the vessel per timestamp are the emissions of the main engine and auxiliary engine summed up. This is added as an extra column to the dataframe of each trip.

4.2.4. Project emissions from trips on FIS network

The emissions are estimated per trip in the trip collection. The next step is now to project the sum of all trips on the FIS graph. This means assigning each edge of the graph the emission results of all four emission

products in g/m. The edges of the FIS graph are filtered out one by one and compared to the (closest) edge of each timestamp of each trip in the trip collection, when a match is found the emission of that timestamp is added to the total of emissions on that edge.

4.3. Model output

4.3.1. Emission distribution

The results of the model will be displayed as a projection on the FIS graph. By coupling them to the FIS graph instead of plotting all AIS data points, the emissions can be addressed per fairway section and more accurate insight in the emissions distribution is delivered. The emissions are visualised by plotting each edge according an assigned color scale related to the sum of emissions in g/m. Displaying the emissions per meter fairway, is to avoid that long fairway sections show high emissions due to the fact that vessels spend more time on this section. The emission totals can be plotted or the emissions of one single trip or vessel can be plotted.

4.3.2. Emission statistics

Besides the emission distribution, also some characteristics of the total emissions can be derived. The sum of the emissions of all timestamps of all trips shows the total emissions. Additionally, a split in emissions based on operational modes can also be derived. This can be done by adding up the emissions of all timestamps with the same operational mode. The same way, a split in emissions based on vessel types can be derived.

4.4. Implementation of emission reduction strategies

With the model output known, strategies to reduce emissions van be proposed. To determine the exact strategy a thorough port analysis must be done, which is a research subject on its own. However, once an emission reduction strategy is determined, the developed model can be of added value to determine a good first quantification of the emission reduction.

The model takes in real-time AIS data, however it also has the capability to take in simulated AIS data of a fictive fleet. Due to the scope of this research, setting up a simulation is too comprehensive so to demonstrate reduction strategies another approach is used. Since a bottom-up model is created, which deviates between operational modes, very detailed modifications can be made to the model to simulate measures on the real-time fleet. Specific vessel types can be modified, but also for example all vessels at berth can be modified, or a combination of the two options. These groups are then excluded from the model, which will create a fictive fleet but with unaltered AIS paths. These fleet adjustments may lead to changes in the behaviour of vessels. This is neglected with the current approach, but this could be modeled in an extensive simulation as mentioned earlier. The current approach will be explained by means of certain reduction strategies.

Alternative fuels and energy

The fuel type of the vessel is of large influence on the emissions of the vessel. The model takes in a fuel type specifically assigned to each individual vessel and the unknown fuel types are filled in based on statistics. Now the regulations around fuel characteristics are tightening, a shift in fuel types can be expected. If knowledge around these shift is obtained and a statistical forecast is available, this can be implemented in the model by overruling the assigned fuel types to a certain simulated fuel type distribution. This possibility is also applicable to just one specific vessel type or vessel.

Widely studied subjects in this field are the use of hydrogen as a fuel and battery-powered vessels. Regarding the zero emissions goal, these systems have a lot of potential since the combustion of hydrogen produces zero CO_2 emissions, minimal NO_x and PM_{10} emissions (Port of Antwerp Bruges, 2022) and the battery-powered vessels even zero (The Maritime Executive, 2022b). This is specifically interesting in ports, since with the current technology the batteries can only store enough energy for short voyages (hydrogen energy is also stored on batteries). This is why the first hydrogen and battery-powered vessel types are mostly ferries and tugboats, which mainly operate in ports. Recently the first zero-emission tugboats and ferries are launched in the ports of San-Francisco, Navia, Antwerp and Westhafen. This is an interesting reductions strategy to investigate in this research. Since the model differentiates between vessel types, it is possible to simulate a switch of a normal tugboat fleet to a zero-emission tugboat fleet, by omitting all tugboats from the model since their emissions will be zero. The model with tugboats can be compared to a model without tugboats, and a first estimation of the emission reduction can be quantified.

Another reduction measure gaining popularity, is the use of shore power (also known as cold-ironing). Nowadays, an increasing number of ports are supplying shore power or consider installing shore power. While at berth, vessels can plug into electrical power from shore to take over the power supplied by the auxiliary engines to save fuel and reduce emissions. By focusing on the power consumption of vessels at berth a shore-power scenario can be simulated with the developed model, where all vessels or certain vessels or vessel types can be connected to shore power. The altered model can be compared to the unaltered model, and this way the reduction in emissions can be quantified.

Legislative measures
It is also possible to simulate legislative measures, like emission limits and regulations. For example, only allowing vessels in the port with certain engine certifications. A widely used measure in this category is the speed limit. According Faber et al. (2017), limiting the maximum speed of the global fleet with 10%, reduces the greenhouse gas emissions by 13%. This measure is interesting when investigating fairways, but not so much when looking into ports since the speed in ports is already limited.

Of more interest considering ports, is the application of ECAs. Figure 4.2 shows the current ECAs and the discussed ECAs. From this can be shown that many coastlines are currently considering ECA limits, among which the Black Sea area. This inspires interest, as our second case study is concerning a port located on the coast of the Black Sea. The model is capable of quantifying the difference in emissions when ECA limits apply or not. When applying ECA limits, the sulfur content of the fuel is influenced. This can be varied in our model. The fuel type allocation procedure of the model also changes, simulating the switch in fuel types vessels will be making when entering an ECA.

Figure 4.2: Current and discussed ECAs (Source: Karimpour (2018))

Ship design
A possible way to reduce emissions, is optimizing the ship design. This can be categorized in two parts: optimizing the hull and optimizing the engine system. By improving the hull, the hydrodynamic performance can be improved and the resistance will decrease, leading to lower emissions. By improving the engine system, the efficiency can be increased and so emissions can be decreased. The model takes in certain hull design values (such as the block coefficient and the appendages design), to calculate the resistance. These values can be altered based on new experiments, however there is no direct way to alter these to simulate a more efficient hull design. The method makes use of several assumptions to incorporate engine efficiencies. These are incorporated in the method, such as the engine load correction factor, or processed in for example the emission factors. For both goes that it is difficult to do alterations to these values to simulate improved engine efficiencies in a quantitative matter before doing extensive research. They can however, be updated after additional testing or new insights as long they are of the same form.

Economical changes
To evaluate emission reductions due to economical changes such as an increase or decrease in traffic intensity, changes in fleet composition or shifts between cargo types, a new fictive fleet must be set up. The same goes for changes in cargo handling times or waiting times. This is not part of this research. However, once a fleet simulation is done, the simulated fleet can be implemented in the model and the emission estimation can be performed. The simulated fleet must include the position and speed of the vessel at certain timestamps and the vessel characteristics specified in Section 4.1.1.

II

Results

5

Case study Port of Rotterdam

5.1. The case

With a surface area of approximately 126 km^2 (including Maasvlakte 2) and an average annual throughput of 450 million tonnes of cargo, the port of Rotterdam is Europe's largest port. It is strategically located at the gateway of the inland waterway network of Europe and has the equipment to handle almost every cargo type (Port of Rotterdam, 2021).

The port is directly connected to the North Sea and is located inside an ECA. For the developed model this means that all ships are sailing on their lightest fuel type. It also influences the maximum allowed sulphur content in the fuel, which is inside ECA's 0.10% m/m.

5.2. Model input for case study - Port of Rotterdam

The first step of the case study is to set up the model input. This consists of three important components stated in Section 4.1, which will be addressed.

AIS data and AIS data processing

For this case study two AIS data sets are used: data of the first two weeks of June 2021 (01/06/2021 00:00:00 - 14/06/2021 00:00:00) and data of the first two weeks of January 2022 (01/01/2022 00:00:00 - 14/01/2022 00:00:00). This way the emissions during summer and during winter are observed. To enrich the AIS data, the Δt, distance, calculated speed and vessel types are added. For the scope of this research, not all vessel types are taken into account. The vessels falling outside the ten vessels types stated in Section 2.4 are filtered out. For the two weeks in June 1137 vessels are remaining, and for the two weeks in January 836 vessels are remaining. Figure 5.1 shows how many vessels of each vessel type are present in the filtered AIS data.

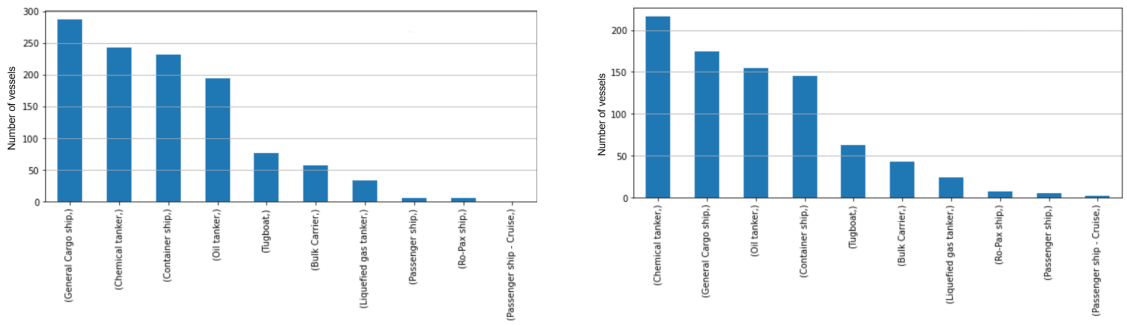

(a) Vessel types in Port of Rotterdam June 1 - 14 2021

(b) Vessel types in Port of Rotterdam January 1 - 14 2022

Figure 5.1: Number of vessels per vessel type after AIS data filtering

Fairway Information System (FIS)
Use is made of an existing FIS graph of the Dutch fairway system. The graph is developed by de Jong et al. (2021) and is open source. From this graph only a polygon is drawn around the area of the Port of Rotterdam and only the edges falling inside this polygon are observed. The down-scaling of the FIS graph is done to spare computational time.

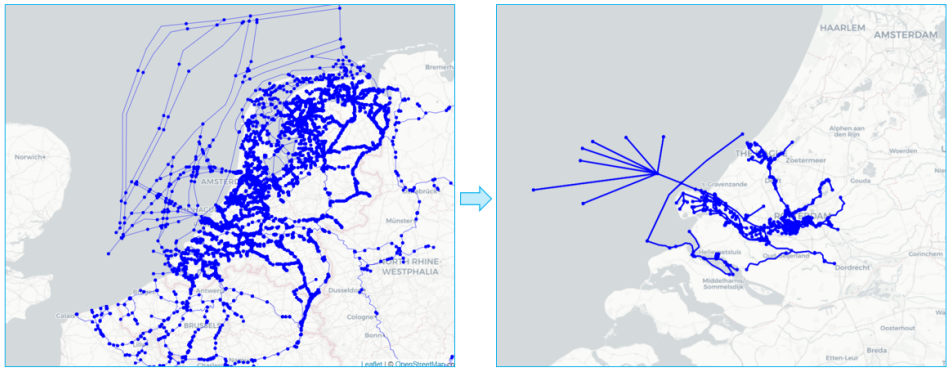

Figure 5.2: FIS graph from de Jong et al. (2021) reduced to FIS graph of Port of Rotterdam area

Sea-web Ships database
The Sea-web Ships database is extracted in April 2022.

5.3. The case study model - Port of Rotterdam

The steps from Section 4.2 are followed to create the model. The steps are repeated below with some remarks specific for this case study.

A) Create a vessel database
First the vessel database is drawn up. Each vessel with an unique mmsi-number is filtered out and its characteristics are complimented with data from the Sea-web Ships database. After this, the missing entries are filled in. A fragment of the vessel database can be found in Section E.1.1 for illustration.

B) Create a trip collection
The enriched AIS data is cut up in trips according the procedure of Section 4.2.2. An example of one trip from the trip collection can be found in subsubsection E.1.2.1.

C) For each trip in the trip collection:

1) **Project AIS points on edges of FIS network and retrieve water depths and fairway lengths**
The closest edge and its water depth and length is assigned to all AIS timestamps. If the FIS graph contains a water depth for the edge, this value is used in the emission calculations. If the water depth is unknown, the average water depth of the Port of Rotterdam is assumed, which is approximately 20 meters (World Port Source, 2022).

2) **Determine the energy consumption of the auxiliary engine**
This step adds a column with the location of the destination, the operational mode and the energy consumption of the auxiliary engine to the trip dataframe. An example of one trip from the trip collection with the auxiliary engine power added can be found in subsubsection E.1.2.2.

3) **Determine the energy consumption of the main engine**
This step adds the emissions from the main engines to each timestamp of the trip dataframe.

4) **Calculate emissions (main engine and auxiliary engine)**
Here the emissions of the main and auxiliary engines are added up. An example of one trip from the trip collection with the emissions of all four emission types in g and in g/m can be found in subsubsection E.1.2.3.

D) Project emissions from trips on FIS network
Now the FIS graph can be plotted with the colors of the edges indicating the amount of of emission on that edge. The results are shown in the next section.

5.4. Model output - Port of Rotterdam

5.4.1. Emission statistics

To state the results from the case study in yearly averages, the results of the emission estimation outcomes of the two weeks in January and the two weeks in June are summed up (this gives a 26 days average). This is translated to a daily average by dividing by 26 and this is translated to a yearly average by multiplying by 365. The results are stated in Table 5.1 below. The CO_2 emissions in the port are approximately 222,000 tonnes per year, which equals the emissions of 950,000 return flights from London to Rome (Kommenda, 2019). In the Netherlands, according Our World in Data (2022b) in 2018 approximately 47.17 mega tonnes CO_2 emissions came from shipping and aviation. With our emission estimation, the port of Rotterdam would contribute 0.5% to this. With the Port of Rotterdam being one of the largest ports worldwide, this seems rather small. The port area of interest is determined by drawing a polygon and a time span of two weeks is maintained. These two variables, makes a great difference in the final results. If few calls or short stops occur in these two weeks, this is magnified when translating this to yearly averages.

When comparing the emission from June with January, the emissions in June are higher. This could be the result of seasonal and economical influences causing oscillating throughput and traffic intensities. The Port of Rotterdam states that the throughput has decreased in the first quarter of 2022 (Port of Rotterdam, 2022c), which also agrees with the research of Nilsson et al. (2018), who observed a higher density of ship traffic over the North Sea for the summer season.

	Total CO_2	**Total** SO_x	**Total** NO_x	**Total** PM_{10}
Total emissions two weeks January	2864.17	0.97	55.20	0.86
Total emissions two weeks June	12951.95	4.37	244.36	3.83
Estimated daily emission	608.31	0.21	11.52	0.18
Estimated yearly emission	**222033.91**	**74.94**	**4205.34**	**65.84**

Table 5.1 Estimated emissions in the Port of Rotterdam in tonnes

The emission types are contributing to the total emissions according the ratios stated in Table 6.2. This is comparable to the ratios derived by the research of Kauffman and Hulskotte (2021) calculating emissions in all ports in the Netherlands. The share of SO_x and PM_{10} emissions are somewhat lower then in 2019. This difference can be explained by the implementation of the 'IMO 2020 rule' in 2020, tightening the restrictions of the sulfur content of the fuel. Due to the lack of information around the scope of the research and the method, the quantitative numbers are not directly comparable.

	Total CO_2	**Total** SO_x	**Total** NO_x	**Total** PM_{10}
Model	98.08	0.03	1.86	0.03
Research of Kauffman and Hulskotte	98.48	0.07	1.40	0.06

Table 5.2 Share of emission type of total emissions [%]

Emission split in operational modes

The emissions per operational mode are evaluated and shown in Figure 5.3. This shows that for each emission type, the split between the operational modes is approximately the same. The largest share of emissions is produced in sailing mode. However, still around 22% of the emissions are produced at berth. Manoeuvring has the smallest contribution to the total emissions. The research of Starcrest consulting group LLC (2020a) shows approximately the same split between operational modes, as well as the research of Fu et al. (2017).

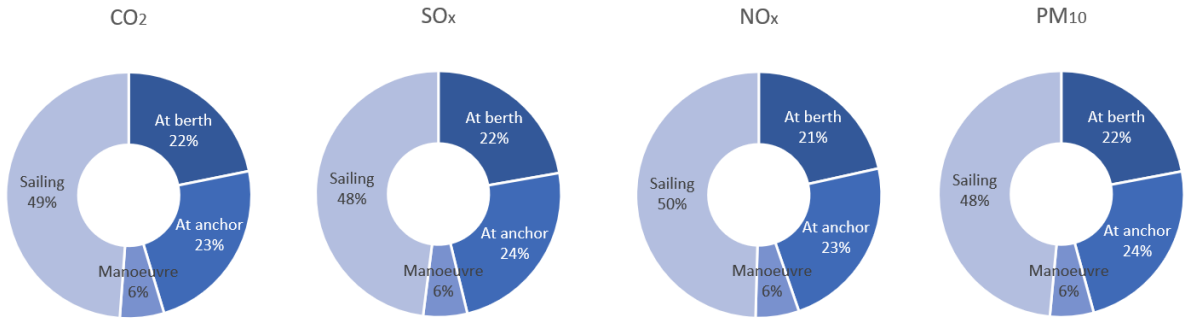

Figure 5.3: Percentage of emissions in each operational mode

Emission split in vessel types

To indicate the emission split per vessel type, their percentage of the total emissions are stated in Figure E.5. Only CO_2 is showed for simplicity, the split of the other three emission types is almost similar and can be found in Section E.2. The four vessel types which are most often visiting the port (see Figure 5.1) are responsible for the largest share of emissions. The contribution to the emissions of tankers seems rather large. This could very well be the case since the energy consumption of tankers at berth is large. However, in reality this share will probably be somewhat lower since the energy consumption of tankers at berth is very roughly estimated. To investigate this further, detailed research on the behaviour of tankers at berth must be performed.

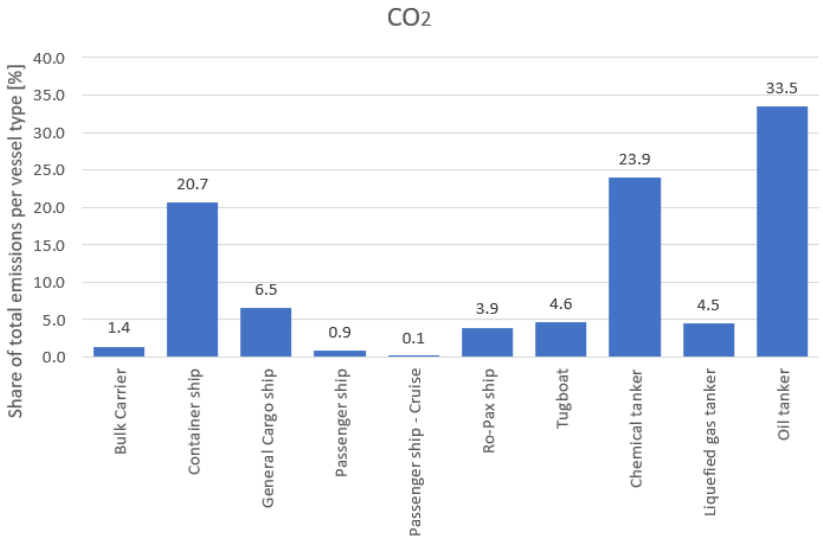

Figure 5.4: Emission split in vessel types in percentage of total emissions

5.4.2. Emission distribution

To get an insight in the emission pattern in the port, the emissions are projected on the FIS graph, see Figure 5.5, Figure 5.6, Figure 5.7 and Figure 5.8 for the results of the two weeks in June, the two weeks in January can be found in Section E.3.

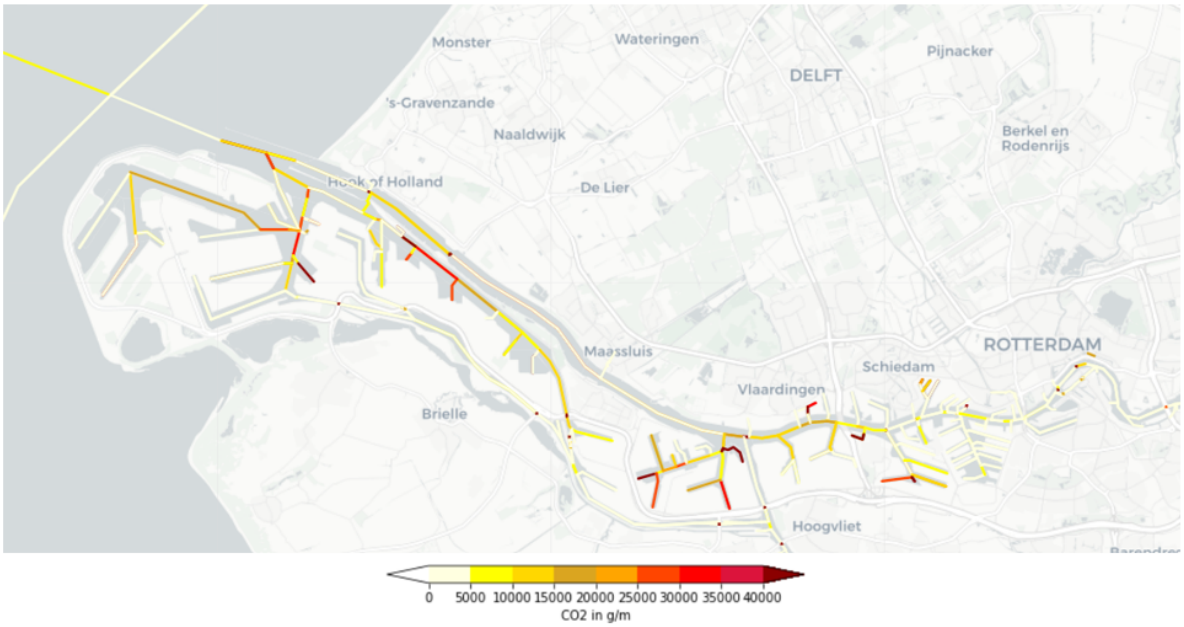

Figure 5.5: Estimated CO_2 emissions in the Port of Rotterdam from June 1 - June 14 2021

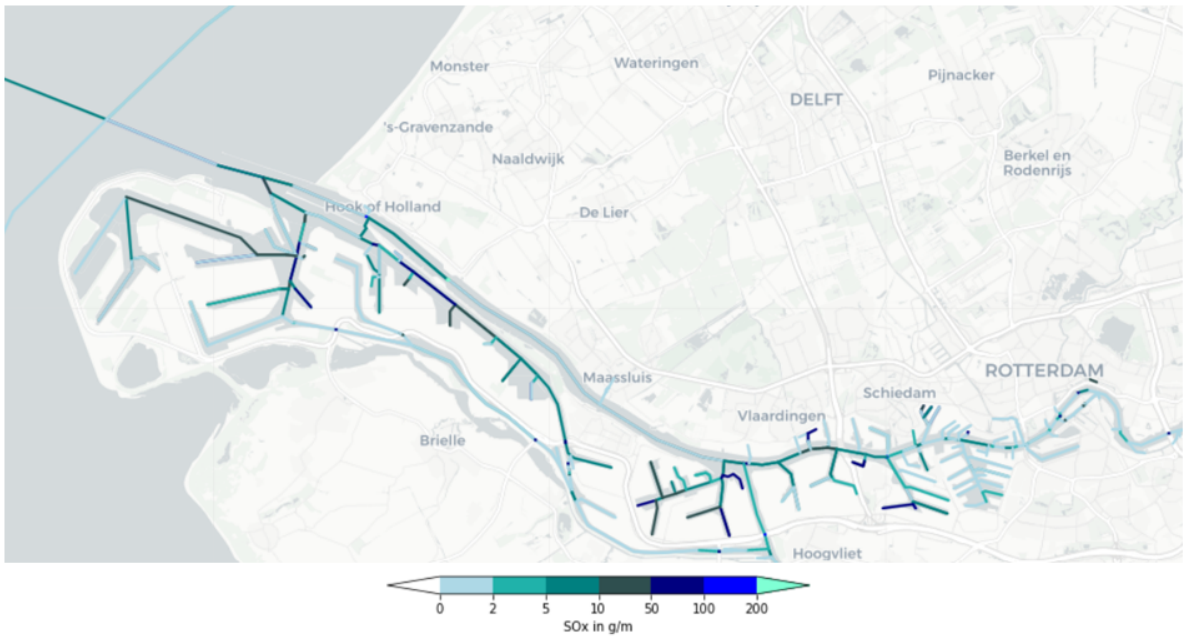

Figure 5.6: Estimated SO_x emissions in the Port of Rotterdam from June 1 - June 14 2021

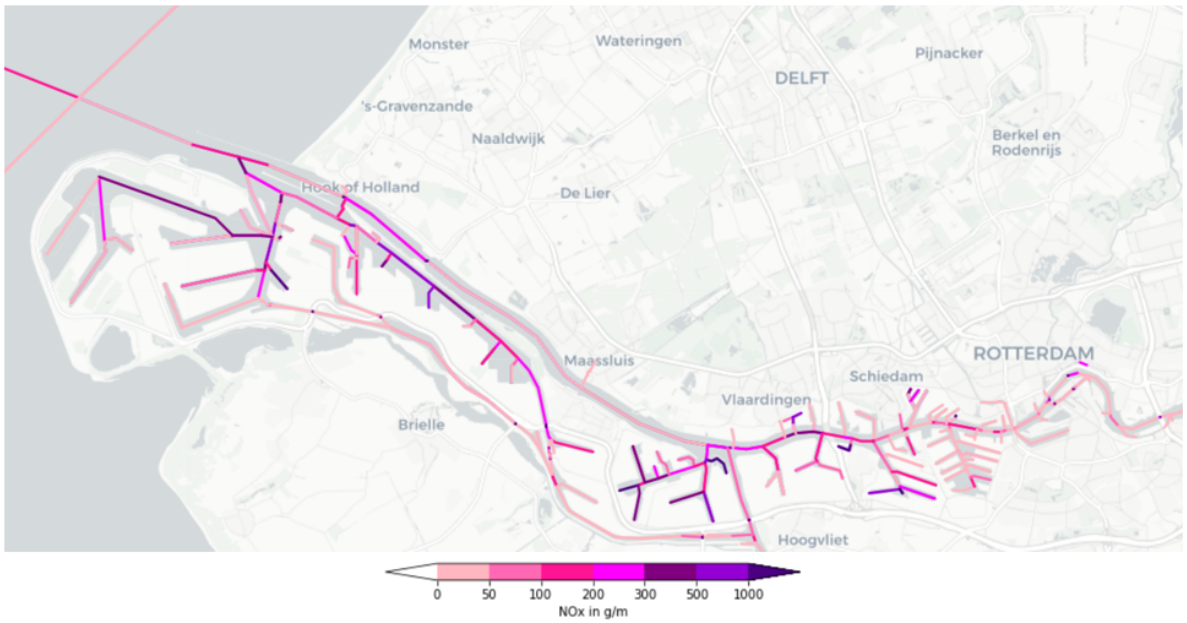

Figure 5.7: Estimated NO_x emissions in the Port of Rotterdam from June 1 - June 14 2021

Figure 5.8: Estimated PM_{10} emissions in the Port of Rotterdam from June 1 - June 14 2021

When comparing the graphs, all the emission types have the highest values at the same edges. In general can be seen that the main waterway through the port is not responsible for the large emissions, but the peaks occur at junctions of fairways and in certain port basins. The exception is the port entry. The entry of the port is a busy fairway, since all vessels are converging here. Due to the high traffic volumes, the emissions are relatively high at this spot. When zooming in, the edges immediately before and after junctions of fairway sections or port basin entrances to the main fairway are also showing high emissions (almost red-dots in Figure 5.5). The locally higher emissions, are probably due to the fact that vessels are slowing down when approaching a junction. Low speed causes main engines to operate at an inefficient stage and thus emit more per consumed kWh and the vessels spend more time on the fairway section also leading to higher emissions.

Low speed also causes the vessel to sail on the fairway section for a longer time and thus emit more. Next, the port basins with high emissions will be evaluated.

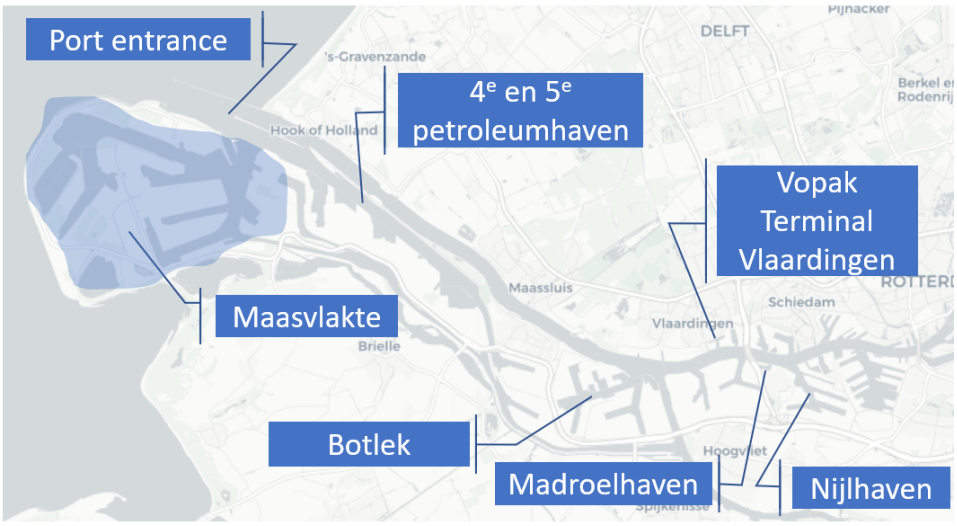

Figure 5.9: Location of the ports with the highest emissions

The Maasvlakte shows high emissions. This is one of the newest and largest deep-sea ports areas of the Port of Rotterdam. These terminals can host large container vessels, responsible for large emissions.

The 4e and 5e Petroleumhaven and the Nijlhaven are oil-terminals. These host large vessels, which take long to load and unload. Due to the their long berthing times these spots will show high emissions. A news article about the Nijlhaven LNG-terminal stated that the terminal was running on high capacity, since it was extraordinary busy due to the high oil prices (Port of Rotterdam, 2022b). This peak can be seen in the results of June 2021 where the edge is marked with high emissions.

The Botlek area contains mainly oil refineries and chemical industry. According Port of Rotterdam (2022a) this is one of the most busiest fairways of the Netherlands and can host very large vessels like the Aframax, Suezmax and Panamax, which typically emit more than smaller vessels. Due to the high traffic intensity and large vessels it is not surprising that this section is marked as an emission hotspot.

The Madroelhaven is mostly used by tugs (Rijksmuseum, 2001). Tugs are likely to drift around until they are needed somewhere in the port. This can cause high emissions since the main engines are always on. It is interesting to investigate the behavior of the vessels around these edge.

An emission hotspot is located at the Vopak Terminal Vlaardingen, which is mostly used for storing oils (Vopak, 2022). The company which owns the terminal recently announced that the terminal will be expanded, which indicates that the terminal is frequently used. The plausibility of an emission hotspot located in this stand-alone basin, will be examined a little further by down-drilling of the emissions. This demonstrates the fact that if exceptional emission patterns are discovered, the method is capable of indicating the source.

Down-drilling procedure Vopak Terminal Vlaardingen
The edge of the fairway section of interest is selected first. The trips of the vessels passing this edge are indicated and the exact AIS messages spend on this edge are established. This is summarized in Table 5.3. The table shows that Vessel #3 is responsible for the high emissions at this fairway section. The tanker has spend over 9 hours at the fairway section. When zooming in on the trip of this vessel, it shows that the vessel is drifting at a very low speed, see Figure 5.10. Following the decision matrix of the operational mode of a tanker (Table 3.1), this means the vessel is berthing. When a tanker is berthed, the auxiliary engine determines the emission and for tankers this is very high. The loading or unloading of this vessel takes over 9 hours and therefore causes locally a large amount of emissions. When the source of the emissions is known, a reduction strategy can be opposed. A possible solution to tackle this locally high emissions could be to connect the vessel to shore power or to shorten the load and unloading time.

Vessels 1,2 and 4 show other behaviour. The vessels have spend approximately half to one and a half hour in the port basin and account for a small amount of emissions. Vessel #4 has two trips passing this fairway section: trip 1 arriving at the basin and trip 2 is the next day leaving the basin. The model has cut up the trip in two trips, which is probably an accurate assumption since the engines of the vessel were most likely switched off during this overnight stay.

The down-drilling procedure shows that only one tanker is berthing for a long enough period to load and unload. While the Port of Rotterdam is a large port and more than one vessel is expected to load and unload in this basin in two weeks time. The basin only shows short visits, which do not account for large emissions. If this is a trend during these two weeks, this could also be a possible explanation for the low estimated yearly emissions discussed in Section 5.4.1.

Vopak terminal - edge (8867982,8864753)					
	Vessel #1	**Vessel #2**	**Vessel #3**	**Vessel #4 trip 1**	**Vessel #4 trip 2**
Start time of AIS message	31-5-2021 10:41:50+00:00	8-6-2021 16:16:21+00:00	6-6-2021 19:59:39+00:00	8-6-2021 22:19:51+00:00	9-6-2021 15:39:59+00:00
Vessel type	General Cargo ship	Chemical tanker	Chemical tanker	General Cargo ship	General Cargo ship
DWT	10,000-19,999	40,000-+	20,000-39,999	10,000-19,999	10,000-19,999
Duration [min]	56.65	85.03	552.12	37.20	29.95
Distance [m]	88.45	57.34	447.91	196.85	2.18
Speed [m/s]	0.03	0.01	0.01	0.09	0.001
CO_2 [g/m]	282.51	3781.20	27868.85	71.45	57.52
NO_x [g/m]	5.33	71.40	463.61	1.31	1.06
SO_x [g/m]	0.097	1.300	9.585	0.025	0.020
PM_{10} [g/m]	0.086	1.148	7.037	0.021	0.017

Table 5.3 Down-drilling of the emissions of the Vopak Terminal Vlaardingen

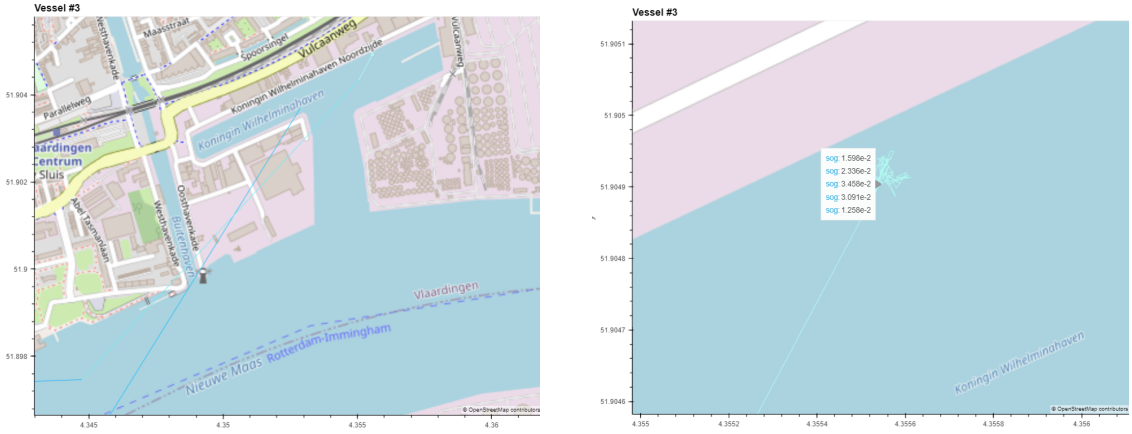

(a) Vessel #3 arriving and leaving

(b) Zoom in on vessel path of vessel #3

Figure 5.10: AIS trajectory of vessel #3 (color indicates speed)

6

Case study Port of Constanța

6.1. The case

The port of Constanța has a surface area of 40 km^2. This is almost four times smaller than the port of Rotterdam. The annual throughput of the port is estimated at 60.37 million tons (PortSEurope, 2021), which is about seven times smaller than the port of Rotterdam. The port of Constanța is sheltered by two breakwaters and has a strategic location close to two Pan-European transport corridors providing a good connection to the hinterland.

The port is located on the western-coast of the Black Sea. No emission control areas are located in the Black Sea, so no ECA limits apply in the port of Constanța. For the developed model this means that the fuel type a vessel is using in the port is the most economical fuel type they have onboard. It also influences the allowed sulphur content in the fuel, which is outside ECA's between 0.10% and 0.50 % m/m.

6.2. Model input for case study - Port of Constanța

The first step of the case study is to set up the model input. This consists fo three important components which will be addressed.

AIS data and AIS data processing

For this case study two AIS data sets are used: data of the first two weeks of January 2021 (01/01/2021 00:00:00 - 14/01/2021 00:00:00) and data of the first two weeks of June 2021 (01/06/2021 00:00:00 - 14/06/2021 00:00:00). This way the emissions during summer and during winter are observed. To enrich the AIS data three columns are added: Δt, distance and calculated speed. The next step is to filter out all the vessels out of the scope of the research. For the two weeks in January there are 209 vessels remaining, and for the two weeks in June 213 vessels. Figure 6.1 shows how many vessels of each vessel type are present in the filtered AIS data.

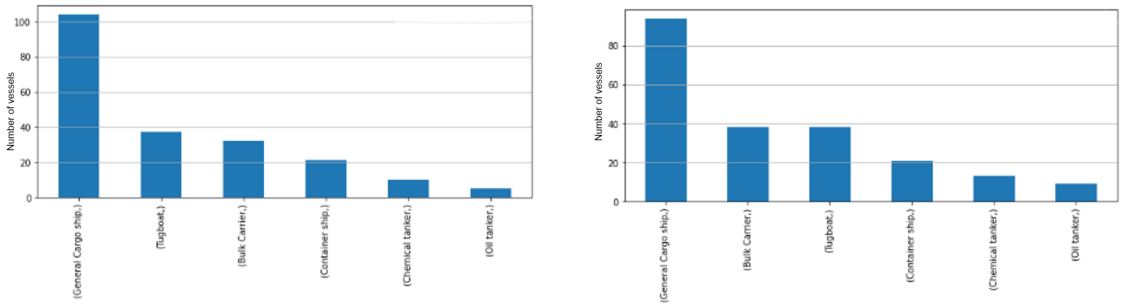

(a) Vessel types in Port of Constanța January 1 - 14 2021

(b) Vessel types in Port of Constanța June 1 - 14 2021

Figure 6.1: Number of vessels per vessel type after AIS data filtering

Fairway Information System (FIS)
No FIS graph is available for this study area, so a new FIS graph is set up manually. This is done by drawing a system of edges and nodes in the port in Google Earth. This creates a shape-file which will be translated with Python to a FIS graph. The graph contains information about the length of the edges. The Python code to create the FIS graph from the shape-dile can be found in Section F.1. The final FIS graph is shown in Figure 6.2.

According the Port Authorities of Constanța, tides in the black sea are negligible and the maximum water level variation due to extreme winds is 0.3 meters (Port of Constanta, 2022). Therefore, the water depth of the port is for simplicity assumed to be constant over time and space and no manually adding of the water depths to the FIS graph is needed. The average water depth of the Port of Constanța is assumed as constant water depth in the port. This is approximately 10 meters (Port of Constanta, 2022).

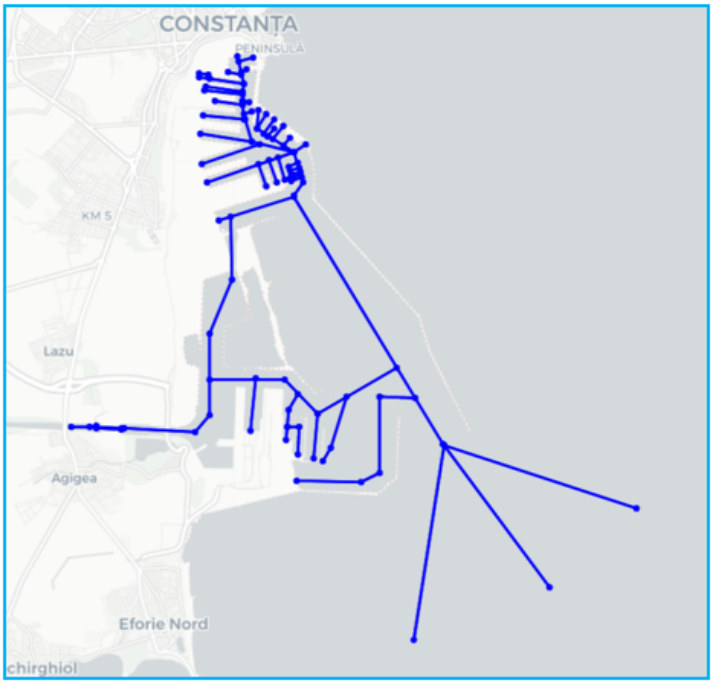

Figure 6.2: FIS graph of the Port of Constanța

Sea-web Ships database
This case study makes use of the same Sea-web Ships database extraction from April 2022 as the first case study.

6.3. The case study model - Port of Constanța

The steps from Section 4.2 are followed to create the model, in the exact same manner as described in the case study of the port of Rotterdam. The steps are stated below with some remarks specific for this case study. For this case study no example dataframes are presented, since the idea is the same as the example dataframes from the case study of the Port of Rotterdam.

A) Create a vessel database

B) Create a trip collection

C) For each trip in the trip collection:

1) **Project AIS points on edges of FIS network**

2) **Retrieve water depths and fairway lengths**
From the closest edge to the AIS data point the water depth and length are derived. This FIS graph does not contain any information about the water depths, therefore a constant water depth of 10 meters is assigned to each edge.

3) **Determine the energy consumption of the auxiliary engine**

4) **Determine the energy consumption of the main engine**

5) **Calculate emissions (main engine and auxiliary engine)**

D) **Project emissions from trips on FIS network**

6.4. Model output - Port of Constanța

6.4.1. Emission statistics

To state the results from the case study in yearly averages, the results of the emission outcomes of the two weeks in January and the two weeks in June are summed up (which gives a 26 days average). This is translated to a daily average by dividing by 26 and this is translated to a yearly average by multiplying by 365. The results are stated in Table 6.1 below. The yearly CO_2 emissions in the port are estimated at 110,500 tonnes. In Romania, according Our World in Data (2022a) in 2018 approximately 420,000 tonnes CO_2 emissions came from shipping and aviation. It seems reasonable that according the current emission estimation, the port of Constanța contributes 1/4 to this.

	Total CO_2	**Total** SO_x	**Total** NO_x	**Total** PM_{10}
Total emissions two weeks January	4273.19	9.43	134.07	2.26
Total emissions two weeks June	3596.29	4.72	66.59	1.14
Estimated daily emission	302.67	0.54	7.72	0.13
Estimated yearly emission	**110475.49**	**198.71**	**2816.93**	**47.65**

Table 6.1 Estimated emissions in the Port of Constanța in tonnes

The emission types are contributing to the total emissions according the ratios stated in Table 6.2. This is comparable to the ratios derived by the research of Florin et al. (2018) calculating the yearly emissions from shipping in the Port of Constanța in 2016. The absolute numbers are incomparable, due to the lack of information on the method and scope of the research.

	Total CO_2	**Total** SO_x	**Total** NO_x	**Total** PM_{10}
Model	97.30	0.18	2.48	0.04
Research of Florin et al.	95.66	1.53	2.60	0.22

Table 6.2 Share of emission type of total emissions [%]

Emission split in operational modes

The emission types split by operational modes are presented in Figure 6.3. The contribution of the vessels at berth and at anchor is exceptionally high.

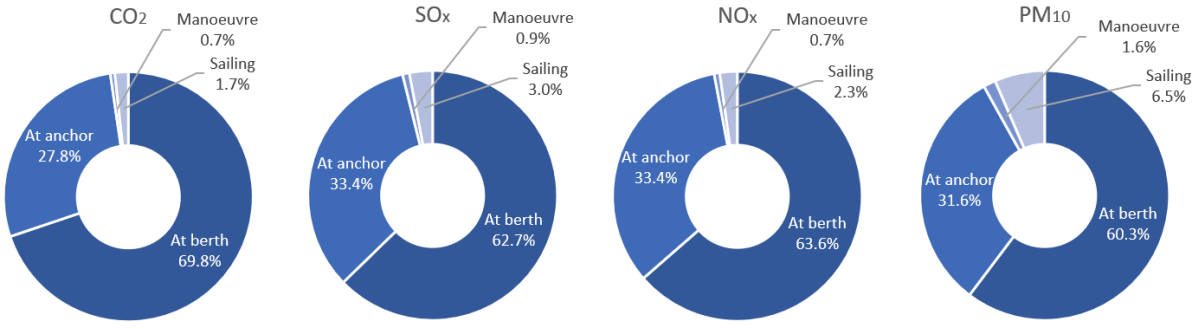

Figure 6.3: Percentage of emissions in each operational mode

The operational mode 'berthing' is assigned when the speed is below 0.5 knots and the vessel is within one nautical mile from its destination. When looking into the data the speeds from the AIS messages are very low. Figure 6.4 shows the average speed of each trip. All the speeds are close to zero, with some outliers. For

this reason, the model identifies approximately 60-70% of the emissions as coming from berthed vessels. The reason why all vessels have such low speeds is unknown, it could be that few vessel movements occur in the Port of Constanța and that the vessels are indeed laying still at berth. However, this many berthed vessels seems rather unlikely. It could also be the result of a disturbed AIS signal.

The other parameter influencing the operational mode is the distance to destination. When looking at Figure 6.4 one can see that the average distance to destination is also very small. This explains why so few vessels are categorized as manoeuvring or sailing, since these modes require a distance over one nautical mile (in combination with higher speeds). The port of Constanța is a small port compared to the port of Rotterdam where the model seems to identify the modes correctly. The length of the terminals is ranging between the 300 - 800 meters and the length of the port measured from the end point of the breakwater to the deepest point land inward is approximately 3000 meters (Google Earth, 2022). When the vessel is leaving berth and should be qualified as first anchoring and then manoeuvring or sailing, the vessel has already almost left the port by the time it reaches the required 1 to 5 nautical mile from destination. A new run with the same model but lowered limits of the distance to destination (1 nm lowered to 0.5 nm and 5 nm lowered to 1.5 nm), gave approximately the same operational mode distribution, which indicates that the main influence in this case must be the speed. This makes sense since the speeds must be over 3 knots to qualify as manoeuvring or sailing at all. The down-drilling ability of the model is used to check several randomly selected vessel trajectories for irregularities. These trajectories and a short elaboration on these trajectories, can be found in Section F.2. They all show very low speeds. Half of these randomly selected trips, show very short trip-lengths.

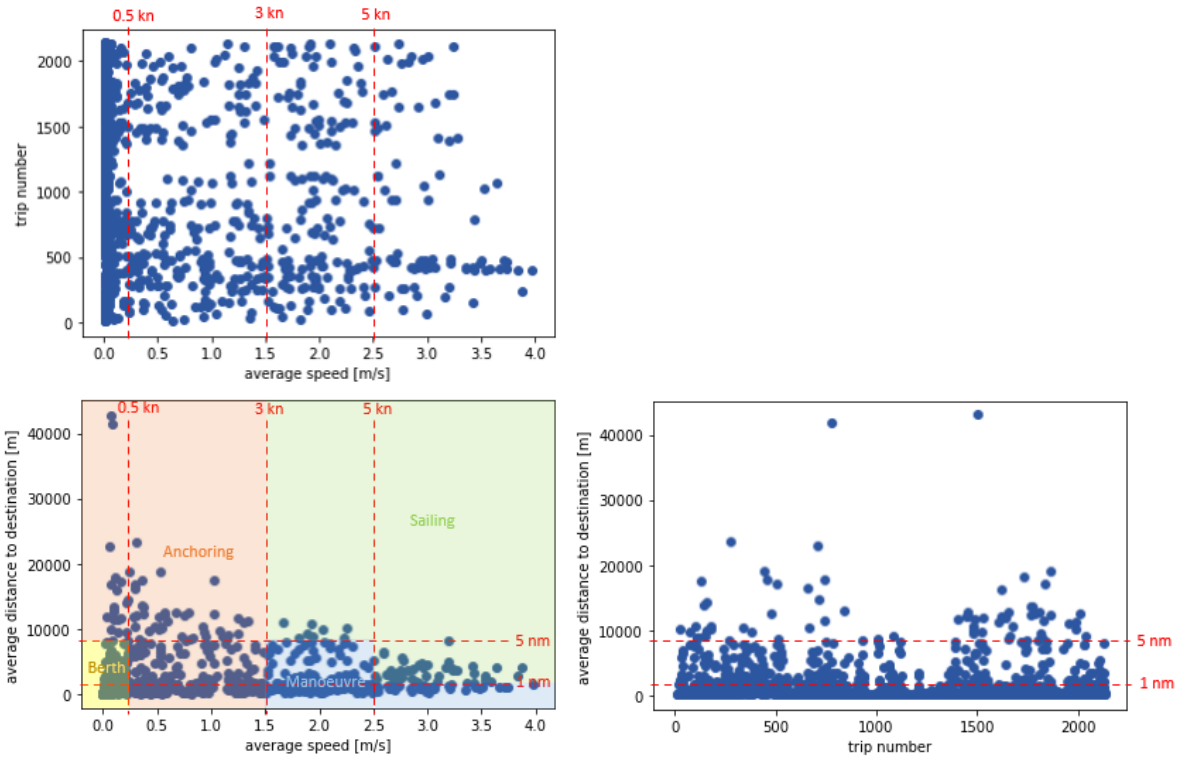

Figure 6.4: Average speed and distance to destination of all trips in June 1 - June 14 2021

How the model performs on smaller ports, is hard to determine with the available AIS data. The low AIS speeds are the reason for the wrongly distributed operational modes in this case study. However, when in the future AIS data is used with higher vessel speeds, the distance to destination could still be a discrepancy of the model. Further research around the operational modes in smaller ports is necessary.

Emission split in vessel types

To indicate the emission split per vessel type, their contribution to the total emissions are stated in Figure F.3 in percentages. Only CO_2 is showed for simplicity, the split of the other emission types is almost similar and

can be found in Section F.3. The contribution of the general cargo vessels is the largest since these vessels are by far responsible for the most port visits. However the oil tankers are not visiting often and are the second largest contributors to the total emissions. This could be due to the fact that tankers emit a lot while at berth and a large part of the AIS messages is from vessels at berth.

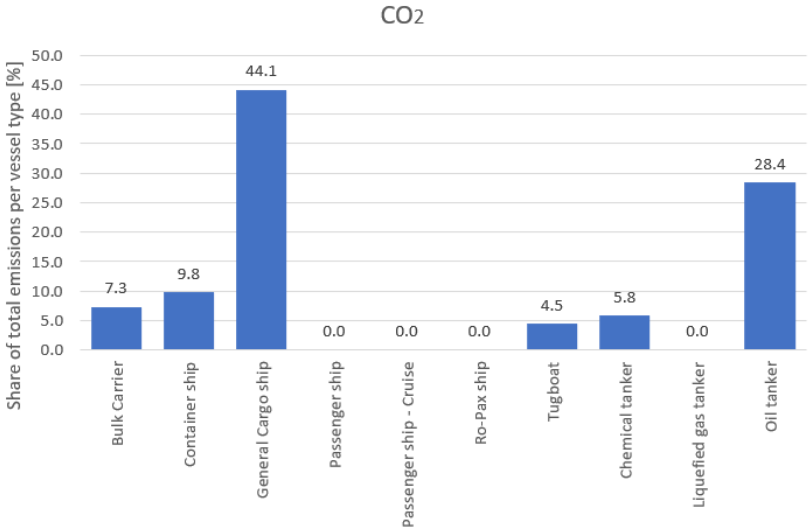

Figure 6.5: Emission split in vessel types in percentage of total emissions

6.4.2. Emission distribution

To get an insight in the emission pattern in the port, the emissions are projected on the FIS graph, see Figure 6.6, Figure 6.7, Figure 6.8 and Figure 6.9 for the results of the two weeks in January, the two weeks in June can be found in Section F.4.

When comparing the graphs, all the emission types have the same distributions. In general can be seen that the main waterway through the port is not responsible for the large emissions, but the peaks occur in certain port basins. This is due to the high share of emissions of vessels at berth.

Another emission hot-spot is the small corridor leading to the Rhine-Danube corridor, which is a busy fairway to Central and Eastern European. Due to the high traffic volumes, the emissions are relatively high at this spot. Next, the port basins with the highest emissions will be evaluated.

Figure 6.6: Estimated CO_2 emissions in the Port of Constanța from January 1 - January 14 2021

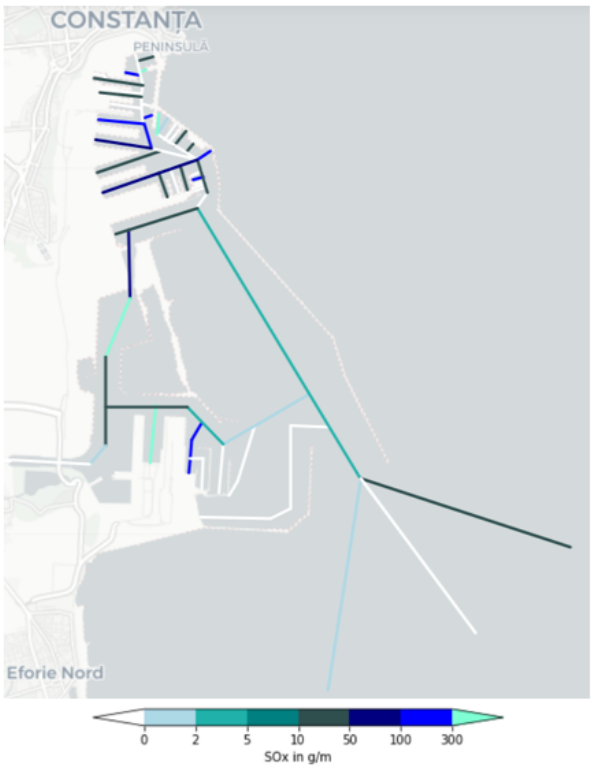

Figure 6.7: Estimated SO_x emissions in the Port of Constanța from January 1 - January 14 2021

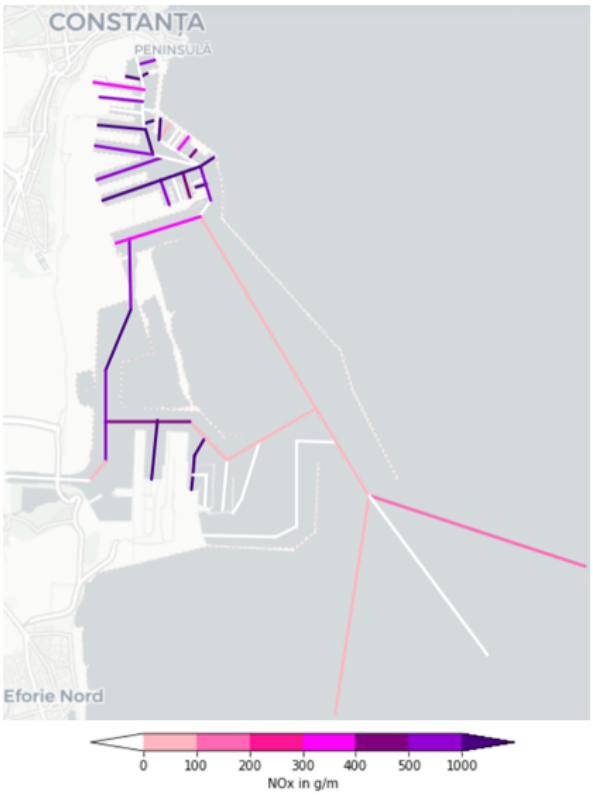

Figure 6.8: Estimated NO_x emissions in the Port of Constanța from January 1 - January 14 2021

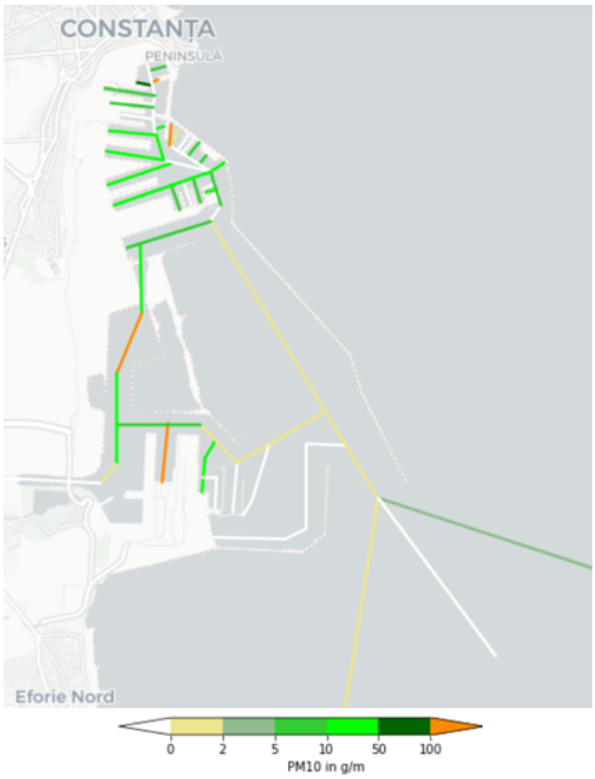

Figure 6.9: Estimated PM_{10} emissions in the Port of Constanța from January 1 - January 14 2021

The emission hotspots are indicated at the map in Figure 6.10.

The container terminals have high emissions, this corresponds to the fact that the port identifies itself as A-hub for the container traffic in the Black Sea. The general cargo terminals show high emissions. This is consistent with the fact that most of the port visits are from general cargo vessels. General cargo vessels and container vessels are large vessels which cause high emissions.

The oil terminal shows high emissions as well. The loading and unloading of oil products can take a long time and their equipment requires much energy. However, the emissions from tankers are probably overestimated with the model.

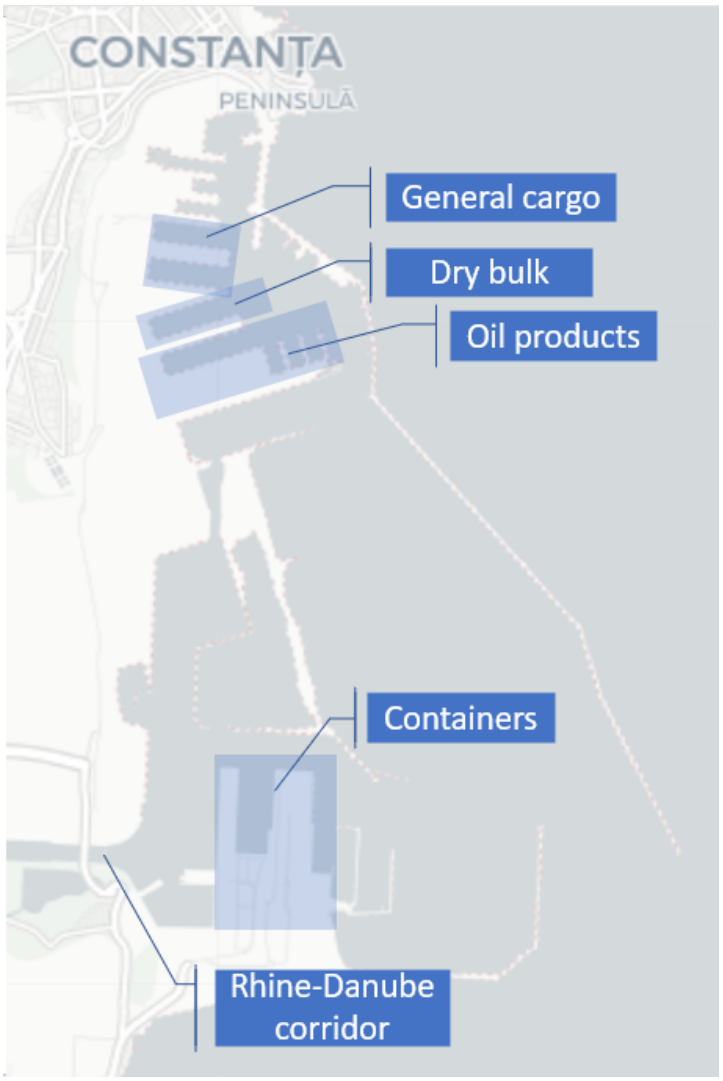

Figure 6.10: Location of the ports with the highest emissions

7

Emission reduction strategies

Insight in emissions is of importance to find the right strategy to reduce emissions. To demonstrate the possibilities of the model on this aspect, several reduction measures are modeled. How to implement the emission reduction strategies is briefly discussed in Section 4.4, now they are actually implemented in one of the case studies.

7.1. Shore power

Since around 22% of the emissions in the port of Rotterdam take place at berth, shore power is an interesting reduction measure to reduce the emissions in this port.

Recently the port authority of the Port of Rotterdam has drawn up a strategy to connect more vessels to shore power. Their aim is that in 2030 at least for 90% of the visits of Roll-on/Roll-off, offshore, ferry and cruise vessels they will connect to shore power, and at least 50% of the visits of container vessels with a TEU capacity greater than 10,000 TEUs will be connected to shore power. The port authority estimates, that this will lead to a reduction of 30 to 35 % of CO_2 and NO_x emission for vessels at berth. (Bonte and Castelein, 2020)

To indicate the results of this strategy a model is set up to mimic these circumstances. For this the model used in the case study of the Port of Rotterdam is adjusted. To reduce computational time, only the two weeks of January 2022 are examined. The results of the two weeks in January from the original case study will be compared to a hypothetical case study with shore power. The two weeks of January are divided by 13 and multiplied by 365 to obtain the yearly averages.

For the hypothetical case with shore power, the strategy of the Port of Rotterdam described in the paragraph above will be mimicked. The vessels connected to shore power are simulated by setting the power from the auxiliary engine from ships at berth to zero. This is done for all the vessels registered as 'Passenger ship', 'Passenger ship - cruise' and 'Ro-Pax ship'. This means that for 100% of the trips they will connect to shore power in stead of the aimed for 90% by the Port of Rotterdam. For the container vessels an assumption is made as well. For the size categories '12,000 - 14,4999', '14,500 - 19,999' and '20,000 - +' the auxiliary engine power at berth is set to zero. These assumptions will lead to a slight over-estimation of the emission reduction.

The comparison of the original situation without shore power and the new situation with shore power is summarized in Table 7.1 and Table 7.2 below. When investigating the shore power case study results from Table 7.1, it shows that even when being on the conservative side, the emission reduction will be approximately 24% for vessels at berth. This is less than the estimated 30% the port authorities predicted.

When looking at the total emission reduction the percentage is even lower. A possible explanation for this could be that sailing vessels are responsible for the largest share of emissions. By connecting vessels to shore power, these emissions are not influenced. Their contribution will now relatively have a larger impact on the total emissions, since the share of emissions of vessels at berth has decreased. This rationale goes for all operational modes except berthing (see Figure 7.1). Quantitatively, the emissions of all operational modes are decreased.

	Total CO_2	Total SO_x	Total NO_x	Total PM_{10}	Total emissions
Original case Estimated yearly emission at berth [tonnes]	17413.2	6.0	326.7	5.2	17751.2
Shore power Estimated yearly emission at berth [tonnes]	13295.1	4.6	249.4	4.0	13553.0
Emission reduction [tonnes]	4118.1	1.4	77.3	1.2	4198.1
Emission reduction [%]	23.6	23.6	23.7	23.7	23.6

Table 7.1 Emission reduction for vessels at berth

	Total CO_2	Total SO_x	Total NO_x	Total PM_{10}	Total emissions
Original case Estimated yearly emission [tonnes]	80417.0	27.3	1549.9	24.2	82018.4
Shore power Estimated yearly emission [tonnes]	70062.4	23.6	1336.8	20.9	71443.6
Emission reduction [tonnes]	10354.6	3.7	213.1	3.3	10574.8
Emission reduction [%]	12.9	13.7	13.7	13.8	12.9

Table 7.2 Total emission reduction

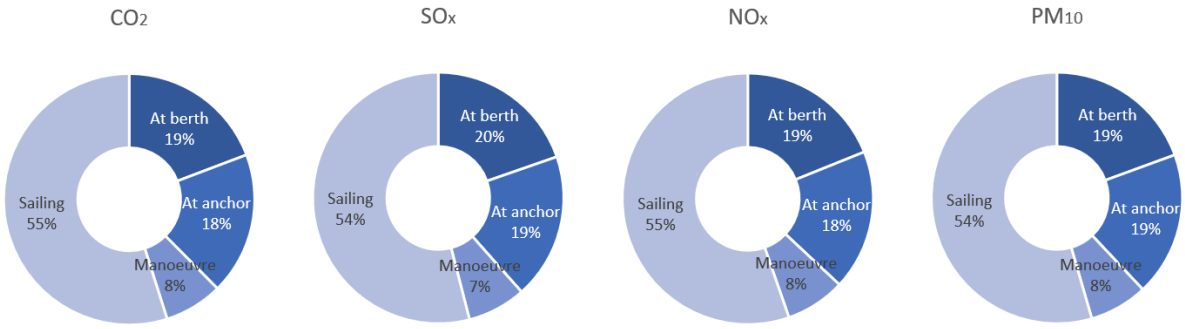

Figure 7.1: Percentage of emissions in each operational mode of the simulated shore power case

7.2. Zero-emission tugboats

Zero-emission vessels are gaining interest in the maritime industry. Hydrogen or battery fueled vessels are especially practical in ports. The two leading zero-emission vessel types are ferries and tugboats. When looking at the emission distribution of the port of Rotterdam, the Madroelhaven was marked as an emission hotspot and was mainly used by tugs. The largest ferry terminal is also marked in the figure. No exceptionally high emissions are detected here. The emissions split per vessel type shown in Figure E.5, where ferries are falling in the category 'Passenger', also confirms no high emissions from ferries. The hypothetical case will therefore be build around zero-emission tugboats.

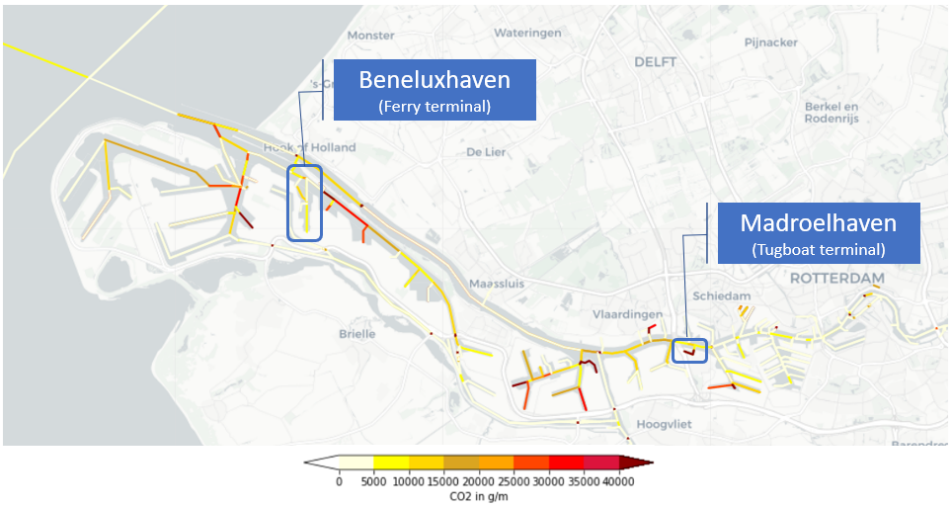

Figure 7.2: CO_2 emissions in the ferry terminal and in the Madroelhaven

The emissions of the port under normal conditions are described earlier in the case study of the Port of Rotterdam. The two weeks of January 2022 are compared to a hypothetical case were zero-emission tugs are adopted. The comparison is stated in yearly averages based on these two weeks; The two weeks of January are divided by 13 and multiplied by 365.

In this new case study all tugboats are excluded from the model, since their emissions will be zero. This means that 63 tugboats of the total 836 vessels are filtered out from the AIS data (7.5 %). The comparison between the two vessel type distributions can be seen in Figure 7.3. All other circumstance stay the same.

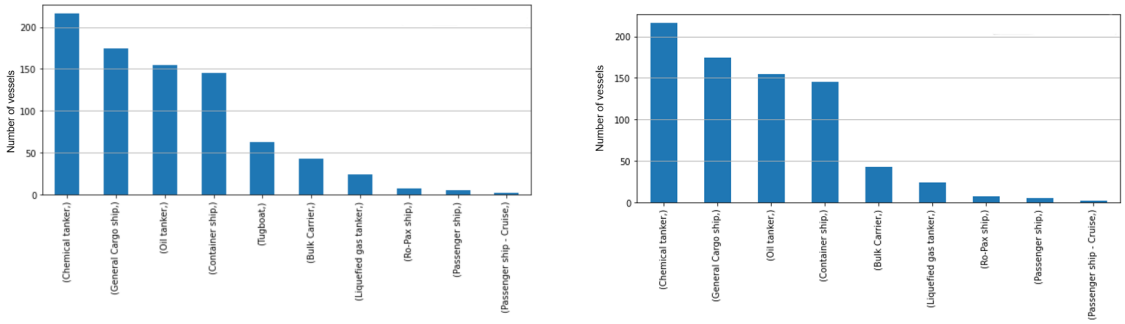

(a) Number of vessels per vessel type - Original case

(b) Number of vessels per vessel type - Zero-emission tugboats case

Figure 7.3: Number of vessels per vessel type comparison of original case to case with zero-emission tugboats

The results of the hypothetical case with zero-emission tugboats are stated in Table 7.3. Replacing all tugs by zero-emission tugs seems to reduce the emissions by approximately 13%. This is an efficient way of reducing emissions, however somewhat less efficient than for example connecting a specific group of vessel to shore power (see the case study about shore power in Section 7.1).

	Total CO_2	**Total SO_x**	**Total NO_x**	**Total PM_{10}**	**Total emissions**
Original Estimated yearly emission [tonnes]	80417.0	27.3	1549.9	24.2	82018.4
Zero-emission tugboats Estimated yearly emission [tonnes]	70034.8	23.6	1344.2	20.9	71423.5
Emission reduction [tonnes]	10382.2	3.8	205.7	3.3	10595.0
Emission reduction [/%]	12.9	13.7	13.3	13.6	12.9

Table 7.3 Estimated emissions with hybrid tugs

When comparing the split in operational modes from this reduction measure with the original case study (Figure 5.3), this measure has the most effect in the berth and anchor mode, since these percentages have decreased. However, the expectation is that tugs also consume a lot of energy while manoeuvring, causing high emissions. By introducing zero-emission tugs, a decrease in the emissions in the manoeuvring mode would also be expected which does not show from the results. This discrepancy can be due to the method to estimate the energy consumption of the main engine in which the power prediction method of Holtrop and Mennen (1982) is used. This method might not be suited to describe the energy consumption of tugboats, whereas they have very different resistance patterns than other vessels.

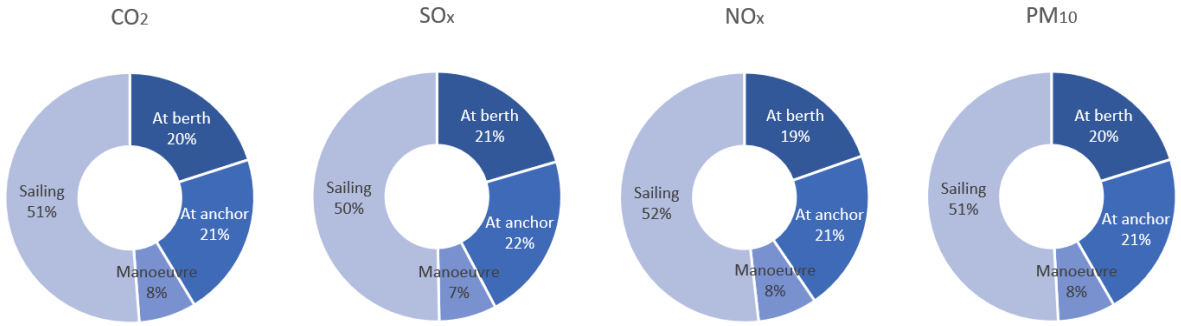

Figure 7.4: Percentage of emissions in each operational mode of the simulated zero-emission tugs case

When looking at the emission distribution in Figure 7.5, a decrease in emissions in the Madroelhaven can be observed. This matches with the prediction that the emissions from this terminal were mainly due to tugboats. This case study illustrates the purpose of the model well since it is the typical approach of first identifying the emission hotspot with the model, proposing a suitable emission reduction strategy and quantifying the effect of this strategy with the model.

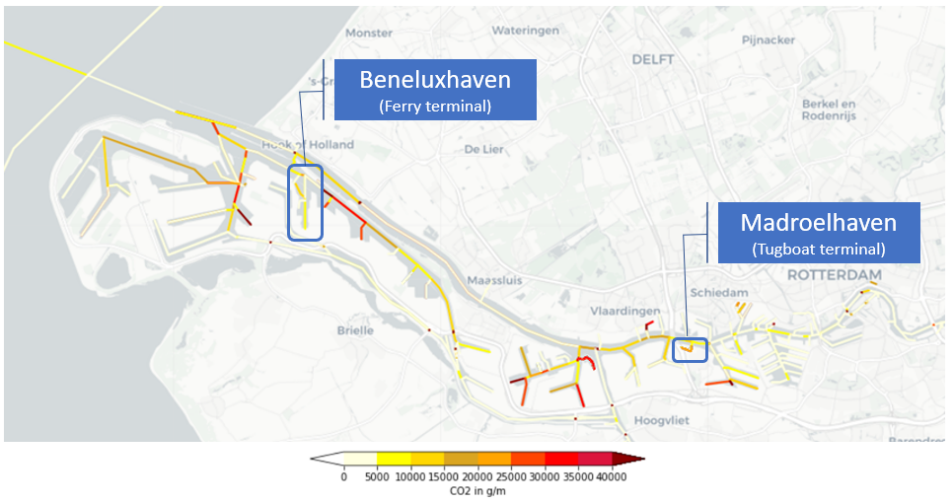

Figure 7.5: *CO2* emissions in the Madroel haven from the case study with zero-emission tugboats

7.3. Applying ECA limits

The Port of Constanța shows multiple fairway sections with high emissions. Therefore the port would benefit from an emission reduction measure lowering all emissions gradually. The possibility of applying ECA limits will be examined. To indicate the potential reduction of emissions when applying ECA limits, a new hypothetical case is set up. The model composition is the same as the one from the case study performed in Chapter 6 with some alterations. The fuel types of the vessels are changed from the most economical fuel type to the lightest fuel type on board. The second alteration is the sulphur content in the fuel, this is changed to a maximum of 0.10% m/m.

The results of the original case study of the Port of Constanța are compared to the results of the new case study. This is summarized in Table 7.4. It shows that applying this reduction measure mainly reduces the SO_x emissions. It is a relative easy measure to apply and the effect on the SO_x emissions is large. When large cuts in emissions must be made, applying ECA limits is not the leading strategy and other options for reducing emissions must be examined. When the SO_x emissions must be regulated, this is however a very effective method.

	Total CO_2	**Total** SO_x	**Total** NO_x	**Total** PM_{10}	**Total emissions**
Original Estimated yearly emission [tonnes]	119978.1	264.8	3764.3	63.4	124070.6
Zero-emission tugboats Estimated yearly emission [tonnes]	115187.8	72.4	3898.8	62.3	119221.3
Emission reduction [tonnes]	4790.2	192.4	134.4	1.1	4849.2
Emission reduction [/%]	4.0	72.6	3.6	1.7	3.9

Table 7.4 Estimated emissions when applying ECA limits

Furthermore, these results show that the fuel type allocation of the developed model simulates the reality well and that changes in the fuel type translate to an effect on the emission outcomes. However a reduction of SO_x emissions of 70% with the model seems somewhat high.

III

Discussion, conclusions and recommendations

8

Discussion

The obtained results are an estimation of the actual emissions. This is due to some limitations of the method and model. The exact limitations are addressed in this chapter, starting with the method limitations, followed by the model limitations and a reflection on the results.

8.1. method

A correction for the limited water depth is taken into account in the method, however the effects of a limited fairway width are neglected. The resistance a vessel experiences is less affected by lateral restrictions than by depth restrictions. In case of narrow waterway cross sections the effects become larger. Most ports must accommodate large ocean-going vessels, which need to be able to pass each other and perform manoeuvring actions. It is therefore likely that not many narrow waterway cross sections occur in ports. However, in port basins the lateral effects can be quite complex. Also many vessels congregate in ports and passing vessels influence the flows around surrounding vessels. The effect this has on the resistance is also neglected in this research. For future studies, it could be of importance to look further into flows around vessels in ports. Also other external influences on the resistance such as wind and waves are interesting to look at. In this research, those external influences are neglected since ports are mostly sheltered.

The method takes into account the speed over water, which depends on the currents of the fairway. It means that when a ship is sailing against the current the speed is smaller than the speed relative to the ground and vice versa when sailing along with the current. Currents are time-dependent as they vary throughout the day. Currents are also directional and do not need to be in the lateral direction of the fairway. Detailed data about currents in ports is not available for each port. Due to the scope of the research and since the method must be applicable for many ports, the effect of currents is neglected. However, they can be of influence on the emission estimations since the vessel speed determines the resistance of the vessel. The main engine power estimates can be improved by taking into account currents, the auxiliary engine power is not effected by currents as it does not depend on the speed of the vessel. In the operational modes 'berth' and 'anchor', solely the auxiliary engine determines the emission of the vessel, meaning that these outcomes are not sensitive to currents. In ports a large share of the total emissions (approximately 40-50%) comes from vessels operating in the 'berth' or 'anchor' operational mode and the approach will estimate these emissions accurately. (Note: the categorization of the operational modes depends on speed *over ground* and therefore will not be influenced by currents.)

The number of operational modes considered in this research is four, while in reality many other operational modes are possible. The assumption of four modes is a simplification of reality. Determining the operational mode is done by setting criteria for the vessel speed in combination with the distance to its destination. However, the speed at which a vessel is switching between operational modes, differs per vessel type and size and captain. This is neglected in this research.

The emission factors used from the IMO are based on tests on different engine types and after this updated every four years. The last update was in 2020 and new engine types have come on the market since then. The auxiliary engine power consumption is also based on estimations from the IMO, who have validated these by

peer-reviewing, verification from experts and validation against noon-reports (International Maritime Organization, 2021). However, these two characteristics can vary per vessel and are again also dependent of the behavior of a captain, which leads to an uncertainty in the emission estimation. Furthermore, the values can change over the years and it is important to evaluate these numbers from time to time. In the current model the emission factors and auxiliary engine energy consumption values are stated in a separate input file which can be easily updated so that the model itself does not need adjustments.

In addition to that, the IMO uses the auxiliary energy consumption to estimate emissions of vessels on a higher abstraction level. They obtained their values by averaging the measurements over vessel types and operational modes, where there is for example no need to differentiate in the berthing mode between loading and unloading. However, when estimating emissions in ports this is interesting when considering tankers. Since no better data source is available, the values of the IMO are considered sufficient for this research. It might be interesting to look at port-specific values in future studies, since they are a key-input in this research.

The decision matrix for the operational modes is also based on the IMO approach. This approach assumes that between 1 and 3 knots the vessel is anchoring no matter what distance to destination. This means that when a vessel leaves berth and in reality is manoeuvring or sailing away from the port basin, it is wrongly assigned some time in anchoring mode. This leads to an over-estimation of the share of emissions of anchoring vessels.

The method is based on the energy consumption of the main engine and auxiliary engine. For tankers this leads to a limitation since their loading and unloading power is supplied by the boilers. This leads to a significant under-estimation of the energy consumption in berthing load, on which is anticipated by adding the power consumption of the boiler to the power consumption of the auxiliary engine, which assumes that the boiler has the same engine characteristics as the auxiliary engines. However, this is large simplification and leads to inaccuracy of the emission estimation of tankers. The method of this research is therefore not suitable for this vessel type. A possible recommendation could be to add an approach to estimate the emissions from boilers to the method.

Besides tankers, the emissions from tugboats have a higher uncertainty than the rest. The power consumption of tugboats is estimated less accurately, since tugboats have deviating operational modes and the power prediction method of Holtrop and Mennen (1982) is not suitable for the resistance patterns of tugboats. A different categorization of operational modes should be set up for tugboats, with for example an extra mode 'assisting'. Further research is needed to establish these operational modes and their characteristics for tugs. To add this eventually to the model, knowledge about the energy consumption of the auxiliary engine must be available for each mode.

Some vessel types are excluded from the research, as they are not part of the largest emitters. With the right information about these vessel types, they can easily be added to the research. Their power consumption must have the same pattern as the current method assumes. The vessel types that in the future could be added must be large sea-going vessels since their resistance can be calculated with the approach of Holtrop and Mennen (1982). For example RoRo ships are a welcome addition to the research, where as refrigerated bulk vessels are less suitable since their cargo requires power.

The assumption that the main engine is turned off when a vessel is berthing or anchoring is not in all cases true; sometimes a captain leaves the engines idling for a while. The same goes for the assumption that a captain turns off the engines of a berthing/anchoring vessel after approximately 30 minutes. Human behavior is hard to include in calculation models and therefore for future research it could be of interest to validate these assumptions.

Another important assumption is that the vessels always have their auxiliary engines on when they are berthing. This omits the possibility that the vessel could be connected to shore power. The vessels using shore power are therefore responsible for an overestimation of the emissions. From the case study in Section 7.1 can be derived that connecting a group of vessels types to shore power can already lead to a reduction of 13% of the total emissions. In the future of marine shipping it is conceivable that more ports will install shore power, so it is important to monitor this trend.

8.2. Model

8.2.1. Model input

The model input consists of AIS data, a fairway information system and a vessel database. First the AIS data is discussed.

AIS data

The quality of the AIS data is important. The quality can be affected by technical problems such as signal disturbance, but a greater unreliability comes from the fact that some data needs to be put in manually by captains. The transmission of the signal goes automatically, but filling in fields containing vessel characteristics and switching the transmitter on and off, are the responsibilities of the captain. It is hard to quantify how many of the entries are wrongly put in. The missing entries are easier to quantify. For example looking at the AIS datasets used in the case studies, 1.5 to 1.8 % of the vessel lengths and widths are missing, which is not a large percentage. The vessel characteristic with a somewhat higher unreliability than the others is the draught of the vessel. The draught varies over time as it depends on how much the vessel is loaded and external conditions. From practice it shows that most vessels register a constant draught for each trip. This can well be the case, as most of the trips are going to a destination to load and unload and will not lose any weight during the trip. For further research, to see if the draught varies over time one could look at two trips of the same vessel reaching and leaving berth. Another point of interest concerning the AIS data quality are the low AIS speeds in the second case study of the Port of Constanța. To avoid this in the future, making an assessment of the quality of the AIS data prior to the data processing, could be of added value to the model.

Retrieving the AIS data is done manually so personal interpretations play a role. The area of interest must be determined (in this case a polygon needs to be drawn around the port area) and the time span of the data must be determined. This causes deviations in emission estimation as for example seen in the case study of the Port of Rotterdam. To compare the quantitative amount of emissions to other researches, a clear definition of the port area and time span of the AIS data must be stated. Th case study of the Port of Rotterdam shows that a two week timeframe is to short to quantify emissions. When in the future possibly external influences are added to the research, the time-dependency of the emissions will become of even more influence.

The vessels from the RoyalHaskoningDHV AIS data are divided into certain vessel types based on their own developed categories. It is important to note that when other sources are used, these categories could differ. In this research the vessel types are divided into ten categories and the ones falling outside these categories are rejected. Vessels might be assigned an incorrect vessel type, leading to a erroneous emission output or leading to dismissing the wrong vessels.

Fairway Information System (FIS)

Using an existing FIS graph is convenient and saves a lot of time. However, this is not available for all ports and the model must be generic for all ports worldwide. This adds an extra step to the model, which comes with some discussion. Construction of a FIS graph is done manually by adding nodes to a map. This leads to room for own interpretation. The number of nodes and edges can vary. The more nodes and edges the more accurate the representation of the fairway but this also leads to more construction and computational time. It could also lead to a too detailed fairway system making it harder to determine the closest edge to the AIS data points, which could lead to outliers in the vessel path. Assigning the vessel's position to an edge on the graph, is based on the distance of the vessel to the surrounding edges. In ports many surrounding edges representing bends and junctions are present, making it difficult to determine the correct route of the vessel over the edges. In general, more information on how to create a FIS graph must be gathered. This will improve the accuracy of the emission estimation and the projection of the emissions.

The characteristics of the fairway are assigned to each edge. Not all edges contain the needed fairway properties for the emission calculation. For example, from the FIS graph of the area around the Port of Rotterdam used in the first case study, 15 % of the edges contain a water depth and for the remaining ones the average water depth is used. This leads to a higher inaccuracy. However, the model has the ability to take the accurate water depths into account once the information is available. In reality the water depth does not only vary in space, but also in time. These fluctuations are neglected in this research. Information about the bottom of the fairway as well as the water level per a certain time period are needed to take into account these variations. This will decrease the uncertainty of the emission estimation.

Database

The database used to retrieve vessel characteristics is the Sea-web Ships database. When relying on one database, not all characteristics can be filled in. For example, the used database consists of 64,055 vessels and has 1.76% missing entries. The world fleet consists of 74,505 vessels, so this means that 14% of the vessels are lacking from the database (The Maritime Executive, 2022a). To improve the model an option for future research could be to combine information from multiple databases. However, the procedure of filling in the missing entries seems to suffice since no mistakes in the vessel type patterns are observed.

Most databases are updated daily, weekly or monthly. When applying the model, it is important to make sure the information is not outdated and to check regularly if more recent data is available. The annual growth of the world fleet is on average 1.75%, which resembles 567 new vessel per year (The Maritime Executive, 2022a). At least a yearly update is therefore advisable.

8.2.2. The model

The model starts with creating a vessel database and trip collection. The vessel database saves a lot of computational time. The trip collection cuts vessel trajectories when a vessel is not transmitting a signal for more than 30 minutes and dismisses trips shorter then one kilometer. This is not the exact representation of reality. In reality sometimes the signal might be turned off too soon while the engines are still running, or the signal is turned on too late making the stop longer than 30 minutes. Furthermore, the time before switching of the auxiliary engine differs per vessel type, this is neglected in this research.

Next, per trip some calculations are performed which starts with determining the operational mode. The mode is considered to be consistent during each timestamp, however in reality during one timestamp the vessel can operate in multiple operational modes. This is a case of seconds or minutes, which will have minor influence on the total results. The model predicts the operational mode well in large ports as the Port of Rotterdam. In small ports the model seems to predict the modes fairly however, the limits for categorizing the distance to destination in small ports should be investigated. Based on the conditions (very low vessel speeds in AIS data), no conclusion can be drawn about the accuracy of operational modes in small ports. It is recommended to do a sensitivity analysis on the operational modes to see the accuracy of the classification. This way the 'anchor' mode between berthing and leaving the berth can also be investigated.

8.3. Results

When interpreting the results, a few things must be taken in mind. First of all, the emissions are an estimation of the actual emissions. Some vessel types and trips are filtered out and their emissions are not added to the total. The actual emissions will therefore be higher than predicted with the model. The model is expected to predict approximately 90% of the total emissions, since the vessel types taken into account are estimated to be responsible for 90 % of the emissions. By adding tugboats the percentage increases, but by dismissing some of the trips the percentage decreases.

When looking at the case study of the Port of Rotterdam, the quantification of the emissions is off. The port's emissions are expected to be a hundred times higher. A plausible reason could be that a mistake is made in setting up the case study rather than the model itself, as the quantification of the emissions of the case study of the Port of Constanța is in the right order. Other aspects that could have influenced the outcome is that not a clear definition of a port area is outlined. This might lead to inclusion or, in this case, exclusion of certain edges and emissions compared to other researches. The chosen time span is also of influence on the emission totals. When looking at the case study of the Port of Rotterdam, the down-drilling procedure shows three tankers making a short stop and only one tanker making a elaborate stop. For such a large port, more takers are expected to pass this edge and more time at berth during these stops is expected. By taking a large timescale (more than four weeks) these effects probably even out more.

The Port of Constanța shows higher estimated emissions per meter fairway (dark shaded fairway sections) than the Port of Rotterdam, while the Port of Rotterdam has twice the amount of yearly emissions. This is probably due to the surface area over which the emissions are spread out. The Port of Rotterdam is three times larger, but only shows twice the number of estimated yearly emissions.

9

Conclusions

This research is conducted to answer the following question:

How to estimate vessel emissions in ports using AIS data in order to identify emission distribution patterns and evaluate emission reduction strategies?

To formulate a concrete answer, the question is divided into sub-questions. In this chapter, we look back on the performed research and address the answers to these sub-questions to see what conclusion can be drawn.

How can a method be developed for estimating emissions in ports in space and time?
A bottom-up approach is the best suitable method to estimate the emission of a single vessel in space and time. This type of approach can take into account data about vessel characteristics and geographical information of the study area. This leads to a detailed approach with the ability to evaluate emissions on a smaller scale, like in a port. With a bottom-up approach use can be made of local real-time data, which aligns well with the goal of this research.

To derive the emission rate of a vessel, the fuel or energy consumption of the engine is multiplied by a vessel-specific emission factor. These emission factors are derived from research of the International Maritime Organization (2021), since these can be applied to vessels in ports all around the world. The fuel-based approach is used to estimate CO_2 and SO_x emissions, of which the emissions are directly proportional to the fuel consumption and therefore depend on the engine load. The energy-based approach is used to estimate NO_x and PM_{10} emissions, of which the emissions can not be directly related to the fuel consumption but depend on engine characteristics. The fuel consumption is determined by multiplying the energy consumption of the engine with a fuel consumption factor specific to each vessel, meaning the fuel consumption is related to the energy consumption.

The main engines and auxiliary engines are the main emission sources on board of a vessel. The emissions of a single vessel in space and time are therefore estimated as the sum of the emissions of the main engine and the auxiliary engine. A method to estimate both emissions separately leads to a more accurate result, than for example assuming the auxiliary engine emissions as a percentage of the main engine emissions. Splitting these two emission sources makes it also possible to determine targeted emission reduction measures. For tankers, the boiler emissions at berth are also considerable, since tankers use their boilers intensively to heat the cargo and drive the unloading pumps. The power consumption of the boilers at berth is added to the auxiliary engine's power consumption, which assumes that the engine characteristics of the boiler and the auxiliary engine are the same. In reality, this is not the case and therefore, the emissions of these vessels estimated with the current method followed in this research are less reliable.

The energy consumption of the main engines depends on the resistance a vessel experiences from sailing through the water and is therefore related to the vessel's speed. The research of Holtrop and Mennen (1982) provides a good resistance estimation based on vessel speed. This estimation is however limited as it does not take into account fairway restrictions. The method of Zeng et al. (2018) is applied to account for the effect on the resistance of a limited water depth. The effect of wind and waves is expected to be limited in ports,

since they are most of the times sheltered. The effect of currents are neglected in this research. However, they are considerable and the method can be improved by taking these into account.

The resistance of the vessel times the speed and taking in the efficiencies of the engine, gives the energy consumption of the main engine. Meaning that when a vessel is sailing at low speed, it requires less energy. However, in ports the vessel's speed alone is not a good indicator of the energy consumption, since this neglects the amount of energy the auxiliary engines consume. Their energy consumption is dependent on how much energy the electrical systems of a vessel require at that moment, which can be high when a vessel is for example at berth or manoeuvring. Therefore, the energy consumption is related to the operations a vessel performs. This leads to an approach which takes into account the vessel's resistance and operational modes.

According to the operational mode, the main engine power consumption is estimated zero when the vessel is laying still, or calculated with the method of Holtrop and Mennen if the vessel is sailing. The IMO provides values for the energy consumption of the auxiliary engine during different operational modes.

The emissions must be displayed in such a manner that the emissions in ports can be derived and emission patterns can be observed. This is done by developing a model, containing the algorithms to calculate the emissions according the described method per vessel at each timestamp and subsequently projects them on a fairway network of a port. The emissions must be displayed per meter fairway to avoid that long fairway sections show high emissions due to the fact that vessels spend more time on this section.

What aspects of a vessel movement in a port should be distinguished when evaluating emissions of a vessel in a port?
As mentioned before the emissions of the main engine are related to the vessel speed. However, in ports the emissions of the auxiliary engines are also important. These emissions are related to the operations a vessel performs. The different types of operations are called 'operational modes' and should be distinguished from an AIS track a vessel is sailing.

The operational modes are categorized based on speed, since the energy consumption of the main engine is speed-dependent. Speed alone is not good enough to determine the operational mode, since slow speeds do not indicate whether a vessel is just slowly sailing or manoeuvring. To encounter this the operational modes are related to the distance of the vessel to its destination. It is assumed that at the end of each trip the vessel is berthing to load and unload cargo. Close to the berth, the vessel will encounter operations like manoeuvring or anchoring (to wait for the berth) and further away or when reaching higher speeds, the vessel is classified as 'sailing'.

Based on previous research, different categorizations in operational modes are made based on vessel speed. They all have the same scope comprising 'sailing', 'manoeuvring' and 'hotelling'. In ports it is important to make a distinction in the hotelling-mode between 'at anchor' and 'at berth' since these two operations both occur in ports and require a different power consumption of the auxiliary engine. They occur at different locations influencing the spatial emission distribution. When a ship is berthing or anchoring it is assumed that the main engine is turned off and the auxiliary engine is on to power the vessel's electrical systems. When a vessel is manoeuvring or sailing the power consumption of the main engine is estimated based on the vessel's resistance according the method of Holtrop and Mennen (1982). The auxiliary engine power consumption will have a smaller contribution in these modes.

What data is needed for developing a model to estimate emissions?
To determine emissions, data about the speed and location of the vessel, data about vessel characteristics and data about fairway characteristics is necessary. The vessel characteristics in combination with the speed and location of the vessel and the fairway characteristics are needed to determine the operational mode and resistance of a vessel. The fairway characteristics and the location of the vessel in time are also needed to visualize the emission patterns.

This data is presented to the model in the form of a vessel database, a trip collection and a FIS graph. The vessel database includes the characteristics of the vessels present in the AIS data. These characteristics are derived from the Sea-web Ships database and some characteristics, as the dimensions of the vessel, are derived from the AIS data itself. When entries are missing, a statistical procedure is used to fill these in.

The trip collection consists of the trajectories of all vessels which are cut up in trips. The trajectory is split into two when a ship has reached berth and the engines are turned off. Practice and previous research show that when a vessel is laying still for more than 30 minutes, the engines are most likely switched off. For creating

the trajectories and cutting them up in trips, the Python package MovingPandas is used. Ships shorter than one kilometer are considered unrealistic and are rejected.

The FIS graph is a collection of nodes and edges resembling the fairway network of a port. This graph contains the fairway characteristics needed to calculate the resistance. The calculated emissions will also be displayed on the FIS graph for a detailed insight in the emission distribution in space.

How can emissions patterns in a port be estimated and how can important emission sources be identified with the developed method?
To derive the emission patterns in a port, the results of the model will be displayed as a projection on a FIS graph. By coupling them to the FIS graph, the emissions can be addressed per fairway section and more accurate insight in the emissions distribution is delivered. The emissions per timestamp are coupled to an edge of the FIS graph and the emissions of all trips are summed up. The emissions are visualised by plotting each edge according an assigned color scale related to the sum of emissions in g/m. Displaying the emissions per meter fairway, is to avoid that long fairway sections show high emissions due to the fact that vessels spend more time on this section. The emission totals can be plotted or the emissions of one single trip or vessel can be plotted.

The fairway sections which are subjected to high emissions can be identified immediately based on their color and so the emission hotspots can be identified. Due to the ability of the model of down-drilling to a single vessel in space and time, a vessel or a group of vessels responsible for the emissions at a certain hotspot can be identified. Identifying an important emission source offers the possibility to design targeted emission reduction strategies.

To provide extra insight in the emission patterns in a port, the model is also capable of deriving a distribution of emissions in operational modes and vessel types. This can be done by adding up the emissions of all timestamps with the same operational mode or vessel type.

How can the effects of emission reduction measures be quantified with this method?
By indicating the location and source of the emission hotspots, targeted emission reduction measures can be taken. Several strategies are discussed in the report. The most suitable strategies for ports are established and the measures which require additional research or a AIS data simulation, are not tested with the model. The model has the capability to take in simulated AIS data of a fictive fleet, since the model takes in real-time AIS data which can be replaced by simulated AIS data. However, due to the scope of this research, setting up a simulation is too comprehensive so to demonstrate reduction strategies another approach is used. Since a bottom-up model is created, which deviates between operational modes and vessel types, very detailed modifications can be made to the model to simulate measures on the real-time fleet. Specific vessel types can be modified, but also for example all vessels at berth can be modified, or a combination of the two options. These groups are then excluded from the model, which will create a fictive fleet but with unaltered AIS paths. These fleet adjustments may lead to changes in the behaviour of vessels. This is neglected with the current approach, but this could be modeled in an extensive simulation as mentioned earlier.

The current approach is applied to three case studies about emission reduction measures. The first strategy concerns installing shore power. The model is able to simulate vessels connected to shore power, by setting their emission rate at berth to zero. This simulation is compared to the original situation without using shore power. Out of the evaluated reduction measures, this seems the best strategy to reduce emissions since it shows the largest reduction of the total emissions. Besides that, it is an effective measure especially for ports, since the largest emissions reduction takes place at berth. The second evaluated strategy shows also good results and is about switching from a normal tugboat fleet to a zero-emission tugboat fleet. The model simulates this switch by eliminating all the tugboats from the fleet since their emissions will be zero. This new case is compared to the original situation with normal tugboats. The third option to reduce emissions is applying Emission Control Area (ECA) limits which do not seem to have a lot of effect on reducing emissions except for the SO_x emissions. This is derived from comparing the original situation without ECA limits, to a new case study where a situation with ECA limits is simulated. This means that the fuel types of the vessels are changed from the most economical fuel type to the lightest fuel type on board and that the sulphur content in the fuel is altered.

How does the method perform when applied on AIS data of global ports?
The performance of the method is tested by two case studies on two different ports. The case studies show that the developed model provides an insight in the emission distribution patterns in a port. The fairway

sections which are subjected to high emissions can be identified immediately and so the emission hotspots can be determined. The model provides the ability for down-drilling, due to which the source of the emission hotspot can be identified. The results of the case studies show the capability of the model for down-drilling to vessel types, operational modes and all the way down to a single vessel in space and time.

By the down-drilling to operational modes in the case study in the Port of Constanța, the model shows a high number of berthed vessels. The model assigns these modes due to low vessel speeds and thus performs as expected on this front. However the sensitivity of the model to the distance to destination in small ports can therefore not be checked. Further research is needed to draw a conclusion. The Port of Rotterdam shows reliable results around the categorization of the AIS messages in operational modes.

The quantity of emissions is hard to validate since the scope of previous and upcoming researches is most of the time different. The port of Constanța shows a good quantification of the emissions. However, the emission estimation of the Port of Rotterdam is far from the expected amount of emissions. The quantification of emissions is assumed to be unreliable and further research is needed to validate these.

By indicating the exact location of the hotspot and identifying the cause of these high emissions by down-drilling, a concrete reduction strategy can be set up. The strategies can be simulated with the developed model and the effect of these measures can be quantified by comparing the emission reduction strategy to a situation without these measures. Three strategies are proposed and tested with the model in three separate case studies. The first strategy concerns installing shore power, the second strategy shows the effects of switching from a normal tugboat fleet to a zero-emission tugboat fleet, and the third strategy showed the effects of applying ECA limits. These case studies showed that the model has the ability to evaluate specific emission reduction strategies. However, the zero-emission tugboat fleet case study showed that the emissions of tugboats must be subjected to further research, as applying this measure did not show a decrease in emissions during manoeuvring. This could be due to the fact that the operational modes maintained in this research do not seamlessly coincide with the operations of tugboats.

With the sub-questions answered, the research question can be answered:

How to estimate vessel emissions in ports using AIS data in order to identify emission distribution patterns and evaluate emission reduction strategies?
A bottom-up method is developed to estimate CO_2, SO_x, NO_x and PM_{10} emission of a single vessel in space and time. This is done breaking down the emissions of a vessel into emissions coming from the main engines and the auxiliary engines. The contribution of both engines is operational mode-specific. Four operational modes are established and assigned to each timestamp based on speed and distance to destination, both derived from the AIS data. The emissions from the main engine are based on a resistance calculation method and the emissions from the auxiliary engines are based on values provided by the IMO. The resistance calculation takes into account the characteristics of the vessel from a vessel database and characteristics of the fairway from a FIS graph.

The developed model makes use of AIS data, local waterway properties, empirical emission factors and operational modes. This data is used in a physics based method to estimate the resistance and the energy consumption. If this information is available, all this combined makes the approach in principle applicable to any port.

The developed model provides an insight in the emission distribution patterns and provides the ability for down-drilling to find the source of the emission hotspots. A targeted emission reduction strategy can be proposed and the model performs well when modelling the effect of these measures. The quantification of the emissions must however be subjected to further research.

10

Recommendations

10.1. Recommendations for emission reduction strategies

Many emission reduction strategies are possible of which some are discussed in this report. The model is capable of running with simulated AIS data. Further research on how to simulate fleets is required before applying the model to this and therefore this research does not include recommendations of emission reduction strategies based on simulated fleet data. Three measures suitable for reducing emissions specifically in ports are established providing three case studies of emission reduction measures.

The emission reduction measure with the largest impact is the installation of shore power. It can be used to target specific vessel types and the effects show a decrease locally since only the vessels at berth are effected. Combining these two characteristics, emission hotspots can be targeted very efficiently. Also almost all vessel types can be connected to shore power. This way the port basins which are marked by the model as emission hotspots can be tackled. To reduce emissions in ports this reduction strategy would be recommended. The investment costs can be a drawback, since they are high and need to be paid by the port itself or sometimes with financial support of municipalities. Applying regulations does not bring costs for these stakeholders. The regulations however, do affect the shipowner companies as some vessels need to be re-equipped. When discussing regulations not only ECAs can be considered, but other rules and sub-mechanisms, like emission taxes could encourage captains and shipbuilders to reduces their emissions. However the effect of such measures is limited. For example, applying ECA limits is only very effective at reducing SO_x emissions. When stricter regulations around sulphur emissions are drawn up, this is a relative easy method to reduce these.

To reduce emissions, an option often looked at is the use of cleaner fuels. Adopting zero-emission tugboats showed that the emissions in all operational modes were reduced. However the model applied to tugs comes with a higher uncertainty, so the before applying this measure more research needs to be done.

As the results from the case studies showed that high emissions are caused by the larger vessels, here great strides can be made. This can be achieved by decreasing the time of these vessels in the port. This can be achieved by decrease the loading and unloading time and keeping port delays to a minimum. It is also advised to connect these specific groups of vessels to shore power.

From the case study results is also concluded that fairway junctions are often emission hotspots. Therefore, when designing a port, it must be kept in mind that junctions between fairways cause higher emissions, so these should be kept to a minimum.

Small changes can lead to big reductions. Every little bit helps, when working towards a climate neutral industry.

10.2. Recommendations for future research

As in any research, there is always room for improvement. Based on the limitations of the model several recommendations are supported.

The method does not take into account the effect of currents. The main engine power consumption estimation can be improved by taking currents into account in further research. Currents variate in space and time and are directional. Therefore, detailed data about currents at different locations in the port is needed to improve the method.

The water depth also varies in time and space. The depth is of influence on flows around a vessel. The bathymetry of the port is needed and multiple water height measurement locations must be evaluated. The information must also be available for the time span the emissions are calculated in.

This study focuses on the ten vessels which are responsible for the largest share of emissions. The model can be improved by adding more vessel types to the calculation. Note that information about the characteristics of the vessel types must be available. RoRo ships would be suggested as first addition since their power consumption patterns fits well with the method used in this research. The research has shown that tankers do not follow this power consumption patterns and the approach for these vessels must be adjusted. It is recommended to add an approach for estimating emissions from boilers. Furthermore, the emission pattern of tugboats needs further examination as it could not be demonstrated that the split of emissions into operational modes is correctly.

With developing the method, several assumptions have been made. The behavior of captains is generalized by setting limits for turning on and off the engines and AIS transmitters. Also tugboat assistance is of influence on the emission patterns of a vessel. Studies about the behaviour of captains and vessels in ports could be of great value when determining emissions.

By improving the input data, the model will improve as well. When all vessel characteristics are known a more accurate estimation of emissions can be done. This study uses data from the Sea-web Ships database. A recommendation could be to combine multiple databases, to reduce the number of missing vessels and entries. The energy consumption estimates and emission factors from the IMO can also be evaluated. Although excessive testing is done by the IMO, more accurate ways to measure these are becoming available. The values changes change over time, so frequently updating the values is advised.

Lastly, the computational time can be reduced. This can be achieved by smart coding solutions, like object-based programming, or running parts of the model simultaneously or with different programs. AIS data is becoming more widely available and its quality is improving rapidly, therefore it is likely that the size of the datasets will increase as well.

Appendices

A

Energy consumption of the main engine

A.1. Resistance calculation

The total resistance a vessel experiences is the sum of multiple resistance components (see Equation 3.5). These components are explained in the following sections.

A.1.1. Frictional resistance R_f

The frictional resistance component is caused by the friction of the water acting on the entire wetted area of the hull. This force is dependent on the wetted surface area (S), the velocity profile, the surface roughness and water viscosity. The function according the ITTC-1957 friction formula becomes:

$$R_f = C_f \frac{1}{2} \rho V_0^2 S \tag{A.1}$$

With:

- R_f = frictional resistance [N]
- C_f = friction coefficient [-]
- ρ = density of water [kg/m^3]
- V_0 = velocity of the vessel [m/s]
- S = wetted surface area [m^2]

The friction coefficient is estimated according the method from ITTC57 and is explained in subsubsection A.1.1.2. The density of water in ports is ranging from 1025 kg/m^3 close to the harbour entrance (sea water) to 1000 kg/m^3 further inland (fresh water). To keep this method widely applicable the average is taken of these values.

It must be noted that in this equation the velocity of the vessel must be stated with respect to the water (speed through water). However, since currents are neglected due to the scope of this research, the speed over ground is used.

The wetted surface area is determined according the method of Holtrop and Mennen and is explained in subsubsection A.1.1.1.

A.1.1.1. Wetted surface area S

$$S = L\,(2T + B)\sqrt{C_M}\,(0,453 + 0.4425\,C_B - 0.2862\,C_M - 0.003467\frac{B}{T} + 0.3696\,C_{wp}) + 2.38\frac{A_{BT}}{C_B} \tag{A.2}$$

With:

- S = wetted surface area [m^2]
- L = length of the vessel [m]
- T = draught of the vessel [m]
- B = width of the vessel [m]
- C_M = midship section coefficient [-]

- C_B = block coefficient [-]
- C_{wp} = waterplane area coefficient [-]
- A_{BT} = transverse sectional area of the bulb [m^2]

The block coefficient is the ratio between the underwater volume of the vessel's hull to a rectangular block underwater with the same length and width of the vessel's underwater dimensions and the depth of the rectangle equal to the draught of the vessel. The block coefficient varies strongly per vessel type. For each of the vessel types a typical block coefficient is derived from MAN Energy Solutions (MAN Energy Solutions, 2018).

Vessel Type	C_B
Bulk carrier	0.8
Oil tanker	0.805
Chemical tanker	0.74
Liquefied gas tanker	0.7
Container ship	0.66
General cargo ship	0.775
Passenger ship	0.6
Passenger ship - Cruise	0.65
Ro-Pax ship	0.6
Tugboat	0.5

Table A.1 Vesseltypes and their corresponding block coefficients

The midship section coefficient and the waterplane area coefficient both depend on the block coefficient. These coefficients are determined with formula of Schneekluth and Bertram (1998):

$$C_M = 1.006 - 0.0056 C_B^{-3.56} \tag{A.3}$$

$$C_{wp} = \frac{1 + 2C_B}{3} \tag{A.4}$$

The transverse sectional area of the bulb is calculated with the following formula:

$$A_{BT} = C_{BB}\ B\ T\ C_M \tag{A.5}$$

Where C_{BB} stands for breadth parameter which represents the ratio of the maximum breadth of the bulb area to the beam of the vessel (B_B/B_{MS}). The breadth parameter typically varies between 0.17 and 0.2. In this study no detailed information of the bulbous bow is available, hence for simplification a value of 0.19 for all ocean-going vessels is maintained.

A.1.1.2. Friction coefficient C_f

The dimensionless friction coefficient is determined with the ITTC57-method. This method neglects flow and waterway restrictions, which is in reality not the case in ports. For simplification, the lateral waterway restrictions are not taken into account, since they are generally of less influence. However, the limited water depth in ports is of large influence and can therefore not be neglected (see Section 2.2.3). For this reason, a modification is made by Zeng et al. (2018) to take in shallow water effects.

The original friction resistance correlation line defined by ITTC57, is as follows:

$$C_{f0} = \frac{0.075}{(log R_e - 2)^2} \tag{A.6}$$

In which R_e is the Reynolds number which can be calculated according:

$$R_e = \frac{V_0 L}{\nu} \tag{A.7}$$

With L being the ship length and with ν the kinematic viscosity which is assumed to be $10^{-6} m^2/s$.

The modification made by Zeng et al. (2018) is based on a regression analysis performed on Computational Fluid Dynamics calculations. This method leads to a frictional resistance coefficient for deep water (D/L

> 1) and a proposed frictional resistance coefficient for shallow water (D/L < 1). The proposed frictional coefficient can not be used directly, because also the non-horizontal wetted surface areas need to be taken into account. The frictional resistance coefficient for deep water needs no further alternations and can be described with:

$$C_{f,deep} = \frac{0.08169}{(logR_e - 1.717)^2} \tag{A.8}$$

The final modified frictional resistance coefficient for shallow water is:

$$C_{f,shallow} = C_{f0} + (C_{f,proposed} - C_{f,Katsui}) \frac{S_B}{S} \left(\frac{V_1}{V_0}\right)^2 \tag{A.9}$$

With the proposed frictional resistance coefficient for shallow water as:

$$C_{f,proposed} = \frac{0.08169}{(logR_e - 1.717)^2} \left(1 + \frac{0.003998}{(logR_e - 4.393)} \left(\frac{D}{L}\right)^{-1.083}\right) \tag{A.10}$$

And the frictional resistance coefficient of a flat plate in unrestricted conditions determined with Katsui's line as:

$$C_{f,Katsui} = \frac{0.0066577}{(logR_e - 4.3762)^a} \tag{A.11}$$

In which:

$$a = 0.042612\ logR_e + 0.56725 \tag{A.12}$$

The other variables are:

- S_B = L * B = area of the flat bottom which is $[m^2]$
- V_1 = corrected velocity of the vessel, velocity under the ship's bottom $[m/s]$
- D = h - T = water depth minus draft of the vessel $[m]$

The corrected velocity underneath the bottom of the ship is determined by Zeng et al. (2018) with linear regression on empirical data. The formula derived is:

$$V_1 = 0.4277\ V_0\ exp\left(\left(\frac{h}{T}\right)^{-0.07634}\right) \tag{A.13}$$

The formula is only valid for h / T ≤ 4. If h / T > 4 the velocity under the vessel bottom remains uncorrected ($V_1 = V_0$).

A.1.2. Viscous resistance $1 + k_1$

Viscosity is the resistance of the fluid to changes in shape. It quantifies the internal frictional force between adjacent layers of fluid that are interacting. A high viscosity means lot of interaction between fluid particles. This gives a high frictional resistance of the vessel. The viscosity is taken into account by multiplying the frictional resistance (R_f) with a form factor ($1 + k_1$). The form factor is calculated according the method of Watson (1998), which is an updated version of the formula determined by Holtrop and Mennen:

$$1 + k_1 = 0.93 + 0.487 c_{14} \left(\frac{B}{L}\right)^{1.068} \left(\frac{T}{L}\right)^{0.461} \left(\frac{L}{L_R}\right)^{0.122} \left(\frac{L^3}{\Delta}\right)^{0.365} (1 - C_p)^{-0.604} \tag{A.14}$$

With:

- $1 + k_1$ = form factor [-]
- c_{14} = coefficient accounting for the specific shape of the after body [-]
- L_R = length of the run $[m]$
- Δ = water displacement $[m^3]$
- C_p = prismatic coefficient [-]

The prismatic coefficient can be expresses as a ratio between the block coefficient and the midship section coefficient:

$$C_p = \frac{C_B}{C_M} \tag{A.15}$$

The coefficient c_{14} can be calculated according Watson (1998):

$$c_{14} = 1 + 0.0011\ C_{stern} \tag{A.16}$$

With the coefficient C_{stern} depending on the shape of the after body according:

= -25 to -20 for a barge-shaped after body

= -10 for an after body with V sections

= 0 for a normal shaped after body

= +10 for an after body with U sections and Hogner stern

For simplification, all vessels are assumed to be normal shaped, hence C_{stern} is equal to zero. This leads to a c_{14} of one.

The length of the run is the length of the immersed shaped stern. This can be calculated according Holtrop and Mennen (1982):

$$L_R = L\ (1 - C_p\ + \frac{0.06\ C_p\ lcb}{4C_p - 1}) \tag{A.17}$$

With lcb the longitudinal position of the centre of buoyancy forward (+) or in the direction of the stern (-). this can be calculated according Saha and Sarker (2010):

$$lcb = -13.5 + 19.4 C_p \tag{A.18}$$

To calculate the water displacement the block coefficient (C_B) is necessary. The formula is (Schneekluth and Bertram, 1998):

$$\Delta = C_B\ L\ B\ T \tag{A.19}$$

A.1.3. Appendage resistance R_{App}

The appendage resistance component accounts for the extra frictional resistance caused by the appendages of a ship. It is expressed as follows (Holtrop and Mennen, 1982):

$$R_{APP} = 0.5\ \rho\ V_0^2\ S_{APP}(1 + k_2)\ C_f \tag{A.20}$$

With:

- R_{APP} = appendage resistance [N]
- S_{APP} = wetted area of the appendages [m^2]
- $1 + k_2$ = appendage resistance factor [-]

The equivalent $(1 + k_2)$ value for a combination of appendages is determined according Holtrop and Mennen (1982):

$$(1 + k_2)_{eq} = \frac{\Sigma(1 + k_2)S_{APP}}{\Sigma S_{APP}} \tag{A.21}$$

Filling this in in Equation A.20 means that the part '$S_{APP}(1 + k_2)$' equals the sum of all appendage types surface areas times the appendage type resistance factor. The appendage resistance factor and surface area differs per appendage type. A distinction is made for single-screw and double-screw vessels. For single-screw vessels the appendage components having the most influence on the total appendage resistance are the bilge keels and the rudders. For double-screw vessels the important components are the balance rudders and the shaft brackets (the shafts itself have a small surface area and are therefore neglected). For cruise vessels the stabilizer fins are also considered. The resistance factors are stated in Table A.2 and are determined by Holtrop and Mennen (1982).

Appendages	**$(1 + k_2)$ value**
Rudder behind skeg	1.5 - 2.0
Rudder behind stern	1.3 - 1.5
Twin-screw balance rudders	2.8
Shaft brackets	3.0
Skeg	1.5 - 2.0
Strut bossings	3.0
Hull bossings	2.0
Shafts	2.0 - 4.0
Stabilizer fins	2.8
Dome	2.7
Bilge keels	1.4

Table A.2 Approximate $(1 + k_2)$ values

For single screw vessels the sum of the rudder and bilge keel components is derived. As a rule of thumb the surface area of a rudder is approximated as 1.5 % of the underwater lateral area of a ship (L * T) (Bertram and Volker, 2012). The appendage resistance coming from the rudder component is 1.5 * 0.015 * L * T with the factor 1.5 representing the resistance factor derived from Table A.2. An average bilge keel is approximately 20 centimeters in width but does not reach over the entire length of the vessel, for this reason the area of the bilge keel is estimated a little smaller than 0.2 times the LOA and is estimated as 0.15 * L. The total appendage resistance coming from the bilge keel is then 1.4 * 0.15 * L. This gives the following sum for single-screw vessels:

For single screw vessels:

$$S_{APP}\ (1 + k_2)_{eq} = (1.5 * 0.015 * L * T + 1.4 * 0.15 * L) \tag{A.22}$$

For double-screw vessels the sum is derived of the twin-screw balance rudders and shaft brackets components. The surface area of a rudder multiplied by two since it is a double-screw vessel. The total appendage resistance coming from the rudders is 2.8 * 2 * 0.015 * L * T with the factor 2.8 derived from Table A.2. For convenience it is assumed that four shaft brackets are present. The surface is estimated as a the area of triangular shape. The triangle reaches over the whole draught and sticks out approximately 30 centimeters. The area of one shaft bracket is multiplied by four and by the resistance factor of 3.0. This gives the following sum for double-screw vessels:

For double-screw vessels:

$$S_{APP}\ (1 + k_2)_{eq} = (2.8 * 2 * 0.015 * L * T + 3.0 * 4 * \frac{1}{2} * 0.30 * T) \tag{A.23}$$

For cruise vessels the stabilizer fins are added to this. The average size of stabilizing fins is determined by Kim and Kim (2011) after a survey on modern cruise vessels and is approximately 50 m^2. With the $(1 + k_2)$-factor 2.8 derived from Table A.2 this gives the following equation for cruise vessels:

For (double-screw) cruise vessels:

$$S_{APP}\ (1 + k_2)_{eq} = (2.8 * 2 * 0.015 * L * T + 3.0 * 4 * \frac{1}{2} * 0.30 * T + 50 * 2.8) \tag{A.24}$$

A.1.4. Resistance due to limited water depth - Karpov method

Additional resistance is caused by the fact that the water depth is limited. When a ship sails in limited water depth it reaches its critical speed sooner and when approaching the critical speed the resistance increases. In subsubsection A.1.1.2 a correction is applied to the frictional resistance according the method of Zeng et al. (2018). This correction is also necessary for the non-frictional resistance components, since the wave pattern of the vessel changes in shallow water, leading to a change in the wave making resistance. This correction is made by applying the Karpov method (Terwisga, 1989). This method replaces the actual speed (V_0) of the vessel with a corrected speed V_2. The corrected speed can be determined with:

$$V_2 = \frac{V_0}{\alpha^{**}} \tag{A.25}$$

With α^{**} as a function of the depth Froude number and ratio between the depth of the fairway and the draft (h/T). The depth Froude number can be calculated according:

$$Fr_h = \frac{V_0}{\sqrt{gh}} \tag{A.26}$$

The figure below (Figure A.1) shows the α^{**} coefficient for different h/T ratios. The h/T ratio closest to the occurring h/T ratio is chosen. With the function corresponding to that line and with the determined Froude number, the alpha is calculated. With the calculated α^{**} the corrected speed can be determined which will be used in the resulting resistance calculations.

The figure is derived from the research of Segers (2020). For each h/T curve, an 6th order polynomial approximation in Excel is applied to determine the α^{**} for each corresponding depth Froude number. The resulting equations for each h/T ratio are implemented in the model.

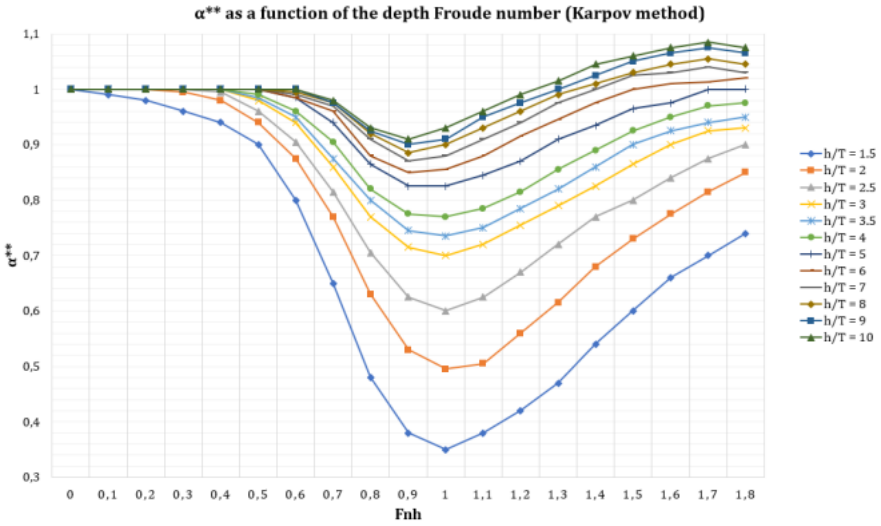

Figure A.1: Karpov method: estimation of α^{**} based on the depth Froude number Fr_h for different h/T ratios

The formulas corresponding to each curve from Figure A.1 are stated in the table below (Table A.3). These formulas are used as input for the model.

h/T ratio		**Formula for α^{**}**		
Curve in Excel	**Range in model**	$\boldsymbol{Fr_h \leq 0.4}$	$\boldsymbol{Fr_h > 0.4}$	
1.5	0 - 1.75	(-4 * 10 ^{-12}) * $Fr_h{}^3$ - 0.2143 * $Fr_h{}^2$ - 0.0643 * Fr_h + 0.9997	-0.9274 * $Fr_h{}^6$ + 9.5953 * $Fr_h{}^5$ - 37.197 * $Fr_h{}^4$ + 69.666 * $Fr_h{}^3$ - 65.391 * $Fr_h{}^2$ + 28.025 * Fr_h - 3.4143	
2	1.75 - 2.25	-0.8333 * $Fr_h{}^3$ + 0.25 * $Fr_h{}^2$ - 0.0167 * Fr_h + 1	2.2152 * $Fr_h{}^6$ - 11.852 * $Fr_h{}^5$ + 21.499 * $Fr_h{}^4$ - 12.174 * $Fr_h{}^3$ - 4.7873 * $Fr_h{}^2$ + 5.8662 * Fr_h - 0.2652	
2.5	2.25 - 2.75	-1.25 * $Fr_h{}^4$ + 0.5833 * $Fr_h{}^3$ - 0.0375 * $Fr_h{}^2$ - 0.0108 * Fr_h + 1	1.2205 * $Fr_h{}^6$ - 5.4999 * $Fr_h{}^5$ + 5.7966 * $Fr_h{}^4$ + 6.6491 * $Fr_h{}^3$ - 16.123 * $Fr_h{}^2$ + 9.2016 * Fr_h - 0.6342	
3	2.75 - 3.75	1	-0.4085 * $Fr_h{}^6$ + 4.534 * $Fr_h{}^5$ - 18.443 * $Fr_h{}^4$ + 35.744 * $Fr_h{}^3$ - 34.381 * $Fr_h{}^2$ + 15.042 * Fr_h - 1.3807	
4	3.75 - 4.5	1	0.3067 * $Fr_h{}^6$ - 0.3404 * $Fr_h{}^5$ - 5.0511 * $Fr_h{}^4$ + 16.892 * $Fr_h{}^3$ - 20.265 * $Fr_h{}^2$ + 9.9002 * Fr_h - 0.6712	
5	4.5 - 5.5	1	0.3212 * $Fr_h{}^6$ - 0.3559 * $Fr_h{}^5$ - 5.1056 * $Fr_h{}^4$ + 16.926 * $Fr_h{}^3$ - 20.253 * $Fr_h{}^2$ + 10.013 * Fr_h - 0.7196	
6	5.5 - 6.5	1	0.9252 * $Fr_h{}^6$ - 4.2574 * $Fr_h{}^5$ + 5.0363 * $Fr_h{}^4$ + 3.3282 * $Fr_h{}^3$ - 10.367 * $Fr_h{}^2$ + 6.3993 * Fr_h - 0.2074	
7	6.5 - 7.5	1	0.8442 * $Fr_h{}^6$ - 4.0261 * $Fr_h{}^5$ + 5.313 * $Fr_h{}^4$ + 1.6442 * $Fr_h{}^3$ - 8.1848 * $Fr_h{}^2$ + 5.3209 * Fr_h - 0.0267	
8	7.5 - 8.5	1	0.1211 * $Fr_h{}^6$ + 0.628 * $Fr_h{}^5$ - 6.5106 * $Fr_h{}^4$ + 16.7 * $Fr_h{}^3$ - 18.267 * $Fr_h{}^2$ + 8.7077 * Fr_h - 0.4745	
9	8.5 - 9.5	1	**if $\boldsymbol{Fr_h < 0.6}$**	**if $\boldsymbol{Fr_h \geq 0.6}$**
			1	-6.4069 * $Fr_h{}^6$ + 47.308 * $Fr_h{}^5$ - 141.93 * $Fr_h{}^4$ + 220.23 * $Fr_h{}^3$ - 185.05 * $Fr_h{}^2$ + 79.25 * Fr_h - 12.484
10	≥ 9.5	1	**if $\boldsymbol{Fr_h < 0.6}$**	**if $\boldsymbol{Fr_h \geq 0.6}$**
			1	-6.0737 * $Fr_h{}^6$ + 44.97 * $Fr_h{}^5$ - 135.21 * $Fr_h{}^4$ + 210.13 * $Fr_h{}^3$ - 176.72 * $Fr_h{}^2$ + 75.728 * Fr_h - 11.893

Table A.3 Formulas used in model to calculate α^{**} for each h/T ratio with corresponding depth Froude number

A.1.5. Wave-making and wave breaking resistance R_w

A vessel creates waves when moving through water. This wave results in additional resistance the vessel needs to overcome: the resistance component 'wave-making and wave breaking'. The height of the wave is determined by the speed of the vessel; a higher vessel speed results in a higher wave. A higher wave on its turn results in a higher wave resistance.

When approaching limited water depth, the wave resistance increases even more. Therefore the calculation of R_w makes use of the corrected speed for shallow water (V_2) determined in the section above (Section A.1.4). Therefore the Froude number used in this calculation changes to:

$$Fr_{V2} = \frac{V_2}{\sqrt{gL}} \tag{A.27}$$

The calculation is split up in three parts: an approach for R_{W1}, R_{W2} and R_{W3}. The choice for which of the three components is used, depends on the Froude number. For $Fr < 0.4$ the approach for R_{W1} is followed, and for $Fr \geq 0.55$ the approach for R_{W2} is followed and for Froude numbers between 0.4 and 0.55 the approach for R_{W3} is followed. The latter one only takes in the R_{W1}, R_{W2} and the Froude number mentioned earlier. (Sarris, 2011)

For $Fr_{V2} < 0.4$:

$$R_{W1} = c_1 c_2 c_5 \Delta \rho g e^{m_1 Fr_{V2}^{-0.9} + m_4 cos(\lambda Fr_{V2}^{-2})} \tag{A.28}$$

For $Fr_{V2} > 0.55$:

$$R_{W2} = c_{17} c_2 c_5 \Delta \rho g e^{m_3 Fr_{V2}^{-0.9} + m_4 cos(\lambda Fr_{V2}^{-2})} \tag{A.29}$$

For $0.4 < Fr_{V2} < 0.55$:

$$R_{W3} = R_{W1} + \frac{(10 Fr_{V2} - 4)(R_{W2} - R_{W1})}{1.5} \tag{A.30}$$

With:

- R_{Wi} = wave resistance [N]
- c_i = coefficients [-]
- Δ = water displacement (Equation A.19) [m^3]
- m_i = coefficients [-]
- Fr_{V2} = Froude number based on corrected speed [-]
- λ = wave-making length [-]

The coefficients c and m will be explained in the section below (subsubsection A.1.5.1).

The wave-making length depends on the ratio between L and B:

For L/B < 12:

$$\lambda = 1.446 C_p - 0.03 \frac{L}{B} \tag{A.31}$$

For L/B > 12:

$$\lambda = 1.446 C_p - 0.036 \tag{A.32}$$

A.1.5.1. Coefficients c_i and m_i

Coefficient c_1 (Holtrop and Mennen, 1982)
The first coefficient in the formula for R_{W1} is c_1:

$$c_1 = 2223105\ c_7^{3.78613} \left(\frac{T}{B}\right)^{1.07961} (90 - i_E)^{-1.37165} \tag{A.33}$$

With i_E as the half angle of entrance in degrees, which represents the angle of the waterline at the bow:

$$i_E = 1 + 89\ exp\left(-\left(\frac{L}{B}\right)^{0.80856} (1 - C_{wp})^{0.30484} (1 - C_p - 0.225\ lcb)^{0.6367} \left(\frac{L_R}{B}\right)^{0.34574} \left(\frac{100\ \Delta}{L^2}\right)^{0.16302}\right) \tag{A.34}$$

The coefficient c_7 depends on the ratio between B and L according:

For B/L < 0.11:

$$c_7 = 0.229577 \left(\frac{B}{L}\right)^{0.33333} \tag{A.35}$$

For 0.11 < B/L < 0.25:

$$c_7 = \frac{B}{L} \tag{A.36}$$

For B/L > 0.25:

$$c_7 = 0.5 - 0.0625\frac{B}{L} \tag{A.37}$$

Coefficient c_2 (Holtrop and Mennen, 1982)
The c_2 coefficient account for the reduction on the wave resistance caused by the presence of a bulbous bow:

$$c_2 = e^{-1.89\sqrt{c_3}} \tag{A.38}$$

With c_3 determining the influence of the bulbous bow on the wave resistance:

$$c_3 = 0.56\frac{A_{BT}^{1.5}}{B\ T\ (0.31\ \sqrt{A_{BT}} + T - h_B)} \tag{A.39}$$

The variable h_B describes the position of the centre of the transverse area A_{BT} above the keel line. The value for h_B should not exceed the upper limit of 0.6 T. For simplicity the centre is assumed to be positioned in the middle of the vessel, so that h_B = 0.5 T.

Coefficient c_5 (Holtrop and Mennen, 1982)
The c_5 coefficient accounts for the transom stern influence on the wave resistance:

$$c_5 = 1 - \frac{0.8\ A_T}{B\ T\ C_M} \tag{A.40}$$

With A_T the immersed part of the transverse area of the transom. This is assumed to be 0.2 B T.

Coefficient c_{17} (Sarris, 2011)
The coefficient c_{17} can be estimated according:

$$c_{17} = 6919.3\ C_M^{-1.3346}\left(\frac{\Delta}{L^3}\right)^{2.00977}\left(\frac{L}{B} - 2\right)^{1.40692} \tag{A.41}$$

Coefficient m_1 (Holtrop and Mennen, 1982)
The coefficient m_1 is described as:

$$m_1 = 0.0140407\ \frac{L}{T} - 1.75254\frac{\Delta^{1/3}}{L} - 4.79323\frac{B}{L} - c_{16} \tag{A.42}$$

In which c_{16} depends on the prismatic coefficient:

For C_P < 0.8:

$$c_{16} = 8.07981\ C_P - 13.8673\ C_P^2 + 6.984388\ C_P^3 \tag{A.43}$$

For C_P > 0.8:

$$c_{16} = 1.73014 - 0.7067\ C_P \tag{A.44}$$

Coefficient m_4 (Sarris, 2011)
The coefficient m_4 is described as:

$$m_4 = 0.4\ c_{15}\ e^{-0034\ Fr_{V2}^{3.29}} \tag{A.45}$$

In which c_{15} depends on the ratio between L and Δ:

For L^3/Δ < 512:

$$c_{15} = -1.69385 \tag{A.46}$$

For 512 < L^3/Δ < 1727:

$$c_{15} = -1.69385 + \frac{\left(\frac{L}{\Delta^{1/3}} - 8\right)}{2.36} \tag{A.47}$$

For L^3/Δ > 1727:

$$c_{15} = 0 \tag{A.48}$$

Coefficient m_3 (Sarris, 2011)
The coefficient m_3 is described as:

$$m_3 = -7.2035\left(\frac{B}{L}\right)^{0.326869}\left(\frac{T}{B}\right)^{0.605375} \tag{A.49}$$

A.1.6. Residual terms R_B, R_{TR}, R_A

The residual resistance terms according Holtrop and Mennen (1982) consist of three terms: the additional pressure resistance of the bulbous bow near the water surface (R_B), the additional resistance caused by the immersed transom stern (R_{TR}) and the model-ship correlation resistance (R_A).

A.1.6.1. Bulbous bow resistance R_B

The additional resistance caused by the presence of a bulbous bow near the surface is expressed as follows:

$$R_B = \frac{0.11\ e^{-3Pb^{-2}} Fr_{im}^3 A_{BT}^{1.5}\ \rho\ g}{1 + Fr_{im}^2} \tag{A.50}$$

With:

- R_B = bulbous bow resistance [N]
- P_B = emergence of the bow [-]
- Fr_{im} = Froude number based on the immersion [-]

The emergence of the bow can be expressed as:

$$P_B = \frac{0.56\sqrt{A_{BT}}}{T - 1.5h_B} \tag{A.51}$$

The Froude number based on immersion can be calculated according:

$$Fr_{im} = \frac{V_2}{\sqrt{g\ (T - h_B - 0.25\sqrt{A_{BT}}) + 0.15V_2^2}} \tag{A.52}$$

A.1.6.2. Immersed transom stern resistance R_{TR}

The resistance of the immersed transom stern is calculated according:

$$R_{TR} = 0.5\rho V_2^2 A_T c_6 \tag{A.53}$$

With the coefficient c_6 dependent on the Froude number based on the transom immersion. For $Fr_T > 5$ the coefficient c_6 is assumed zero. For $Fr_T < 5$ the coefficient can be determined according:

$$c_6 = 0.2(1 - 0.2Fr_T) \tag{A.54}$$

The Froude number based on the transom immersion can be determined according:

$$Fr_T = \frac{V_2}{\sqrt{2gA_T/(B + BC_{wp})}} \tag{A.55}$$

A.1.6.3. Model-ship correlation resistance R_A

The model-ship correlation resistance is expressed as:

$$R_A = \frac{1}{2} V_2^2 S C_A \tag{A.56}$$

With the correlation allowance coefficient C_A as:

$$C_A = 0.006(L + 100)^{-0.16} - 0.00205 + 0.003\sqrt{L/7.5}\ C_B^4 c_2 (0.04 - c_4) \tag{A.57}$$

With the coefficient c_4 depending on the ratio between T and L:

For T / L ≤ 0.04:

$$c_4 = \frac{T}{L} \tag{A.58}$$

For T / L > 0.04:

$$c_4 = 0.04 \tag{A.59}$$

A.2. Efficiency components

The calculation of the energy consumption of the main engine takes in some efficiency components. To get from the effective power (P_e) to the delivered horse power (P_d), the open water efficiency of the propeller, the relative rotative efficiency and the hull efficiency need to be determined. In the same manner, to get from the delivered horse power (P_d) to the brake horse power (P_b), the transmission efficiency and gearing efficiency need to be determined.

A.2.1. Open water efficiency η_o

The open water efficiency describes the propeller efficiency when working on open water. With open water is meant a homogeneous wake field with the hull of the vessel disregarded. This efficiency is dependent on many propeller characteristics (such as the thrust force, the number of blades, the disk area ratio, etc.) which are hard to derive from the available AIS data. Typical values for open water efficiency vary between 0.55 and 0.7 (MAN Energy Solutions, 2018). A value of 0.6 is assumed for all vessel types to be on the average though conservative side.

$$\eta_o = 0.6 \tag{A.60}$$

A.2.2. Relative rotative efficiency η_r

The relative rotative efficiency of the propeller accounts for the losses of the propeller relative to the open water situation. Compared to open water flow conditions, the flow is not constant and the wake field is not homogeneous. The efficiency differs for ships with a single and double propeller arrangement. Typical values for relative rotative efficiency are 1 - 1.07 for ships with a single screw and approximately 0.98 for ships with two screws. For ships with a single screw a value of 1 is assumed (MAN Energy Solutions, 2018).

The number of screws depends on the vessel type. For vessels which require high efficiencies, the number of screws is typically one. For vessels which require a high reliability or smooth manoeuvring, two or more screws are needed. The AIS data provides the number of screws for each specific vessel.

For single screw vessels:

$$\eta_r = 1.0 \tag{A.61}$$

For double screw vessels:

$$\eta_r = 0.98 \tag{A.62}$$

A.2.3. Hull efficiency η_h

The hull efficiency accounts for the interaction between the hull and the propeller. It describes the ratio between the amount of work required to tow a certain hull at a given speed to the amount of work required to drive it with a certain propeller. The efficiency can be expressed as (Terwisga, 1989):

$$\eta_h = \frac{1-t}{1-w} \tag{A.63}$$

With:

- η_h = hull efficiency [-]
- t = thrust deduction coefficient [-]
- w = wake fraction coefficient [-]

A.2.3.1. Wake fraction coefficient

The wake fraction coefficient is expresses as:

$$w = 0.11 \frac{0.16}{x} C_B \sqrt{\frac{\Delta^{1/3}}{D_s}} - \Delta w \tag{A.64}$$

With:

- w = wake fraction coefficient [-]
- x = number of screws [-]
- D_s = diameter of the screw [-]
- Δw = velocity correction coefficient [-]

The diameter of the screw can be approached with a rule of thumb. For single-screw ships 0.7T - 0.8T is typical, for double-screw ships 0.6T - 0.7T. For simplicity both values are assumed to be 0.7T.

The velocity correction coefficient depends on the Froude number. If $Fr < 0.2$ the velocity correction coefficient is zero. If $Fr \leq 0.2$ the coefficient is 0.1. The Froude number can be calculated with:

$$Fr = \frac{V_0}{\sqrt{gL}} \tag{A.65}$$

A.2.3.2. Thrust deduction coefficient

The thrust deduction coefficient depends on the number of screws:

For single-screw vessels:

$$t = 0.6w(1 + 0.67w) \tag{A.66}$$

For double-screw vessels:

$$t = 0.8w(1 + 0.25w) \tag{A.67}$$

A.2.4. Gearing efficiency η_g

The gearing efficiency takes into account the losses at the shaft and the gearbox. A typical value for the gearing efficiency is 0.96 (Watson, 1998).

$$\eta_g = 0.96 \tag{A.68}$$

B

Energy consumption of the auxiliary engine

The values for the power demand of the auxiliary engine are derived from research of International Maritime Organization (2021). This research states that they based these values on the following approach:

- Updating the values from the Third IMO GHG Study (Smith et al., 2015).
- Starcrest's Vessel Boarding Program (VBP) reports from 2012 to 2018 (Starcrest Consulting Group LLC, 2020):
  Provides operational data from more than 1,200 different ships allowing for a representative sample of their powering needs. Ship types that are monitored include containers, bulk carriers, tankers of different types, Ro-Ro, cruise, general cargo among others. This study also has access to on-board data, albeit, for a reduced number of specific ships, for fuel consumption and power output.
- Auxiliary engine and boiler fuel consumption data provided by ClassNK:
  Provides hourly observations for the auxiliary machinery power demanded on-board liquefied gas tankers converted to energy consumption.
- Auxiliary engine fuel consumption provided by continuous monitoring data:
  Provides hourly observations for the auxiliary machinery power demanded on-board liquefied gas tankers. The hourly observations provide speeds and main engine maximum continuous ratings, allowing for the auxiliary engine power output to be classified per operational modes.
- Expertise/Professional judgement from experts on the field:
  The tentative power output for both auxiliary engines and boilers at different operational modes have been sent to ship operators and experts to fine-tune the numbers.

After adding the power consumption of the boilers to the power consumption of the auxiliary engines for the three tanker types, the final power consumption values are stated in the table below.

Ship Type	Size	Unit	Auxiliary Engine Power Output (kW)			
			At berth	Anchored	Manoeuvring	Sea
Bulk carriers	0-9,999	dwt	110	180	500	190
	10,000-34,999		110	180	500	190
	35,000-59,999		150	250	680	260
	60,000-99,999		240	400	1100	410
	100,000-199,999		240	400	1100	410
	200,000-+		240	400	1100	410
Chemical tankers	0-4,999	dwt	780	170	190	200
	5,000-9,999		1000	490	560	580
	10,000-19,999		1330	490	560	580
	20,000-39999		2140	550	900	660
	40,000-+		2140	550	900	660
Container ships	0-999	TEU	370	450	790	410
	1,000-1,999		820	910	1750	900
	2,000-2,999		610	910	1900	920
	3,000-4,999		1100	1350	2500	1400
	5,000-7,999		1100	1400	2800	1450
	8,000-11,999		1150	1600	2900	1800
	12,000-14,499		1300	1800	3250	2050
	14,500-19,999		1400	1950	3600	2300
	20,000-+		1400	1950	3600	2300
General cargo ships	0-4,999	dwt	90	50	180	60
	5,000-9,999		240	130	490	180
	10,000-19,999		720	370	1450	520
	20,000-+		720	370	1450	520
Liquefied gas tankers	0-49,999	cbm	1240	240	360	240
	50,000-99,999		2700	1700	2600	1700
	100,000-199,999		4000	2000	2300	2650
	200,000-+		9750	7200	7200	6750
Oil tankers	0-4,999	dwt	750	250	375	250
	5,000-9,999		1125	375	560	375
	10,000-19,999		1940	500	580	490
	20,000-59,999		3420	520	600	510
	60,000-79,999		3870	490	770	560
	80,000-119,999		4800	640	910	690
	120,000-199,999		9000	770	1300	860
	200,000-+		9500	770	1300	860
Passenger ships	0-299	gt	190	190	190	190
	300-999		190	190	190	190
	1000-1999		190	190	190	190
	2000-+		520	520	520	520
Passenger ships - Cruise	0-1,999	gt	450	450	580	450
	2,000-9,999		450	450	580	450
	10,000-59,999		3500	3500	5500	3500
	60,000-99,999		11500	11500	14900	11500
	100000-149999		11500	11500	14900	11500
	150000-+		11500	11500	14900	11500
RoPax ships	0-1999	gt	105	105	105	105
	2000-4999		330	330	330	330
	5000-9999		670	670	670	670
	10000-19999		1100	1100	1100	1100
	20000-+		1950	1950	1950	1950
Tugboats	0-+	gt	100	80	210	80

Table B.1 Power output auxiliary engine per vessel type and size (International Maritime Organization, 2021)

C

Base emission factors

The base emission factors used in this research are derived from fourth IMO greenhouse gas study (International Maritime Organization, 2021). The EF_{base} for each emission type is dependent on certain fuel characteristics and engine characteristics. The method to determine the correct base emission factor for each individual vessel is described in detail in this appendix.

C.1. Base emission factor CO_2

The base emission factor for CO_2 is fuel based. To determine the EF_{base} the fuel type of the vessel must be known. The corresponding emission factor can then be derived from Table C.1.

Fuel type	**EF** CO_2 **[g** CO_2 **/ g fuel]**
HFO	3.114
MDO	3.206
LNG	2.750
Methanol	1.375

Table C.1 Base emission factor for CO_2 for different fuel types

C.1.1. Fuel type

The IHS database has two categories for the fuel type of the vessel: 'Fuel Type 1' and 'Fuel Type 2'. The first fuel type is the lightest fuel type registered to the vessel. Due to the scope of this research it is assumed that when a vessel is sailing in port area located inside an ECA, it operates on its lightest fuel type.

If the lightest fuel type is registered in the IHF database as 'HFO' and the vessel is sailing in an ECA, this is an outdated entry since the vessel must comply with the 0.1% m/m stringent ECAs since 2020. All these vessels are assumed to have switched to 'MDO'. This is a generalisation and it must be noted that also other low-sulphur fuel oils can be used to comply with the 0.1% m/m stringent ECAs, but the share of these fuel oils was (in 2018) less than 2% and is therefore neglected in this research (International Maritime Organization, 2021).

When the port is *not* located inside an ECA, the vessel will most likely not sail on the lightest fuel but on the most economical fuel. When more than one fuel is allocated to the vessel, a representative main fuel is allocated. This allocation procedure is based on conditional logic. Table C.2 describes the possible fuel arrangements and the logic behind the main fuel type allocation. In the database the fuel type 'LPG' and 'Ethane' occur. LNG, LPG and Ethane are used for many of the same applications so for simplicity of the research the fuel types LPG and Ethane are replaced by LNG. It is important to note that the use of scrubbers is neglected in this research, so the emission of vessels operating on HFO is over estimated.

Main Fuel	Condition	Explanation
HFO	Fuel Type 1 or Fuel Type 2 is 'Residual Fuel'	HFO is the cheapest fuel on the market. When the port area is not inside an ECA, a vessel having this fuel on board is economically seen most likely to use HFO.
	Exception: When the vessel type is 'Liquefied gas tanker' and the engine type is 'Turbine'	These vessels are allocated LNG.
MDO	Fuel Type 1 and Fuel Type 2 is 'Distillate Fuel'	The vessel only has distillate fuel on board, so no other fuel can possibly be used.
	Fuel Type 1 or Fuel Type 2 is 'Distilled Fuel' and the remaining column is 'Not Applicable'	The vessel has only reported distillate fuel, so no other fuel can be assigned.
	Fuel Type 1 is 'Coal' and Fuel Type 2 is 'Distillate Fuel'	Coal is not able to compete with distillate fuel in terms of costs and energy. The vessel is most likely to be sailing the largest part of the trip on distillate fuel.
LNG	Fuel Type 1 is 'Lng' and Fuel Type 2 is 'Distillate Fuel'	Based on the cost of the investment to make a vessel operating on distillate fuel compatible with LNG, it is most likely that LNG is used to earn back the costs.
	Fuel Type 1 is 'Lng' and Fuel Type 2 is 'Not Applicable'	The vessel has only reported LNG fuel, so no other fuel can be assigned.
	Fuel Type 1 is 'Gas Boil Off' and Fuel Type 2 is 'Distillate Fuel'	Gas Boil Off engines use LNG as fuel.
	Fuel Type 2 is 'Gas Boil Off'	Gas Boil Off engines use LNG as fuel.
	Vessel type is 'Liquefied gas tanker', engine type is 'Turbine' and Fuel Type 1 or Fuel Type 2 is 'Residual Fuel'	A liquefied gas tanker with a steam turbine uses LNG
Methanol	Fuel Type 1 is 'Methanol' (and Fuel Type 2 is in this case always 'Distillate Fuel')	Methanol is likely to be more widely used in the nearby future.
Nuclear	Fuel Type 1 is 'Nuclear' and Fuel Type 2 is 'Distillate Fuel'	All vessels in this category are passenger vessels or cruise vessels with a high power demand. To supply enough energy, nuclear fuel is the most likely main fuel.
	Fuel Type 1 is 'Nuclear' and Fuel Type 2 is 'Not Applicable'	The vessel has only reported nuclear fuel, so no other fuel can be assigned.
Coal	Fuel Type 1 is 'Coal' and Fuel Type 2 is 'Not Applicable'	The vessel has only reported coal as fuel, so no other fuel can be assigned.
Hydrogen	Fuel Type 1 is 'Hydrogen' and Fuel Type 2 is 'LNG'	All vessels in this category are passenger vessels or cruise vessels. This fuel type is used for short distances.

Table C.2 Main fuel type allocation procedure

C.2. Base emission factor SO_x

The base emission factor SO_x is fuel based. To determine the EF_{base} the fuel type of the vessel must be known. The emissions factor is determined directly from the fuel sulphur content according to International Maritime Organization (2021):

$$EF_{SO_x} = 2 * 0.97753 * \text{sulphur content in fuel} \tag{C.1}$$

The formula shows a factor 0.97753 because 97.753% of sulphur in the fuel is converted to SO_x (the other 2.247% is converted to sulphate aerosols which is part of particulate matter). The factor 2 comes from the ratio of the molecular weight of SO_2 to sulphur because, for ship emissions, the vast majority of SO_x is SO_2 (International Maritime Organization, 2021).

The sulphur content in fuel depends on if the vessel is sailing inside or outside an emission control area, due to the newly implemented "IMO 2020" rule. This rule limits the sulphur in the fuel oil used on board ships to 0.50% m/m (previous limit of 3.5%) and within defined emission control areas the limits were already stricter (0.10%). Due to this stricter requirements there has been a shift in the average sulphur content in fuels and the annual world sulphur content averages from preceding years can not be used. The most recent research is the sulphur monitoring program for 2020 done by the IMO. This report gives an average yearly sulphur content for three categories: fuel oil not exceeding 0.10% (fuel used inside the emission control areas), fuel oil not exceeding 0.50% but above 0.10% (fuel used outside the emission control areas) and fuel oil exceeding 0.50% (fuel oil used in conjunction with equivalent means). These values are stated in Table C.3.

Category	**Inside ECA** ≤ **0.10%**	**Outside ECA** > **0.10 to** ≤ **0.50%**	**In conjunction** > **0.50%**
HFO	0.1216	0.4556	2.5558
MDO	0.0564	0.2126	0.5210

Table C.3 Average sulphur content per fuel type in 2020 [%]

With Equation C.1 and the average sulphur content, the emission factors for SO_x are calculated. The values are stated in Table C.4. Dependent on in which area (inside an ECA or outside an ECA) the investigated port is located, the corresponding column is used. Most European ports are likely to handle the < 0.1% sulphur content requirement. Ports in other places around the world are slowly adapting towards the < 0.1% sulphur content requirement.

The values exceeding 0.5% do not represent the actual amount of sulphur (or particulate matter) emitted in the atmosphere since the vessels using fuel with this sulfur content are most likely to have scrubbers. However, the use of scrubbers is neglected in this research. It is of importance for future research to evaluate this trend, since neglecting scrubbers will cause an over-estimation of the actual amount of SO_x (and PM_{10}) emissions.

	EF SO_x [**g** SO_x **/ g fuel**]	
Fuel type	**Inside ECA** ≤ **0.10%**	**Outside ECA** > **0.10 to** ≤ **0.50%**
HFO	0.0023774	0.0089073
MDO	0.0011027	0.0041565
LNG	0.0000317	0.0000317
Methanol	0.00264	0.00264

Table C.4 Base emission factor for SO_x for different fuel types

C.3. Base emission factor NO_x

The base emission factor for NO_x is energy based. The age dependency, captured in the tiers (Section C.3.2), and the engine speed dependency (Section C.3.1) are the criteria for determining the emission factor. Further it is necessary to determine if the vessel is fuelled with LNG, Methanol or any other fuel type, since for first two fuels different values apply. When these characteristics are known, the corresponding emission factor can be determined with Table C.5, Table C.6 and Table C.7.

	EF NO_x [g NO_x / kWh]			
Engine type	**Tier 0**	**Tier 1**	**Tier 2**	**Tier 3**
SSD	18.1	17	14.4	3.4
MSD	14.00	13.00	10.5	2.6
HSD	10.00	9.8	7.7	2.0
Auxiliary Engine	11.2			
Turbine	4.2			

Table C.5 Base emission factor for NO_x for all fuel types except Methanol and LNG

	EF NO_x [g NO_x / kWh]			
Engine type	**Tier 0**	**Tier 1**	**Tier 2**	**Tier 3**
Methanol-SS	18.1	17	14.4	3.4
Methanol-MS	14.00	13.00	10.5	2.6

Table C.6 Base emission factor for NO_x for fuel type Methanol

	EF NO_x [g NO_x / kWh]			
Engine type	**Tier 0**	**Tier 1**	**Tier 2**	**Tier 3**
LNG-Otto-SS	1.30			
LNG-Otto-MS	1.30			
LNG-Diesel	18.10	17.00	14.40	3.40
LBSI	1.30			
Auxiliary Engine	1.30			
Turbine	1.30			

Table C.7 Base emission factor for NO_x for fuel type LNG

C.3.1. Engine type and speed

The engine speed of the vessel depends on the engine type and the RPM. The following classification is used in this research:

Oil engines

The oil engines are all vessels from the IHS database which have stated 'Oil' in the category 'engine type'. These can be divided into three engine speed groups depending on their RPM:

- **Slow-speed Diesel (SSD)**: All vessels with oil engines which have an engine speed of ≤ 300 RMP are considered slow-speed engines. Slow-speed diesel engines are the most common engines and therefore SSD is the default engine type when no RPM is known and the engine type is 'Oil'.
- **Medium-speed Diesel (MSD)**: All oil engines with an engine speed between 300 and 900 RPM are classified as MSD.
- **High-speed Diesel (HSD)**: All oil engines with an engine speed > 900 RPM are classified as HSD.

LNG engines

All vessels from the IHS database which have according stated 'LNG' as fuel type (determined according the procedure from Section C.1.1) are considered to have an LNG engine. The LNG engines can be subdivided into four groups:

- **LNG-Otto SS**: Engines that fall in this category operate similar to the Otto cycle and are two-stroke, dual-fuel, slow-speed engines. These engines are either manufactured by Wärtsilä and have an 'X' or 'DF' in their model name or are manufactured by MAN Energy Solutions and have 'ME-GA' as model name. In this research, the engines are identified by their model names.

- **LNG-Otto MS**: Engines that fall in this category operate on the Otto cycle and are four-stroke, dual-fuel, medium-speed engines. The engines are identified by having the number four in the category 'Engine Stroke Type' and have an engine speed over 300 RMP (with exception of LBSI engines). LNG-Otto MS engines are the most common LNG engines and are therefore the default engine type when the engine is unclassified and the engine type is 'LNG'.
- **LNG-Diesel**: Engines that fall in this category operate on the Diesel cycle and are two-stroke, dual-fuel, slow-speed engines. These engines are only manufactured by MAN Energy Solutions and have 'ME' in their model name. These engines are identified by their model name, but the 'ME-GA' (described in the LNG-Otto MS section) engines are excepted.
- **LBSI**: Engines that fall in this category run on only natural gas (mono-fueled) and operate similar to the Otto cycle. The engines are four-stroke, medium-speed engines and are called 'lean burn spark ignition'. These engines are mainly manufactured by Rolls-Royce/Bergen, but to a lesser extend also by Mitsubishi and Hyundai. The latter two manufactures are neglected and the engines are identified by having 'Rolls-Royce/Bergen' in the category 'Engine Design'.

Other engines
Other engines that do not fall under the above named categories are:

- **Methanol**: Engines that fall in this category are methanol fueled (determined according the procedure from Section C.1.1). They can be subdivided into slow speed and medium speed when their engine speed is ≤ 300 RPM and > 300 RPM respectively.
- **Gas and steam turbines**: Engines that fall in this category have stated 'turbine' in the category 'engine type'. Vessels that are classified with slow speed and medium speed oil engines but have the fuel type 'gas' are considered gas turbines and therefore also fall in this category.
- **Sail**: Engines that fall in this category have stated 'sail' in the category 'engine type'. These vessels are not part of this research as they do not emit any greenhouse gasses.
- **Batteries**: Engines that fall in this category have stated 'Batteries' in the category 'engine type'. These vessels do not emit any greenhouse gasses and are therefore neglected in this research.
- **Non-propelled**: Engines that fall in this category have stated 'non-propelled' in the category 'engine type'. These vessels do not contribute to the emission of greenhouse gasses and are therefore not part of this research.

C.3.2. Engine tier

The engine tier is depending on the construction year of the vessel. Vessels constructed after the 1st of January 2000 must comply with a maximum NO_x emissions. These requirements became stricter throughout the years, so the construction year of the vessel determines which tier the vessel must comply with. To assign a tier to each vessel the category 'Year' from the IHS database is used. The classification is as follows:

Tier	Construction year
0	Before 1st of Jan 2000
I	After 1st of Jan 2000
II	After 1st of Jan 2011
III	After 1st of Jan 2016

Table C.8 Classification of Tiers

Tier III is only applicable for vessels operating inside the nitrogen emission control areas, if not the case then tier II applies. Tier 0 is a non-existing category in the MARPOL regulation but used to identify vessels constructed before 2000 on which tier regulation do not apply if the vessels have a displacement < 90 liters per cylinder and rated output < 5000 kW. If this is not the case, Tier I regulations apply.

C.4. Base emission factor PM_{10}

The base emission factor for PM_{10} is energy based. To determine the EF_{base} the fuel type, engine speed and construction year class (determined in Section 3.3.1) of the vessel must be known.

The base emission factors are given per construction year class in Table C.9, Table C.10 and Table C.11.

Engine type	**Fuel type**	**EF PM_{10} [g PM_{10} / kWh]**
SSD	HFO	1.4
	MDO	0.18
MSD	HFO	1.4
	MDO	0.18
HSD	HFO	1.4
	MDO	0.17
Turbines	HFO	1.42
	MDO	0.145
Auxiliary Engine	HFO	1.4
	MDO	0.17

Table C.9 Base emission factor for PM_{10} for the construction year class 'Built before 1984'

Engine type	**Fuel type**	**EF PM_{10} [g PM_{10} / kWh]**
SSD	HFO	1.39
	MDO	0.18
MSD	HFO	1.39
	MDO	0.18
HSD	HFO	1.4
	MDO	0.18
Turbines	HFO	1.42
	MDO	0.145
Auxiliary Engine	HFO	1.4
	MDO	0.18
LNG-Otto-MS	LNG	0.02
LBSI	LNG	0.02

Table C.10 Base emission factor for PM_{10} for the construction year class 'Built between 1984 and 2000'

Engine type	**Fuel type**	**EF PM_{10} [g PM_{10} / kWh]**
SSD	HFO	1.39
	MDO	0.19
	Methanol	0.14
MSD	HFO	1.39
	MDO	0.18
	Methanol	0.14
HSD	HFO	1.39
	MDO	0.18
Turbines	HFO	1.42
	MDO	0.15
	LNG	0.03
Auxiliary Engine	HFO	1.369
	MDO	0.18
LNG-Otto-MS	LNG	0.02
LNG-Otto-SS	LNG	0.02
LBSI	LNG	0.02
LNG-Diesel	LNG	0.02

Table C.11 Base emission factor for PM_{10} for the construction year class 'Built after 2000'

D

Missing entries vessel database

When vessels in the vessel database have missing entries they are filled in according the procedure described in this Appendix. The missing entries in the database are allocated based on vessel type and size category of the considered vessel. All possible missing entries and the corresponding procedure to fill this characteristic in, are one by one described. At the end of this Appendix, tables with all characteristic values for each vessel type is stated.

D.1. Deadweight tonnage

All vessel characteristics depend on the size category of the vessel and therefore the deadweight tonnage of the vessel. Only a few percentage of the vessels are lacking a deadweight tonnage entry, but for each vessel type specifically an appropriate estimate for the missing entries is determined. The number of vessels in each size category is counted and divided by the total vessel from that vessel type. This gives the probability that a randomly drawn vessel from this vessel type is from a certain size category. This method reflects the current fleet. The probabilities are summarized in Figure D.1 for each vessel type.

When a vessel is lacking the deadweight tonnage, a random number between 0 and 1 is drawn and according to the probability distribution a size category is assigned.

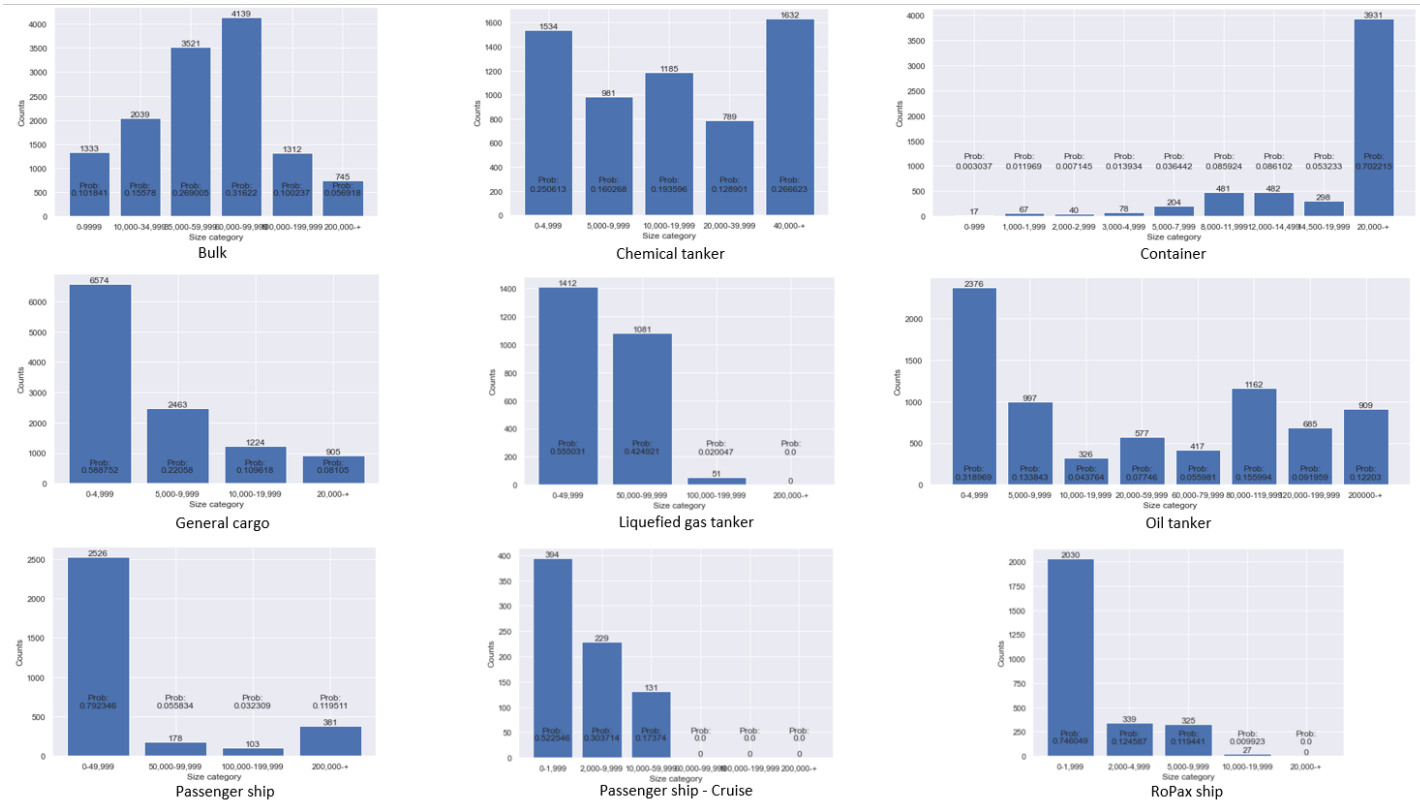

Figure D.1: Deadweight distribution per vessel type

It must be noted that for future research it would be an improvement to correlate the DWT to the dimensions of a vessel. However in the Sea-web Ships database these were unavailable.

D.2. Number of screws

The number of screws of a vessel is estimated based on statistics from the vessels of the same vessel type and size category of which the number of screws is known.

The total number of vessels of which the number of screws is known is determined first, subsequently the vessels having one screw are counted. With these values know, the probability of a vessel having one screw is calculated. The same procedure is repeated for vessels having two, three, four, five and even six screws.

The missing entry in the database is filled in by drawing a random number between zero and one, and according the determined probability distribution the number of screws is assigned. To illustrate this procedure, an example is stated below.

For this example the probabilities of the Bulk Carrier class from size category '0 - 9,999' are stated in the Table D.1. First a random number is drawn, if this number is between 0 and 0.6977 the vessel is assigned one screw, if the number is between 0.6977 and 0.9985 the vessel is assigned two screws, if the number is between 0.9985 and 1 the vessel is assigned three screws.

Number of screws	x = 1	x = 2	x = 3	x = 4	x = 5	x = 6
Probability	0.6977	0.3008	0.0015	0	0	0

Table D.1 Probabilities of the number of screws for the Bulk Carrier size class '0 - 9,999'

D.3. Build year

The build year of the vessel is determined by fitting a distribution on the data of vessels of the same vessel type and size category of which the build year is known.

Approximately forty common distributions are fitted to the data. By means of the sum-square error (SSE) the best fit is determined. When examination the outcome, the distribution occurring the most times as best-fit is the double Weibull distribution. The double Weibull is a very flexible distribution. The formula of the distribution function is given in Equation D.1. For $x < \tau$ the double weibull is equivilant to the Weibull distribution (which is commonly used as a lifetime distribution (Reliawiki, 2018)) and for $x \leq \tau$ it is similar to the reflected Weibull distribution.

$$F(x;\alpha,\beta,\tau) = \begin{cases} \frac{1}{2}\exp\left\{-\left[\frac{\tau-x}{\alpha}\right]^{\beta}\right\} & \text{for } x < \tau \\ 1-\frac{1}{2}\exp\left\{-\left[\frac{x-\tau}{\alpha}\right]^{\beta}\right\} & \text{for } x \geq \tau \end{cases} \tag{D.1}$$

The double Weibull distribution takes in three parameters: the shape parameter 'β' in python referred to as 'c', the location parameter 'x' in python referred to as 'loc' and the scale parameter 'α' in python referred to as 'scale'. These parameters are determined for each vessel type and size class. The missing entry in the database is filled in by drawing a random number from the distribution with these parameters.

To show the distribution and the data, the fit of the bulk carrier class is shown as example below. A SSE of zero means it is a one-on-one fit. When looking to Figure Figure D.2 it shows that when more data is available, the fit gets more accurate. This is important since most missing entries will be from vessels in the size class which contains the most vessels (in this example the lower size classes).

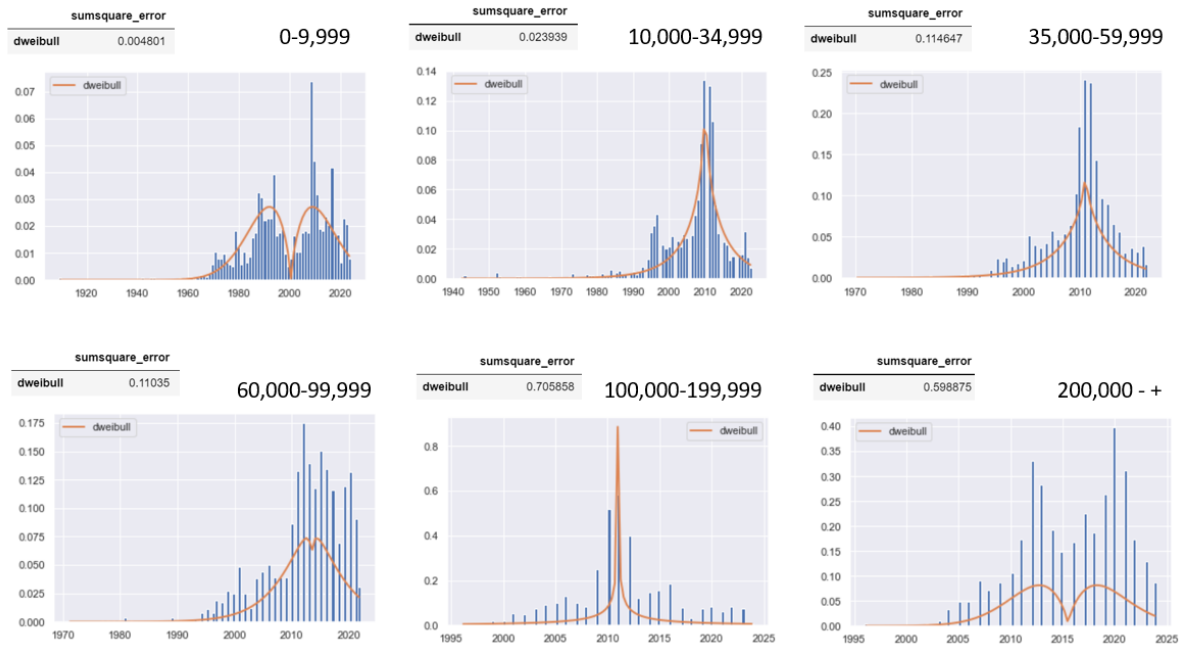

Figure D.2: Fit of the double Weibull distribution on build year data of the Bulk carrier and its size categories

D.4. Installed engine power

Figure D.3 shows that there is a notable linear relation between the dead weight tonnage and the installed engine power. Therefore a linear regression analysis is done to predict the missing entry. A first order polynomial function is fitted through the data to describe this relation for each vessel type and size class separately. The formula corresponding to this polynomial function is derived and used to fill in the missing installed engine power corresponding to the vessels dead weight tonnage.

The correctness of the fit of the polynomial function is identified by means of the R-squared value, where a R-squared of 1 means that the function explains all the variability of the response data around its mean.

The fit of the bulk carrier class is shown as example below. When looking to Figure D.3 it shows that the R-squared value varies between 0.5 and 0.7. The lower R-squareds can be explained by the outliers. For the purpose of this procedure, a linear function is considered a well enough fit.

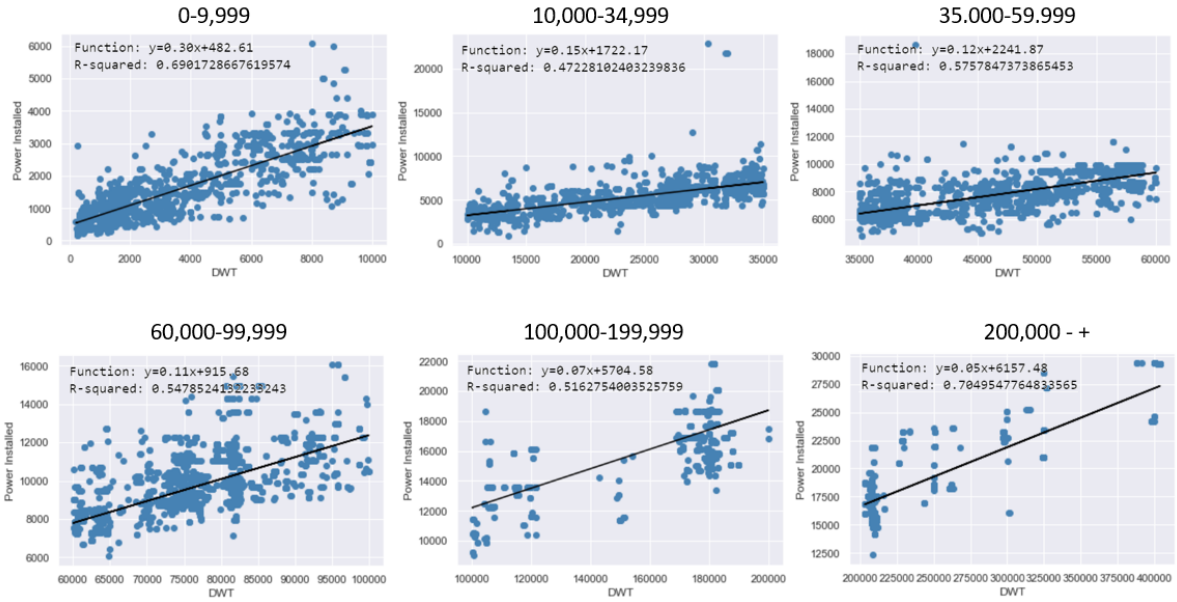

Figure D.3: Linear relation ship of dead weight tonnage and installed engine power of the Bulk carrier and its size categories

D.5. Fuel type

Two types of fuel type can be assigned: inside an ECA where the lightest fuel is taken from the IHS database, and outside an ECA where the procedure is followed from Section C.1.1. This distinction is also made in the method for filling in missing fuel type entries.

Inside ECA

Inside an ECA the missing fuel types is allocated with statistics from the vessels of the same vessel type and size category of which the lightest fuel type is known (Fuel Type 1). In the same manner as determining the probability of the number of screws, the probability is determined for each fuel type.

The missing fuel type entry is filled in by drawing a random number between zero and one, and according the determined probability distribution the fuel type is assigned.

Outside ECA

The fuel type outside an ECA is determined according the procedure from Section C.1.1. The same procedure is performed to allocate the main fuel type from vessels from the IHS database of which Fuel Type 1 and Fuel Type 2 are known from the same vessel type and size category. With these statistics known for each group, the probability that a vessel has a certain fuel type is determined. The missing fuel type can then again be filled in by drawing a number between 0 and 1.

D.6. Engine type

The engine type of a vessel is estimated based on statistics from the vessels of the same vessel type and size category of which the engine type is known. First based on the IHS database entries, the engine type is determined for each of the vessels of which the data is known. Subsequently the probability of all engine types for vessels from that class is determined and by drawing a random number between zero and one the missing engine type is allocated.

D.7. Tables with characteristic values

Vessel type	Bulk Carrier						
Size category		0 - 9999	10,000 - 34,999	35,000 - 59,999	60,000 - 99,999	100,000 - 199,999	200,000 - +
DWT	**Median**	2870	28344	52370	76620	179156	209800
Screws	**Probability x = 1**	0.6977	0.9554	0.9974	0.9971	1.0	1.0
	Probability x = 2	0.3008	0.0436	0.0026	0.0014	0	0
	Probability x = 3	0.0015	0.0005	0	0	0	0
	Probability x = 4	0	0.0005	0	0.0014	0	0
	Probability x = 5	0	0	0	0	0	0
	Probability x = 6	0	0	0	0	0	0
Installed power	**Function**	y=0.30x+482.61	y=0.15x+1722.17	y=0.12x+2241.87	y=0.11x+915.68	y=0.07x+5704.58	y=0.05x+6157.48
Build year	**dweibull c**	1.6912	0.8735	0.9329	1.1411	0.5058	1.6739
	dweibull loc	2000.4137	2010	2011.0	2013.4515	2011.0	2015.5212
	dweibull scale	14.3521	5.5799	4.7811	5.2823	3.3064	4.7608
Fuel type inside ECA	**Probability HFO**	0.0086	0	0	0	0	0
	Probability MDO	0.9794	1.0	0.9997	1.0	0.9877	0.9622
	Probability LNG	0.0120	0	0.0003	0	0.0123	0.0378
	Probability Nuclear	0	0	0	0	0	0
	Probability Coal	0	0	0	0	0	0
	Probability Methanol	0	0	0	0	0	0
Fuel type outside ECA	**Probability HFO**	0.7629	0.9990	0.9997	1.0	0.9877	0.9622
	Probability MDO	0.2251	0.0010	0	0	0	0
	Probability LNG	0.0120	0	0.0003	0	0.0123	0.0378
	Probability Nuclear	0	0	0	0	0	0
	Probability Coal	0	0	0	0	0	0
	Probability Methanol	0	0	0	0	0	0
Engine type	**Probability SSD**	0.3891	0.8587	0.9977	0.9986	0.9878	0.9625
	Probability MSD	0.4408	0.1340	0.0020	0.0014	0	0
	Probability HSD	0.1642	0.0034	0	0	0	0
	Probability LNG-Otto-SS	0.0022	0	0	0	0.0046	0
	Probability LNG-Otto-MS	0.0030	0	0	0	0	0
	Probability LNG-Diesel	0	0	0.0003	0	0.0076	0.0375
	Probability LBSI	0	0	0	0	0	0
	Probability Methanol-SS	0	0	0	0	0	0
	Probability Methanol-MS	0	0	0	0	0	0
	Probability Turbine	0.0007	0.0034	0	0	0	0

Table D.2 Characteristic values for missing entries - Bulk Carrier

Vessel type	Chemical tanker					
Size category		0 - 4,999	5,000 - 9,999	10,000 - 19,999	20,000 - 39,999	40,000 - +
DWT	**Median**	1774	7035	14803	34798	49990
Screws	**Probability x = 1**	0.9107	0.8603	0.9662	0.9518	0.9933
	Probability x = 2	0.0821	0.1346	0.0287	0.0241	0.0061
	Probability x = 3	0.0046	0	0.0017	0.0101	0.0006
	Probability x = 4	0.0007	0.0051	0.0034	0.0139	0
	Probability x = 5	0	0	0	0	0
	Probability x = 6	0.0020	0	0	0	0
Installed power	**Function**	y=0.44x+399.40	y=0.30x+962.03	y=0.20x+1878.74	y=0.14x+3503.90	y=0.06x+5597.53
Build year	**dweibull c**	1.6436	0.9174	0.8948	1.6275	1.6300
	dweibull loc	1999.4085	2009.0000	2009.0000	2011.5978	2012.3873
	dweibull scale	13.6030	7.2141	4.9766	6.9729	6.0672
Fuel type inside ECA	**Probability HFO**	0.0297	0.0010	0	0	0
	Probability MDO	0.9690	0.9837	0.9772	0.9822	0.9822
	Probability LNG	0.0013	0.0153	0.0228	0.0178	0.0018
	Probability Nuclear	0	0	0	0	0
	Probability Coal	0	0	0	0	0
	Probability Methanol	0	0	0	0	0.0159
Fuel type outside ECA	**Probability HFO**	0.6271	0.9673	0.9788	0.9822	0.9822
	Probability MDO	0.3716	0.0184	0	0	0
	Probability LNG	0.0013	0.0143	0.0212	0.0178	0.0018
	Probability Nuclear	0	0	0	0	0
	Probability Coal	0	0	0	0	0
	Probability Methanol	0	0	0	0	0.0159
Engine type	**Probability SSD**	0.2568	0.3585	0.7508	0.9135	0.9755
	Probability MSD	0.6441	0.5230	0.2247	0.0674	0.0067
	Probability HSD	0.0984	0.1032	0.0017	0	0
	Probability LNG-Otto-SS	0	0	0	0	0
	Probability LNG-Otto-MS	0.0007	0.0153	0.0228	0.0178	0.0018
	Probability LNG-Diesel	0	0	0	0	0
	Probability LBSI	0	0	0	0	0
	Probability Methanol-SS	0	0	0	0	0.0159
	Probability Methanol-MS	0	0	0	0	0
	Probability Turbine	0	0	0	0.0013	0

Table D.3 Characteristic values for missing entries - Chemical tanker

Vessel type	Container ship						
		0 - 999	1,000 - 1,999	2,000 - 2,999	3,000 - 4,999	5,000 - 7,999	8,000 - 11,999
Screws	**Probability x = 1**	0	0.5224	0.4500	0.7308	0.9559	0.9854
	Probability x = 2	0.5882	0.3881	0.5500	0.2692	0.0441	0.0146
	Probability x = 3	0.4118	0.0746	0	0	0	0
	Probability x = 4	0	0.0149	0	0	0	0
	Probability x = 5	0	0	0	0	0	0
	Probability x = 6	0	0	0	0	0	0
Installed power	**Function**	y=1.53x+-370.06	y=0.70x+619.61	y=-0.80x+3484.39	y=0.65x+-107.33	y=0.87x+-1508.46	y=0.85x+-1606.96
Build year	**dweibull c**	0.9413	1.0486	1.5660	1.4487	0.8992	0.8504
	dweibull loc	2011.0000	2007.3521	2002.2278	2001.8833	1996.0000	2006.0000
	dweibull scale	3.2545	11.6374	15.5834	10.8503	5.6215	5.2542
Fuel type	**Probability HFO**	0.0400	0.0400	0	0.0769	0	0
inside ECA	**Probability MDO**	0.9600	0.9600	1.0	0.8846	1.0	1.0
	Probability LNG	0	0	0	0	0	0
	Probability Nuclear	0	0	0	0	0	0
	Probability Coal	0	0	0	0	0	0
	Probability Methanol	0	0	0	0	0	0
Fuel type	**Probability HFO**	0.1200	0.1200	0.2381	0.7200	1.0	0.9958
outside ECA	**Probability MDO**	0.8800	0.8800	0.7619	0.2800	0	0.0042
	Probability LNG	0	0	0	0	0	0
	Probability Nuclear	0	0	0	0	0	0
	Probability Coal	0	0	0	0	0	0
	Probability Methanol	0	0	0	0	0	0
Engine type	**Probability SSD**	0.0000	0.2537	0.2500	0.2949	0.3284	0.3202
	Probability MSD	0.1176	0.3582	0.4000	0.6026	0.6716	0.6798
	Probability HSD	0.8824	0.3881	0.3500	0.1026	0	0
	Probability LNG-Otto-SS	0	0	0	0	0	0
	Probability LNG-Otto-MS	0	0	0	0	0	0
	Probability LNG-Diesel	0	0	0	0	0	0
	Probability LBSI	0	0	0	0	0	0
	Probability Methanol-SS	0	0	0	0	0	0
	Probability Methanol-MS	0	0	0	0	0	0
	Probability Turbine	0	0	0	0	0	0

Table D.4 Characteristic values for missing entries - Container ship - part 1

Vessel type	Container ship			
		12,000 - 14,499	14,500 - 19,999	20,000 - +
Screws	**Probability x = 1**	0.9876	0.9732	0.9908
	Probability x = 2	0.0124	0.0268	0.0092
	Probability x = 3	0	0	0
	Probability x = 4	0	0	0
	Probability x = 5	0	0	0
	Probability x = 6	0	0	0
Installed power	**Function**	y=0.81x+-1937.26	y=0.44x+3304.49	y=0.32x+14220.40
Build year	**dweibull c**	1.1251	1.2911	1.3121
	dweibull loc	2008.7133	2004.3028	2009.5203
	dweibull scale	5.9322	6.8948	5.9754
Fuel type	**Probability HFO**	0	0	0
inside ECA	**Probability MDO**	0.9937	0.9730	0.9901
	Probability LNG	0.0063	0	0.0099
	Probability Nuclear	0	0	0
	Probability Coal	0	0	0
	Probability Methanol	0	0.0270	0
Fuel type	**Probability HFO**	0.9937	0.9662	0.9901
outside ECA	**Probability MDO**	0	0.0068	0
	Probability LNG	0.0063	0	0.0099
	Probability Nuclear	0	0	0
	Probability Coal	0	0	0
	Probability Methanol	0	0.0270	0
Engine type	**Probability SSD**	0.6307	0.8087	0.9812
	Probability MSD	0.3631	0.1644	0.0081
	Probability HSD	0	0	0
	Probability LNG-Otto-SS	0	0	0
	Probability LNG-Otto-MS	0.0062	0	0.0097
	Probability LNG-Diesel	0	0	0
	Probability LBSI	0	0	0
	Probability Methanol-SS	0	0	0
	Probability Methanol-MS	0	0	0
	Probability Turbine	0	0	0.0010

Table D.5 Characteristic values for missing entries - Container ship - part 2

Vessel type	General Cargo ship				
Size category		0 - 4,999	5,000 - 9,999	10,000 - 19,999	20,000 - +
DWT	Median	2100	6763	12767.5	33305
Screws	Probability x = 1	0.7872	0.7966	0.9387	0.9845
	Probability x = 2	0.2076	0.1989	0.0556	0.0155
	Probability x = 3	0.0037	0.0024	0.0041	0
	Probability x = 4	0.0011	0	0.0008	0
	Probability x = 5	0	0	0	0
	Probability x = 6	0.0003	0.0020	0	0
Installed power	Function	y=0.27x+594.59	y=0.48x+-398.94	y=0.38x+-108.82	y=0.05x+6438.33
Build year	dweibull c	1.4018	1.2295	0.9117	1.1008
	dweibull loc	1997.6147	2004.2544	2010	2010.5268
	dweibull scale	13.5124	9.8653	6.9531	6.1118
Fuel type inside ECA	Probability HFO	0.0403	0	0	0
	Probability MDO	0.9566	0.9996	1.0	0.9877
	Probability LNG	0.0026	0.0004	0	0.0112
	Probability Nuclear	0	0	0	0.0011
	Probability Coal	0	0	0	0
	Probability Methanol	0	0	0	0
Fuel type outside ECA	Probability HFO	0.2869	0.9517	0.9983	0.9877
	Probability MDO	0.7105	0.0479	0.0017	0
	Probability LNG	0.0026	0.0004	0	0.0112
	Probability Nuclear	0	0	0	0.0011
	Probability Coal	0	0	0	0
	Probability Methanol	0	0	0	0
Engine type	Probability SSD	0.2769	0.2869	0.5679	0.9436
	Probability MSD	0.5322	0.6254	0.4272	0.0442
	Probability HSD	0.1892	0.0873	0.0041	0
	Probability LNG-Otto-SS	0	0	0	0
	Probability LNG-Otto-MS	0.0009	0.0004	0	0.0110
	Probability LNG-Diesel	0	0	0	0
	Probability LBSI	0	0	0	0
	Probability Methanol-SS	0	0	0	0
	Probability Methanol-MS	0	0	0	0
	Probability Turbine	0	0	0.0008	0.0011

Table D.6 Characteristic values for missing entries - General cargo ship

Vessel type	Liquefied tanker				
Size category		0 - 49,999	50,000 - 99,999	100,000 - 199,999	200,000 - +
DWT	**Median**	4984	80000	121843	121843
Screws	**Probability x = 1**	0.9547	0.5597	0	0
	Probability x = 2	0.0390	0.2664	1.0	1.0
	Probability x = 3	0.0021	0	0	0
	Probability x = 4	0.0042	0.1240	0	0
	Probability x = 5	0	0.0167	0	0
	Probability x = 6	0	0.0333	0	0
Installed power	**Function**	y=0.25x+1855.38	y=0.51x+-13614.32	y=0.03x+33208.71	y=0.03x+33208.71
Build year	**dweibull c**	1.4480	1.1375	0.7464	0.7464
	dweibull loc	2004.5336	2016.4692	2008.0000	2008.0000
	dweibull scale	11.8057	6.9313	2.4480	2.4480
Fuel type inside ECA	**Probability HFO**	0	0	0	0
	Probability MDO	0.9501	0.4287	0.8627	0.8627
	Probability LNG	0.0292	0.4361	0.1373	0.1373
	Probability Nuclear	0	0	0	0
	Probability Coal	0	0	0	0
	Probability Methanol	0	0	0	0
Fuel type outside ECA	**Probability HFO**	0.8073	0.4793	0.8627	0.8627
	Probability MDO	0.1615	0	0	0
	Probability LNG	0.0313	0.5207	0.1373	0.1373
	Probability Nuclear	0	0	0	0
	Probability Coal	0	0	0	0
	Probability Methanol	0	0	0	0
Engine type	**Probability SSD**	0.7208	0.3575	0.8627	0.8627
	Probability MSD	0.2211	0	0	0
	Probability HSD	0.0206	0	0	0
	Probability LNG-Otto-SS	0	0	0	0
	Probability LNG-Otto-MS	0.0291	0.4381	0.1373	0.1373
	Probability LNG-Diesel	0	0	0	0
	Probability LBSI	0	0	0	0
	Probability Methanol-SS	0	0	0	0
	Probability Methanol-MS	0	0	0	0
	Probability Turbine	0.0085	0.2044	0	0

Table D.7 Characteristic values for missing entries - Liquefied tanker

Vessel type	Oil tanker						
Size category		0 - 4,999	5,000 - 9,999	10,000 - 19,999	20,000 - 59,999	60,000 - 79,999	80,000 - 119,999
Screws	Probability x = 1	0.7205	0.7182	0.8804	0.9723	0.9664	0.9923
	Probability x = 2	0.2761	0.2798	0.1166	0.0121	0.0168	0.0052
	Probability x = 3	0.0013	0.0010	0.0000	0.0000	0.0072	0.0000
	Probability x = 4	0.0013	0.0010	0.0000	0.0156	0.0096	0.0026
	Probability x = 5	0.0008	0.0000	0.0031	0.0000	0.0000	0.0000
	Probability x = 6	0.0000	0.0000	0.0000	0.0000	0.0000	0.0000
Installed power	Function	y=0.35x+488.53	y=0.17x+1489.74	y=0.25x+724.54	y=0.10x+4965.87	y=0.04x+8622.95	y=0.03x+10314.67
Build year	dweibull c	1.6439	0.7494	1.1941	1.1204	1.1271	1.7011
	dweibull loc	1999.5399	2009.0000	2008.5315	2005.6888	2007.6319	2012.6113
	dweibull scale	14.1934	7.1109	9.9310	5.3873	3.9618	6.8803
Fuel type	Probability HFO	0.0494	0.0000	0.0000	0.0000	0.0000	0.0000
inside ECA	Probability MDO	0.9506	1.0000	0.9938	0.9965	1.0000	0.9475
	Probability LNG	0.0000	0.0000	0.0062	0.0035	0.0000	0.0525
	Probability Nuclear	0.0000	0.0000	0.0000	0.0000	0.0000	0.0000
	Probability Coal	0.0000	0.0000	0.0000	0.0000	0.0000	0.0000
	Probability Methanol	0.0000	0.0000	0.0000	0.0000	0.0000	0.0000
Fuel type	Probability HFO	0.4178	0.9426	0.9907	0.9965	1.0000	0.9475
outside ECA	Probability MDO	0.5822	0.0574	0.0031	0.0000	0.0000	0.0000
	Probability LNG	0.0000	0.0000	0.0062	0.0035	0.0000	0.0525
	Probability Nuclear	0.0000	0.0000	0.0000	0.0000	0.0000	0.0000
	Probability Coal	0.0000	0.0000	0.0000	0.0000	0.0000	0.0000
	Probability Methanol	0.0000	0.0000	0.0000	0.0000	0.0000	0.0000
Engine type	Probability SSD	0.2888	0.2903	0.5092	0.9480	0.9856	0.9475
	Probability MSD	0.4828	0.5606	0.4264	0.0485	0.0144	0.0009
	Probability HSD	0.2280	0.1491	0.0583	0.0000	0.0000	0.0000
	Probability LNG-Otto-SS	0.0000	0.0000	0.0000	0.0000	0.0000	0.0000
	Probability LNG-Otto-MS	0.0000	0.0000	0.0061	0.0035	0.0000	0.0517
	Probability LNG-Diesel	0.0000	0.0000	0.0000	0.0000	0.0000	0.0000
	Probability LBSI	0.0000	0.0000	0.0000	0.0000	0.0000	0.0000
	Probability Methanol-SS	0.0000	0.0000	0.0000	0.0000	0.0000	0.0000
	Probability Methanol-MS	0.0000	0.0000	0.0000	0.0000	0.0000	0.0000
	Probability Turbine	0.0000	0.0000	0.0000	0.0000	0.0000	0.0000

Table D.8 Characteristic values for missing entries - Oil tanker - part 1

Vessel type	**Oil tanker**		
Size category		120,000 - 199,999	200000 - +
Screws	**Probability x = 1**	0.9693	1.0000
	Probability x = 2	0.0175	0.0000
	Probability x = 3	0.0000	0.0000
	Probability x = 4	0.0073	0.0000
	Probability x = 5	0.0058	0.0000
	Probability x = 6	0.0000	0.0000
Installed power	**Function**	y=0.05x+8826.80	y=0.10x+-3295.83
Build year	**dweibull c**	1.5763	1.6203
	dweibull loc	2013.5646	2013.4405
	dweibull scale	6.6979	6.4062
Fuel type	**Probability HFO**	0.0000	0.0000
inside ECA	**Probability MDO**	0.9839	0.9813
	Probability LNG	0.0161	0.0187
	Probability Nuclear	0.0000	0.0000
	Probability Coal	0.0000	0.0000
	Probability Methanol	0.0000	0.0000
Fuel type	**Probability HFO**	0.9911	0.9802
outside ECA	**Probability MDO**	0.0044	0.0011
	Probability LNG	0.0044	0.0187
	Probability Nuclear	0.0000	0.0000
	Probability Coal	0.0000	0.0000
	Probability Methanol	0.0000	0.0000
Engine type	**Probability SSD**	0.9781	0.9813
	Probability MSD	0.0073	0.0000
	Probability HSD	0.0000	0.0000
	Probability LNG-Otto-SS	0.0000	0.0000
	Probability LNG-Otto-MS	0.0146	0.0187
	Probability LNG-Diesel	0.0000	0.0000
	Probability LBSI	0.0000	0.0000
	Probability Methanol-SS	0.0000	0.0000
	Probability Methanol-MS	0.0000	0.0000
	Probability Turbine	0.0000	0.0000

Table D.9 Characteristic values for missing entries - Oil tanker - part 2

Vessel type	Passenger ship				
Size category		0 - 49,999	50,000 - 99,999	100,000 - 199,999	200,000 - +
DWT	**Median**	50	522.5	1377	79007
Screws	**Probability x = 1**	0.1140	0.1854	0.0485	0.0709
	Probability x = 2	0.7419	0.6292	0.6408	0.1102
	Probability x = 3	0.0685	0.1011	0.0097	0.0210
	Probability x = 4	0.0752	0.0843	0.3010	0.4751
	Probability x = 5	0	0	0	0.1260
	Probability x = 6	0	0	0	0.1969
Installed power	**Function**	y=-2.32x+2502.50	y=4.64x+-12.45	y=4.60x+-555.51	y=4.89x+4984.84
Build year	**dweibull c**	1.1192	1.1319	1.9471	1.3693
	dweibull loc	1998.4713	1993.3535	2003.4997	2007.4672
	dweibull scale	15.3270	16.9145	18.2799	12.3556
Fuel type inside ECA	**Probability HFO**	0.0101	0.0449	0.1053	0.0116
	Probability MDO	0.9836	0.9438	0.8553	0.9043
	Probability LNG	0.0051	0.0112	0.0395	0.0725
	Probability Nuclear	0	0	0	0.0029
	Probability Coal	0.0013	0	0	0
	Probability Methanol	0	0	0	0
Fuel type outside ECA	**Probability HFO**	0.0215	0.1910	0.4474	0.8870
	Probability MDO	0.9722	0.7978	0.5132	0.0290
	Probability LNG	0.0051	0.0112	0.0395	0.0725
	Probability Nuclear	0	0	0	0.0029
	Probability Coal	0.0013	0	0	0
	Probability Methanol	0	0	0	0
Engine type	**Probability SSD**	0.2530	0.1930	0.1613	0.1500
	Probability MSD	0.0553	0.3070	0.5161	0.7500
	Probability HSD	0.6672	0.4825	0.3226	0.0500
	Probability LNG-Otto-SS	0.0004	0	0	0
	Probability LNG-Otto-MS	0.0013	0.0088	0	0
	Probability LNG-Diesel	0	0	0	0
	Probability LBSI	0	0	0	0
	Probability Methanol-SS	0	0	0	0
	Probability Methanol-MS	0	0	0	0
	Probability Turbine	0	0	0	0.0500

Table D.10 Characteristic values for missing entries - Passenger ship

Vessel type	Passenger ship - Cruise						
Size category		0 - 1,999	2,000 - 9,999	10,000 - 59,999	60,000_99,999	100,000 - 199,999	200,000 - +
DWT	Median	379	5974	12000	-	-	-
Screws	Probability x = 1	0.1827	0.0480	0.1145	0.1145	0.1145	0.1145
	Probability x = 2	0.6802	0.1135	0.0229	0.0229	0.0229	0.0229
	Probability x = 3	0.0355	0.0175	0.0305	0.0305	0.0305	0.0305
	Probability x = 4	0.1015	0.5852	0.3130	0.3130	0.3130	0.3130
	Probability x = 5	0	0.0873	0.2137	0.2137	0.2137	0.2137
	Probability x = 6	0	0.1485	0.3053	0.3053	0.3053	0.3053
Installed power	Function	y=4.83x+308.45	y=6.67x+-4646.20	y=1.87x+43846.39	y=1.87x+43846.39	y=1.87x+43846.39	y=1.87x+43846.39
Build year	dweibull c	1.2822	1.4089	2.0151	2.0151	2.0151	2.0151
	dweibull loc	1998.7062	2005.6680	2013.4208	2013.4208	2013.4208	2013.4208
	dweibull scale	20.2481	12.9627	8.3836	8.3836	8.3836	8.3836
Fuel type inside ECA	Probability HFO	0.0402	0.0049	0	0	0	0
	Probability MDO	0.9447	0.9754	0.8092	0.8092	0.8092	0.8092
	Probability LNG	0.0151	0.0148	0.1679	0.1679	0.1679	0.1679
	Probability Nuclear	0	0.0049	0	0	0	0
	Probability Coal	0	0	0	0	0	0
	Probability Methanol	0	0	0	0	0	0
Fuel type outside ECA	Probability HFO	0.2312	0.9507	0.8092	0.8092	0.8092	0.8092
	Probability MDO	0.7538	0.0296	0	0	0	0
	Probability LNG	0.0151	0.0148	0.1679	0.1679	0.1679	0.1679
	Probability Nuclear	0	0.0049	0	0	0	0
	Probability Coal	0	0	0	0	0	0
	Probability Methanol	0	0	0	0	0	0
Engine type	Probability SSD	0.3731	0.1304	0.1094	0.1094	0.1094	0.1094
	Probability MSD	0.1599	0.8130	0.6719	0.6719	0.6719	0.6719
	Probability HSD	0.4594	0.0174	0	0	0	0
	Probability LNG-Otto-SS	0	0	0	0	0	0
	Probability LNG-Otto-MS	0.0076	0.0348	0.1484	0.1484	0.1484	0.1484
	Probability LNG-Diesel	0	0	0	0	0	0
	Probability LBSI	0	0	0	0	0	0
	Probability Methanol-SS	0	0	0	0	0	0
	Probability Methanol-MS	0	0	0	0	0	0
	Probability Turbine	0	0.0043	0	0	0	0

Table D.11 Characteristic values for missing entries - Passenger ship - Cruise

Vessel type	Ro-Pax ship					
Size category		0 - 1,999	2,000 - 4,999	5,000 - 9,999	10,000 - 19,999	20,000 - +
DWT	**Median**	360	3200	6984	11600	-
Screws	**Probability x = 1**	0.1064	0.0354	0.0523	0	0
	Probability x = 2	0.6192	0.6460	0.5077	0.2963	0.2963
	Probability x = 3	0.0389	0.0088	0.0031	0	0
	Probability x = 4	0.2246	0.2802	0.4246	0.7037	0.7037
	Probability x = 5	0.0039	0.0088	0.0092	0	0
	Probability x = 6	0.0025	0.0206	0.0031	0	0
Installed power	**Function**	y=4.77x+1722.92	y=6.06x+-5720.37	y=0.46x+22677.10	y=-0.69x+34088.85	y=-0.69x+34088.85
Build year	**dweibull c**	1.4871	1.5825	1.4527	1.8881	1.8881
	dweibull loc	1995.4720	1997.5870	2005.4713	2005.1687	2005.1687
	dweibull scale	15.8807	14.6288	10.4679	14.2112	14.2112
Fuel type inside ECA	**Probability HFO**	0.0109	0.0893	0	0	0
	Probability MDO	0.9358	0.8694	0.9255	0.8148	0.8148
	Probability LNG	0.0395	0.0344	0.0745	0.1481	0.1481
	Probability Nuclear	0	0	0	0	0
	Probability Coal	0	0.0069	0	0	0
	Probability Methanol	0	0	0	0.0370	0.0370
Fuel type outside ECA	**Probability HFO**	0.1722	0.8179	0.9193	0.8148	0.8148
	Probability MDO	0.7878	0.1409	0.0062	0	0
	Probability LNG	0.0400	0.0344	0.0745	0.1481	0.1481
	Probability Nuclear	0	0	0	0	0
	Probability Coal	0	0.0069	0	0	0
	Probability Methanol	0	0	0	0.0370	0.0370
Engine type	**Probability SSD**	0.2311	0.1686	0.0706	0.0741	0.0741
	Probability MSD	0.2819	0.7426	0.8282	0.7407	0.7407
	Probability HSD	0.4648	0.0533	0.0215	0	0
	Probability LNG-Otto-SS	0	0	0	0	0
	Probability LNG-Otto-MS	0.0202	0.0296	0.0798	0.1481	0.1481
	Probability LNG-Diesel	0	0	0	0	0
	Probability LBSI	0	0	0	0	0
	Probability Methanol-SS	0	0	0	0	0
	Probability Methanol-MS	0	0	0	0.0370	0.0370
	Probability Turbine	0	0	0	0	0

Table D.12 Characteristic values for missing entries - Ro-Pax ship

Vessel type	Tugboat	
Size category		0 - +
DWT	**Median**	188
Screws	**Probability x = 1**	0.0680
	Probability x = 2	0.9162
	Probability x = 3	0.0136
	Probability x = 4	0.0023
	Probability x = 5	0
	Probability x = 6	0
Installed power	**Function**	y=3.35x+1882.02
Build year	**dweibull c**	1.0711
	dweibull loc	2006.4862
	dweibull scale	12.7338
Fuel type inside ECA	**Probability HFO**	0.0233
	Probability MDO	0.9728
	Probability LNG	0.0039
	Probability Nuclear	0
	Probability Coal	0
	Probability Methanol	0
Fuel type outside ECA	**Probability HFO**	0.0471
	Probability MDO	0.9490
	Probability LNG	0.0039
	Probability Nuclear	0
	Probability Coal	0
	Probability Methanol	0
Engine type	**Probability SSD**	0.1257
	Probability MSD	0.3113
	Probability HSD	0.5618
	Probability LNG-Otto-SS	0
	Probability LNG-Otto-MS	0.0011
	Probability LNG-Diesel	0
	Probability LBSI	0
	Probability Methanol-SS	0
	Probability Methanol-MS	0
	Probability Turbine	0

Table D.13 Characteristic values for missing entries - Tugboat

E

Results from case study Port of Rotterdam

E.1. Model input

E.1.1. Vessel database

An example of a vessel from the vessel database of the case study of the Port of Rotterdam is shown in Figure E.1. The bold cells are the characteristics which are needed for the emission estimation.

mmsi	Weight	dead Tonnage	draught	LOA	width	DEFVesselType	Size category	Power_AE at berth	Power_AE anchored	Power_AE manoeuvring	Power_AE sea	C_B	Build year	Total KW Main Eng	Fuel Type 1	Fuel Type 2	Engines Number	Engine Type	Engine Stroke Type	Engines RPM
xxxxxxxxx		255.0	3.34	30.54	11.04	Tugboat	0-+	100	80	210	80	0.500	1996.0	3002.0	Distillate Fuel	NA	2.0	Oil	4.0	900.0

Engine Design	Engine Model	Aux. Engine Total KW	x	Year	P_installed_ME	Fuel_ME_inside	Fuel_ME_outside	Fuel_ME	Fuel_AE	Engine_ME	ProbE	Engine_AE	Engine_speed	Year category	draught-min	draught-max	draught-mean
Deutz	SBV8M628	158.0	2.0	1996.0	3002.00000	MDO	MDO	MDO	MDO	MSD		Auxiliary Engine	MS	1984-2000	3.34	3.34	3.34

Tier	Sapp_oneK2	HFCbase_ME	HFCbase_AE	EF_base_CO2_ME	EF_base_CO2_AE	EF_base_NOx_ME	EF_base_NOx_AE	EF_base_SOx_ME	EF_base_SOx_AE	EF_base_PM10_ME	EF_base_PM10_AE
0	14.580302	185.0	190.0	3.206	3.206	14.0	11.2	0.001103	0.001103	0.18	0.18

Figure E.1: An example of the vessel database from the case study of Port of Rotterdam

E.1.2. Trip collection

E.1.2.1. Create a trip collection

An example of a trip from the trip collection is shown below in Figure E.2. It is a simplification of an AIS dataframe. All the characteristics which are time-dependent are preserved, the rest is placed in the vessel database.

	timestamp	tripnr	dtime	calc_dist	calc_speed	mmsi	latitude	longitude	sog	draught	geometry
0	2022-01-07 04:23:29+00:00	0	0.0	0.000000	0.000000	XXXXXXXXX	51.879507	4.396995	0.034859	7.34	POINT (4.39700 51.87951)
1	2022-01-07 04:26:35+00:00	0	186.0	7.553331	0.040609	XXXXXXXXX	51.879565	4.396938	0.029474	7.34	POINT (4.39694 51.87956)
2	2022-01-07 04:29:33+00:00	0	178.0	3.253689	0.018279	XXXXXXXXX	51.879562	4.396985	0.022945	7.34	POINT (4.39698 51.87956)
3	2022-01-07 04:32:29+00:00	0	176.0	4.867190	0.027654	XXXXXXXXX	51.879537	4.396927	0.018496	7.34	POINT (4.39693 51.87954)
4	2022-01-07 04:35:29+00:00	0	180.0	1.678695	0.009326	XXXXXXXXX	51.879542	4.396950	0.018454	7.34	POINT (4.39695 51.87954)
...	...	...	...	...	...	...	...	...	...	...	...
121	2022-01-07 10:40:08+00:00	0	184.0	7.779504	0.042280	XXXXXXXXX	51.878285	4.421535	0.040046	7.34	POINT (4.42154 51.87828)
122	2022-01-07 10:43:07+00:00	0	179.0	6.767575	0.037808	XXXXXXXXX	51.878248	4.421613	0.035985	7.34	POINT (4.42161 51.87825)
123	2022-01-07 10:46:09+00:00	0	182.0	6.213735	0.034141	XXXXXXXXX	51.878252	4.421523	0.025604	7.34	POINT (4.42152 51.87825)
124	2022-01-07 10:49:07+00:00	0	178.0	3.026167	0.017001	XXXXXXXXX	51.878260	4.421565	0.024950	7.34	POINT (4.42157 51.87826)
125	2022-01-07 10:52:09+00:00	0	182.0	5.998661	0.032960	XXXXXXXXX	51.878312	4.421588	0.034805	7.34	POINT (4.42159 51.87831)

Figure E.2: An example of one trip from the trip collection from the case study of Port of Rotterdam

E.1.2.2. Trip collection with energy consumption of the auxiliary engine

An example of a trip from the trip collection with the closest edge (cl_edge) and the fairway characteristics from this edge, the operational mode of the vessel and the auxiliary engine power is shown below in Figure E.3.

timestamp	index	tripnr	dtime	calc_dist	speed	mmsi	latitude	longitude	sog	draught	geometry	cl_edge	GeneralDepth	L_edge	destination dist	destination lon	destination lat	Mode	Power_aux
2022-01-08 22:14:45+00:00	0	0	0.0	0.000000	0.000000	XXXXXXXXX	51.971933	4.045883	0.000000	4.3	POINT (4.04588 51.97193)	(8864185, 8864615)	20.0	7960.639041	0.0	4.045883	51.971933	Berth	100
2022-01-08 22:15:45+00:00	1	0	60.0	0.000000	0.000000	XXXXXXXXX	51.971933	4.045883	0.000000	4.3	POINT (4.04588 51.97193)	(8864185, 8864615)	20.0	7960.639041	0.0	4.045883	51.971933	Berth	100
2022-01-08 22:17:45+00:00	2	0	120.0	0.000000	0.000000	XXXXXXXXX	51.971933	4.045883	0.000000	4.3	POINT (4.04588 51.97193)	(8864185, 8864615)	20.0	7960.639041	0.0	4.045883	51.971933	Berth	100
2022-01-08 22:19:45+00:00	3	0	120.0	0.000000	0.000000	XXXXXXXXX	51.971933	4.045883	0.000000	4.3	POINT (4.04588 51.97193)	(8864185, 8864615)	20.0	7960.639041	0.0	4.045883	51.971933	Berth	100
2022-01-08 22:29:04+00:00	4	0	559.0	0.000000	0.000000	XXXXXXXXX	51.971933	4.045883	0.000000	4.3	POINT (4.04588 51.97193)	(8864185, 8864615)	20.0	7960.639041	0.0	4.045883	51.971933	Berth	100
...	...	...	...	...	...	...	...	...	...	...	...	...	...	...	...	...	...	...	...
2022-01-09 01:14:04+00:00	98	0	60.0	265.039606	4.417327	XXXXXXXXX	51.968083	4.091483	4.347142	4.3	POINT (4.09148 51.96808)	(8861022, 8860701)	20.0	806.420541	15902.182668	4.045883	51.971933	Sailing	80
2022-01-09 01:15:04+00:00	99	0	60.0	257.641103	4.294018	XXXXXXXXX	51.970167	4.093117	4.351120	4.3	POINT (4.09312 51.97017)	(8860701, 8861022)	20.0	806.420541	16159.823772	4.045883	51.971933	Sailing	80
2022-01-09 01:16:04+00:00	100	0	60.0	243.226442	4.053774	XXXXXXXXX	51.970792	4.096509	4.347449	4.3	POINT (4.09651 51.97079)	(8860701, 8864748)	20.0	359.048792	16403.050213	4.045883	51.971933	Sailing	80
2022-01-09 01:17:04+00:00	101	0	60.0	243.226442	4.053774	XXXXXXXXX	51.971417	4.099900	4.347449	4.3	POINT (4.09990 51.97142)	(8864748, 8866780)	20.0	3263.93837	16646.276655	4.045883	51.971933	Sailing	80
2022-01-09 01:26:35+00:00	102	0	571.0	1786.092557	3.128008	XXXXXXXXX	51.963583	4.122583	3.249325	4.3	POINT (4.12258 51.96358)	(8864217, 8862214)	20.0	423.52937	18432.369212	4.045883	51.971933	Sailing	80

Figure E.3: An example of one trip from the trip collection from the case study of Port of Rotterdam

E.1.2.3. Trip collection with emissions

An example for a trip from the trip collection and the calculated emissions is shown below in Figure E.4. If _ME or _AE is stated in the heading, this is the share of emissions the main or auxiliary engine respectively. The last eight columns state the summed up emissions in g and in g/m.

timestamp	index	tripnr	dtime	calc_dist	calc_speed	mmsi	latitude	longitude	sog	draught	LOA	width	geometry	cl_edge	GeneralDepth	L_edge	destination dist	destination lon	destination lat	Mode	P_aux
2022-01-04 10:08:18+00:00	0	0	0.000000	0.000000	0.000000	XXXXXXXXX	51.910063	4.491260	0.171938	3.1	84.95	9.6	POINT (4.49126 51.91006)	(22161437, B45486_A)	20.0	453.501451	0.0	4.49126	51.910063	Berth	110
2022-01-04 10:14:30+00:00	1	0	372.000000	119.944505	0.322431	XXXXXXXXX	51.909395	4.489892	1.114231	3.1	84.95	9.6	POINT (4.48989 51.90940)	(22161437, B45486_A)	20.0	453.501451	119.944505	4.49126	51.910063	Anchor	170
2022-01-04 10:15:10+00:00	2	0	40.000000	61.832686	1.545817	XXXXXXXXX	51.909500	4.489010	2.134685	3.1	84.95	9.6	POINT (4.48901 51.90950)	(B45486_A, B45486_B)	20.0	11.062703	181.777191	4.49126	51.910063	Anchor	170
2022-01-04 10:15:50+00:00	3	0	40.000000	61.832686	1.545817	XXXXXXXXX	51.909605	4.488127	2.134685	3.1	84.95	9.6	POINT (4.48813 51.90960)	(B45486_B, 8863710)	20.0	484.135662	243.609877	4.49126	51.910063	Anchor	170
2022-01-04 10:16:30+00:00	4	0	40.000000	61.832686	1.545817	XXXXXXXXX	51.909710	4.487245	2.134685	3.1	84.95	9.6	POINT (4.48724 51.90971)	(B4705_B, 8863710)	20.0	136.646594	305.442564	4.49126	51.910063	Anchor	170
2022-01-04 10:17:30+00:00	5	0	60.000000	179.346758	2.989113	XXXXXXXXX	51.908822	4.485070	4.080351	3.1	84.95	9.6	POINT (4.48507 51.90882)	(B4705_B, 8863710)	20.0	136.646594	484.789322	4.49126	51.910063	Anchor	170
2022-01-04 10:18:30+00:00	6	0	60.000000	309.732252	5.162204	XXXXXXXXX	51.906895	4.481822	5.308227	3.1	84.95	9.6	POINT (4.48182 51.90689)	(8863710, 8867528)	20.0	505.434347	794.521574	4.49126	51.910063	Sailing	200
2022-01-04 10:19:30+00:00	7	0	60.000000	327.014479	5.450241	XXXXXXXXX	51.904865	4.478386	5.484015	3.1	84.95	9.6	POINT (4.47839 51.90487)	(8867528, 8863104)	20.0	226.596857	1121.536053	4.49126	51.910063	Sailing	200
2022-01-04 10:20:30+00:00	8	0	60.000000	327.014479	5.450241	XXXXXXXXX	51.902835	4.474950	5.484015	3.1	84.95	9.6	POINT (4.47495 51.90284)	(8863104, 8861047)	20.0	1256.54819	1448.550532	4.49126	51.910063	Sailing	200

em_CO2_ME_g	em_SOx_ME_g	em_NOx_ME_g	em_PM10_ME_g	em_CO2_AE_g	em_SOx_AE_g	em_NOx_AE_g	em_PM10_AE_g	em_CO2_g	em_PM10_g	em_NOx_g	em_SOx_g	em_CO2_g/m	em_PM10_g/m	em_NOx_g/m	em_SOx_g/m
0.000000	0.000000	0.000000	0.000000	0.000000	0.000000	0.000000	0.000000	0.000000	0.000000	0.000000	0.000000	0.0	0.0	0.0	0.0
0.000000	0.000000	0.000000	0.000000	6741.683667	2.318697	127.306667	2.046000	6741.683667	2.046000	127.306667	2.318697	14.865848	0.004512	0.280719	0.005113
0.000000	0.000000	0.000000	0.000000	724.912222	0.249322	13.688889	0.220000	724.912222	0.220000	13.688889	0.249322	65.527589	0.019887	1.237391	0.022537
0.000000	0.000000	0.000000	0.000000	724.912222	0.249322	13.688889	0.220000	724.912222	0.220000	13.688889	0.249322	1.497333	0.000454	0.028275	0.000515
0.000000	0.000000	0.000000	0.000000	724.912222	0.249322	13.688889	0.220000	724.912222	0.220000	13.688889	0.249322	5.305015	0.00161	0.100177	0.001825
0.000000	0.000000	0.000000	0.000000	1087.368333	0.373983	20.533333	0.330000	1087.368333	0.330000	20.533333	0.373983	7.957522	0.002415	0.150266	0.002737
4877.486568	1.677536	107.163366	1.483800	1087.368333	0.373983	20.533333	0.330000	5964.854921	1.813800	127.696699	2.051519	11.801444	0.003589	0.252647	0.004059
5609.814230	1.929406	125.741628	1.741038	1087.368333	0.373983	20.533333	0.330000	6697.182563	2.071038	146.274961	2.303392	29.555235	0.00914	0.645524	0.010165
5609.814230	1.929406	125.741628	1.741038	1087.368333	0.373983	20.533333	0.330000	6697.182563	2.071038	146.274961	2.303392	5.329825	0.001648	0.11641	0.001833

Figure E.4: An example of one trip from the trip collection with corresponding emissions from the case study of Port of Rotterdam

E.2. Emission split in vessel types

To indicate the emission split per vessel type, their percentage of the total emissions are stated.

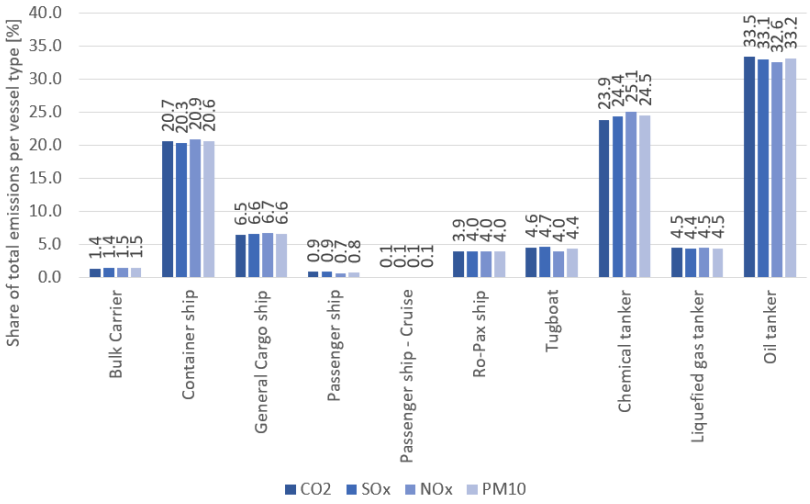

Figure E.5: Emission split in vessel types in percentage of total emissions

E.3. Emission distribution - January 2022

The emission distribution of the Port of Rotterdam is shown below for the four evaluated pollutants. These four figures cover the emissions of the first two weeks of January 2022.

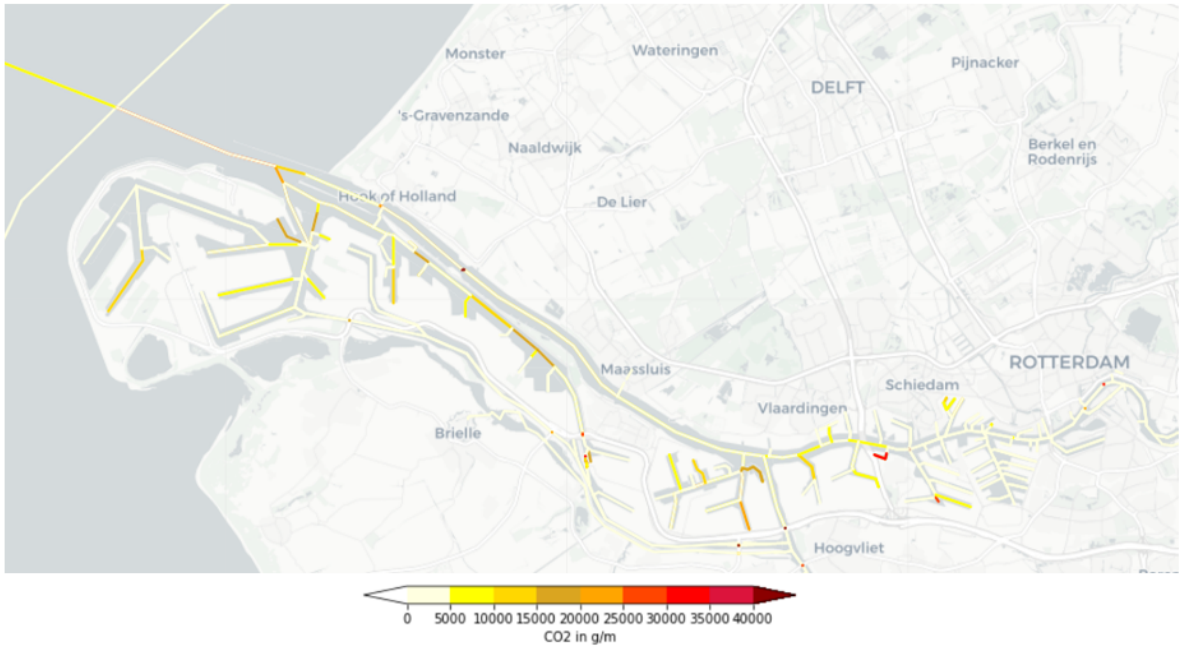

Figure E.6: Estimated CO_2 emissions in the Port of Rotterdam from January 1 - January 14 2022

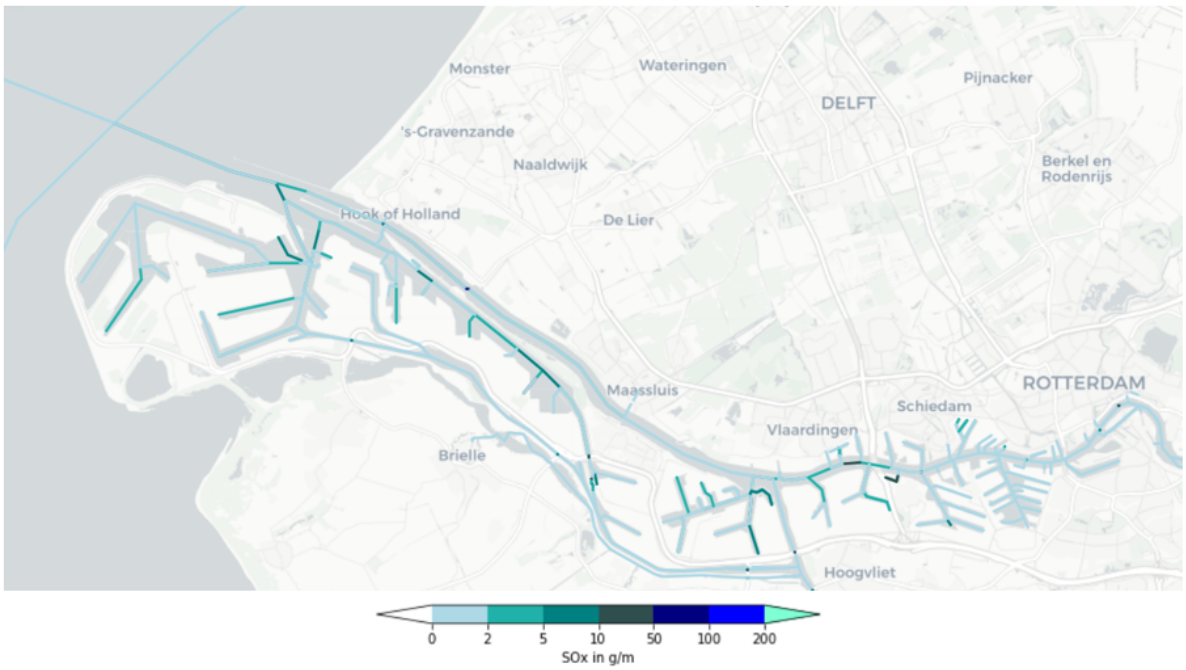

Figure E.7: Estimated SO_x emissions in the Port of Rotterdam from January 1 - January 14 2022

Figure E.8: Estimated NO_x emissions in the Port of Rotterdam from January 1 - January 14 2022

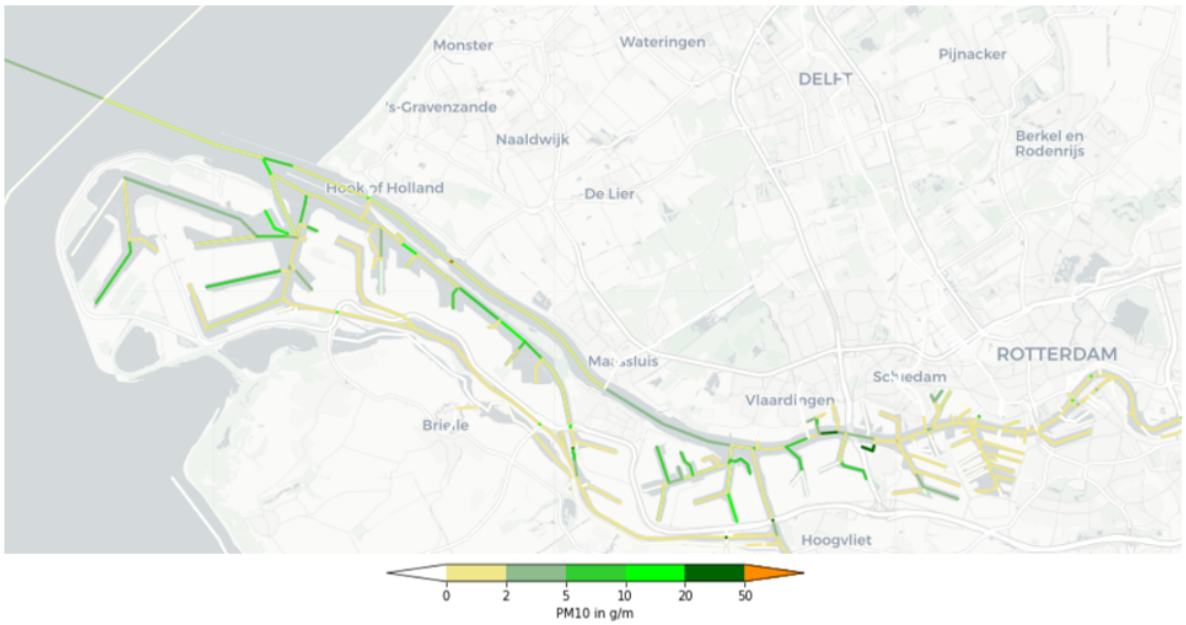

Figure E.9: Estimated PM_{10} emissions in the Port of Rotterdam from January 1 - January 14 2022

F

Results from case study Port of Constanța

F.1. Python code for constructing the FIS graph from a shape-file

The python code for constructing this FIS graph is based on an example from OpenTNSim (2022).

```
from shapely.geometry import shape
import fiona
geoms =[shape(feature['geometry']) for feature in fiona.open("input_file.shp")]
import itertools


# create a list of graphs
G = nx.DiGraph()

for line in geoms:
    line_coords=list(line.coords)
    for i in range(len(line_coords)):
        line_coords[i]=list(line_coords[i])


    # make your preferred Site class out of available mix-ins.
    Node = type('Site', (Identifiable, Locatable), {})

    # Add geometry to nodes
    nodes = []
    for index, coord in enumerate(line.coords):
        data_node = {"name": str(index), "geometry": shapely.geometry.Point(coord[0], coord[1])}
        nodes.append(Node(**data_node))

    # Create sub graphs
    FG = nx.DiGraph()

    for node in nodes:
        FG.add_node(node.name, geometry = node.geometry)



    # add edges
    path = [[nodes[i], nodes[i+1]] for i in range(len(nodes)-1)]

    for index, edge in enumerate(path):

        FG.add_edge(edge[0].name, edge[1].name, weight = 1)

    # add geometry to edge
    for edge in FG.edges:
        point0 = FG.nodes[edge[0]]['geometry']
        point1 = FG.nodes[edge[1]]['geometry']
        FG.edges[(edge[0], edge[1])]['geometry'] = shapely.geometry.LineString([point0, point1])

    #add length
        FG.edges[(edge[0], edge[1])]['length'] = edge_length(FG.edges[(edge[0], edge[1])])



    # toggle to undirected and back to directed to make sure all edges are two way traffic
    FG = FG.to_undirected()
    FG = FG.to_directed()


    # create a positions dict for the purpose of plotting
    positions = {}
    for node in FG.nodes:
        positions[node] = (FG.nodes[node]['geometry'].x, FG.nodes[node]['geometry'].y)


    # collect node labels
    labels = {}
    for node in FG.nodes:
        labels[node] = node

    #Join all seperate FIS graphs
    G = nx.union(FG, G, rename=("FG-", "G-"))

positions = {}
for node in G.nodes:
    positions[node] = (G.nodes[node]['geometry'].x, G.nodes[node]['geometry'].y)

# draw edges, nodes and labels.
plt.axis("off")
nx.draw_networkx_edges(G,  pos=positions, width=3, edge_color="red", alpha=1, arrowsize=0.1, crs="EPSG:4326")
plt.show()
```

Figure F.1: Python code to create FIS graph

F.2. Twelve randomly selected vessel trajectories

Trajectories 1-4, 7, 11 and 12 are berthed vessels. Their signal is drifting in the same area and their speed is low. The model indicates these correctly as berthed vessels.

Trajectories 5, 6, 8, 9 and 10 are moving vessels. Their sailing speeds are however so low, that the model categorizes these vessels as berthed or anchoring no matter how far they are from their destination.

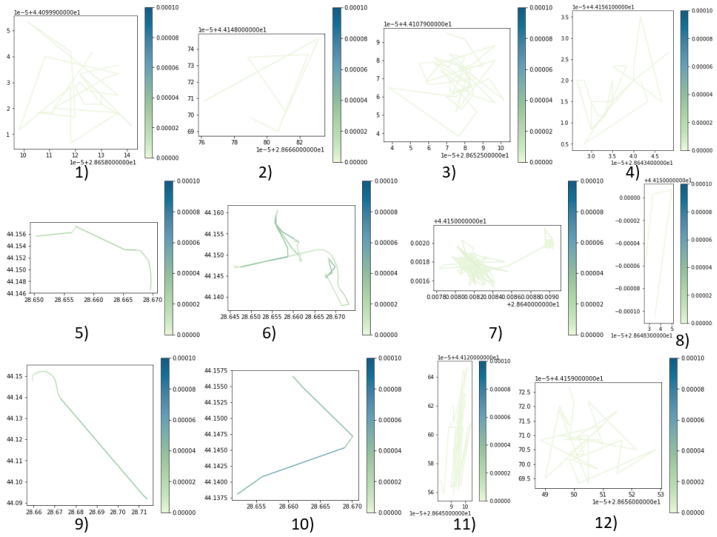

Figure F.2: Twelve randomly selected vessel trajectories with the color indicating the speed in m/s

F.3. Emission split in vessel types

To indicate the emission split per vessel type, their percentage of the total emissions are stated.

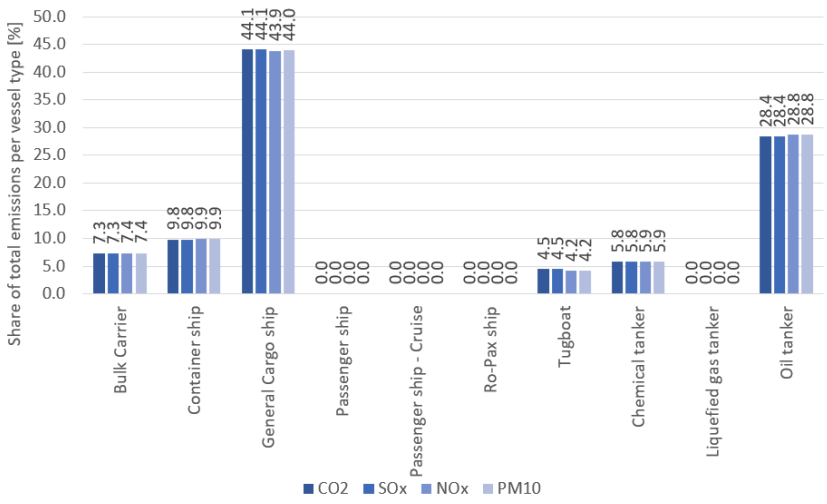

Figure F.3: Emission split in vessel types in percentage of total emissions

F.4. Emission distributions - June 2021

The emission distribution of the Port of Constanța is shown below for the four evaluated pollutants. These four figures cover the emissions of the first two weeks of June 2021.

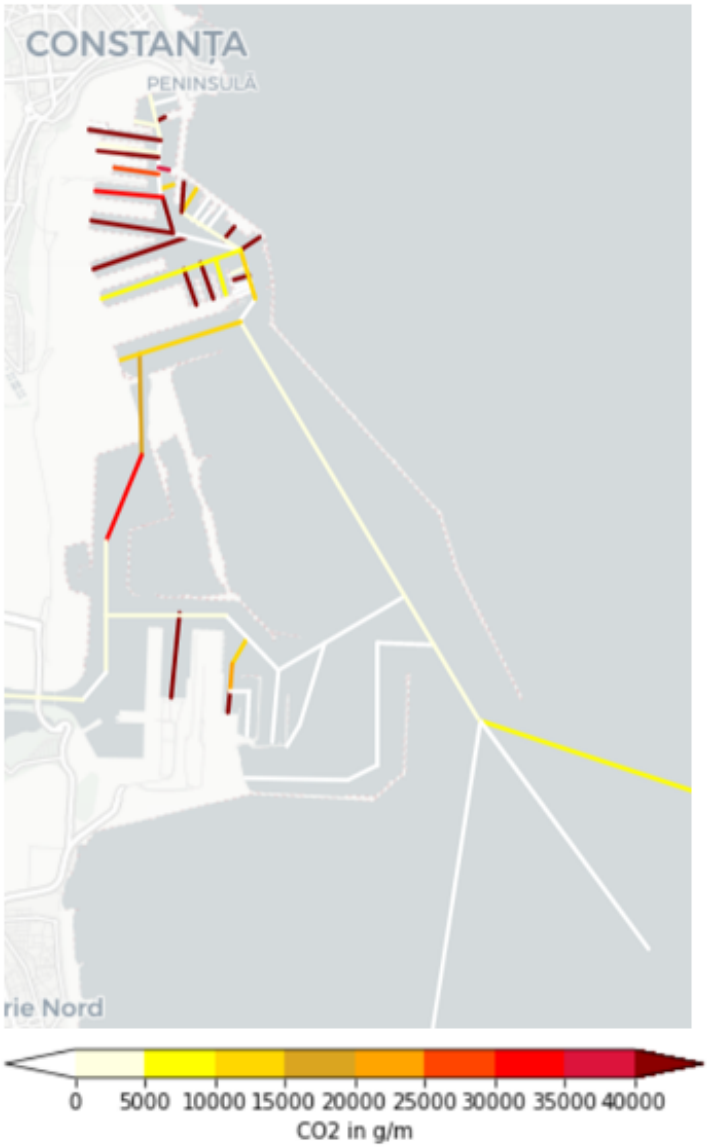

Figure F.4: Estimated CO_2 emissions in the Port of Constanța from June 1 - June 14 2021

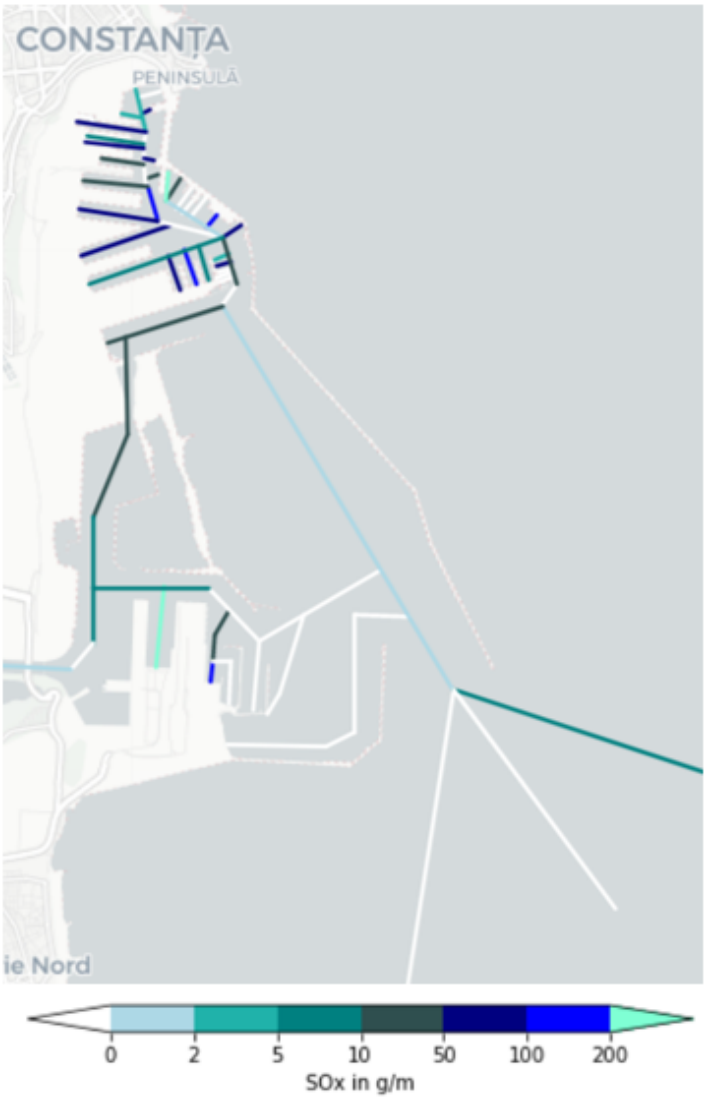

Figure F.5: Estimated SO_x emissions in the Port of Constanța from June 1 - June 14 2021

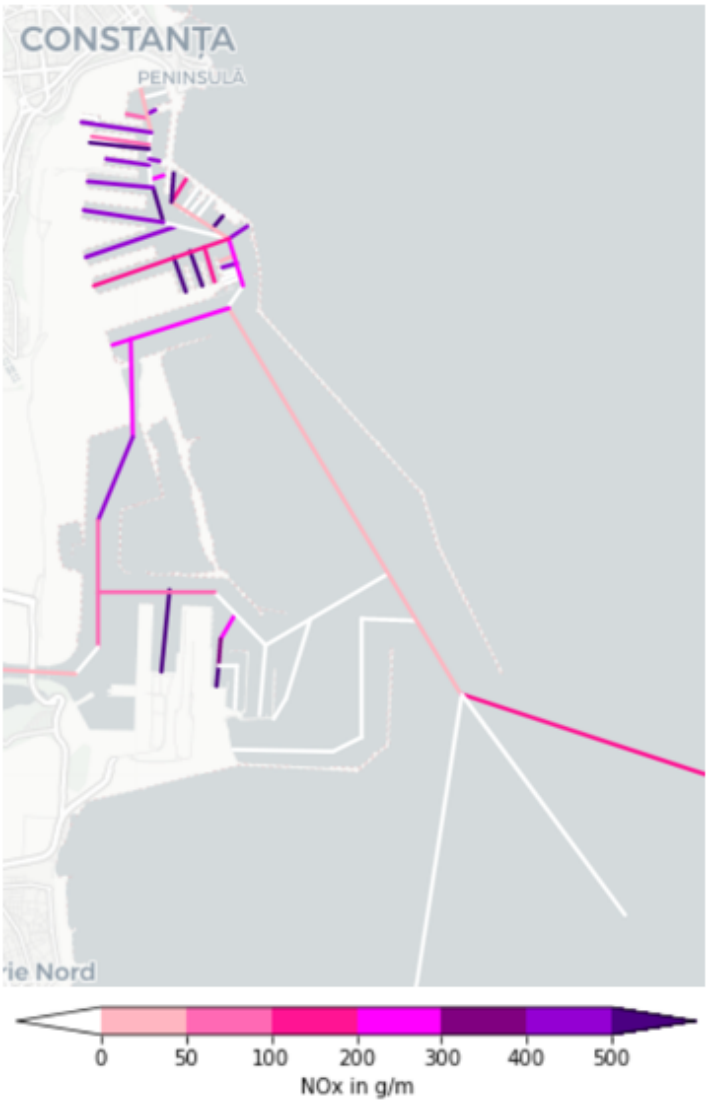

Figure F.6: Estimated NO_x emissions in the Port of Constanța from June 1 - June 14 2021

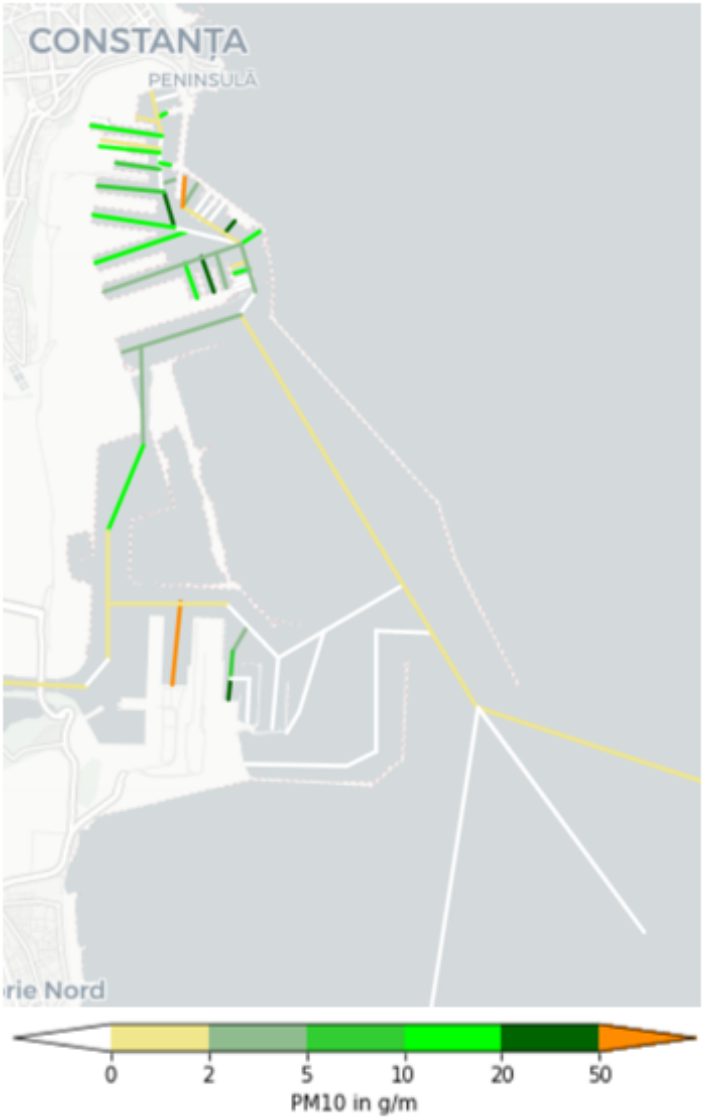

Figure F.7: Estimated PM_{10} emissions in the Port of Constanța from June 1 - June 14 2021

Acronyms

CO_2 carbon dioxide. viii, 1–4, 12, 14–16, 22, 30, 39, 48, 85, 111, 118, 125–127

NO_x nitrogen oxides. viii, 2, 3, 12, 13, 15, 22, 30, 40, 49, 87–89, 112, 120, 125–127

PM_{10} particulate matter. viii, 2, 3, 12, 13, 22, 30, 40, 49, 87, 89, 90, 113, 121, 125–127

SO_x sulfur dioxides. viii, 2, 3, 12, 13, 15, 22, 30, 39, 48, 86, 87, 112, 119, 125–127

AIS Automatic Identification System. v, 5

COP26 26th Conference of the Parties. 1

CSI Clean Shipping Index. 3

ECA Emission Control Area. vi, 65

ECAs Emission Control Areas. 2

ESI Environmental Ship Index. 3

FIS Fairway Information System. v, 5, 27, 36, 44, 61

ICCT International Council on Clean Transportation. 4

ILO International Labour Organization. 1

IMO International Maritime Organisation. 1, 2

RHDHV Royal HaskoningDHV. 25, 26

TNO Nederlandse Organisatie voor toegepast-natuurwetenschappelijk onderzoek. 12

UNFCCC United Nations Framework Convention on Climate Change. 1

VBP Vessel Boarding Program. 83

List of Figures

1.1 CO_2 emissions from shipping in the Netherlands, based on data from CBS (2021) 3
1.2 Report structure 6

2.1 Percentage CO_2 emission per vessel type of total CO_2 emissions of the commercial world fleet . 15

3.1 Overview of the method to estimate emissions of a single vessel 17
3.2 Overview of the operational modes and their influence on the engine power consumption . . . 18
3.3 Schematization of the main engine system of a ship 20

4.1 Overview of the model 25
4.2 Current and discussed ECAs (Source: Karimpour (2018)) 32

5.1 Number of vessels per vessel type after AIS data filtering 35
5.2 FIS graph from de Jong et al. (2021) reduced to FIS graph of Port of Rotterdam area 36
5.3 Percentage of emissions in each operational mode 38
5.4 Emission split in vessel types in percentage of total emissions 38
5.5 Estimated CO_2 emissions in the Port of Rotterdam from June 1 - June 14 2021 39
5.6 Estimated SO_x emissions in the Port of Rotterdam from June 1 - June 14 2021 39
5.7 Estimated NO_x emissions in the Port of Rotterdam from June 1 - June 14 2021 40
5.8 Estimated PM_{10} emissions in the Port of Rotterdam from June 1 - June 14 2021 40
5.9 Location of the ports with the highest emissions 41
5.10 AIS trajectory of vessel #3 (color indicates speed) 42

6.1 Number of vessels per vessel type after AIS data filtering 43
6.2 FIS graph of the Port of Constanța 44
6.3 Percentage of emissions in each operational mode 45
6.4 Average speed and distance to destination of all trips in June 1 - June 14 2021 46
6.5 Emission split in vessel types in percentage of total emissions 47
6.6 Estimated CO_2 emissions in the Port of Constanța from January 1 - January 14 2021 48
6.7 Estimated SO_x emissions in the Port of Constanța from January 1 - January 14 2021 48
6.8 Estimated NO_x emissions in the Port of Constanța from January 1 - January 14 2021 49
6.9 Estimated PM_{10} emissions in the Port of Constanța from January 1 - January 14 2021 49
6.10 Location of the ports with the highest emissions 50

7.1 Percentage of emissions in each operational mode of the simulated shore power case 52
7.2 CO_2 emissions in the ferry terminal and in the Madroelhaven 53
7.3 Number of vessels per vessel type comparison of original case to case with zero-emission tugboats 53
7.4 Percentage of emissions in each operational mode of the simulated zero-emission tugs case . . 54
7.5 $CO2$ emissions in the Madroel haven from the case study with zero-emission tugboats 54

A.1 Karpov method: estimation of α^{**} based on the depth Froude number Fr_h for different h/T ratios 76

D.1 Deadweight distribution per vessel type 92
D.2 Fit of the double Weibull distribution on build year data of the Bulk carrier and its size categories 93
D.3 Linear relation ship of dead weight tonnage and installed engine power of the Bulk carrier and its size categories 94

E.1 An example of the vessel database from the case study of Port of Rotterdam 107
E.2 An example of one trip from the trip collection from the case study of Port of Rotterdam 108

E.3 An example of one trip from the trip collection from the case study of Port of Rotterdam 109
E.4 An example of one trip from the trip collection with corresponding emissions from the case study of Port of Rotterdam 110
E.5 Emission split in vessel types in percentage of total emissions 111
E.6 Estimated CO_2 emissions in the Port of Rotterdam from January 1 - January 14 2022 111
E.7 Estimated SO_x emissions in the Port of Rotterdam from January 1 - January 14 2022 112
E.8 Estimated NO_x emissions in the Port of Rotterdam from January 1 - January 14 2022 112
E.9 Estimated PM_{10} emissions in the Port of Rotterdam from January 1 - January 14 2022 113

F.1 Python code to create FIS graph 116
F.2 Twelve randomly selected vessel trajectories with the color indicating the speed in m/s 117
F.3 Emission split in vessel types in percentage of total emissions 117
F.4 Estimated CO_2 emissions in the Port of Constanța from June 1 - June 14 2021 118
F.5 Estimated SO_x emissions in the Port of Constanța from June 1 - June 14 2021 119
F.6 Estimated NO_x emissions in the Port of Constanța from June 1 - June 14 2021 120
F.7 Estimated PM_{10} emissions in the Port of Constanța from June 1 - June 14 2021 121

List of Tables

3.1 Decision matrix to determine operational mode for all vessel types ∗For liquefied tanker only . 19
3.2 Base hourly fuel consumption 23

4.1 Vessel type classification 26

5.1 Estimated emissions in the Port of Rotterdam in tonnes 37
5.2 Share of emission type of total emissions [%] 37
5.3 Down-drilling of the emissions of the Vopak Terminal Vlaardingen 42

6.1 Estimated emissions in the Port of Constanța in tonnes 45
6.2 Share of emission type of total emissions [%] 45

7.1 Emission reduction for vessels at berth 52
7.2 Total emission reduction 52
7.3 Estimated emissions with hybrid tugs 54
7.4 Estimated emissions when applying ECA limits 55

A.1 Vesseltypes and their corresponding block coefficients 72
A.2 Approximate $(1+k_2)$ values 75
A.3 Formulas used in model to calculate α^{**} for each h/T ratio with corresponding depth Froude number 77

B.1 Power output auxiliary engine per vessel type and size (International Maritime Organization, 2021) 84

C.1 Base emission factor for CO_2 for different fuel types 85
C.2 Main fuel type allocation procedure 86
C.3 Average sulphur content per fuel type in 2020 [%] 87
C.4 Base emission factor for SO_x for different fuel types 87
C.5 Base emission factor for NO_x for all fuel types except Methanol and LNG 88
C.6 Base emission factor for NO_x for fuel type Methanol 88
C.7 Base emission factor for NO_x for fuel type LNG 88
C.8 Classification of Tiers 89
C.9 Base emission factor for PM_{10} for the construction year class 'Built before 1984' 90
C.10 Base emission factor for PM_{10} for the construction year class 'Built between 1984 and 2000' . . 90
C.11 Base emission factor for PM_{10} for the construction year class 'Built after 2000' 90

D.1 Probabilities of the number of screws for the Bulk Carrier size class '0 - 9,999' 92
D.2 Characteristic values for missing entries - Bulk Carrier 95
D.3 Characteristic values for missing entries - Chemical tanker 96
D.4 Characteristic values for missing entries - Container ship - part 1 97
D.5 Characteristic values for missing entries - Container ship - part 2 98
D.6 Characteristic values for missing entries - General cargo ship 99
D.7 Characteristic values for missing entries - Liquefied tanker 100
D.8 Characteristic values for missing entries - Oil tanker - part 1 101
D.9 Characteristic values for missing entries - Oil tanker - part 2 102
D.10 Characteristic values for missing entries - Passenger ship 103
D.11 Characteristic values for missing entries - Passenger ship - Cruise 104
D.12 Characteristic values for missing entries - Ro-Pax ship 105
D.13 Characteristic values for missing entries - Tugboat 106

Bibliography

A. Al-Enazi, E. C. Okonkwo, Y. Bicer, and T. Al-Ansari. A review of cleaner alternative fuels for maritime transportation. *Energy Reports*, 7:1962–1985, 2021. ISSN 2352-4847. doi: https://doi.org/10.1016/j.egyr.2021.03.036. URL https://www.sciencedirect.com/science/article/pii/S2352484721002067.

K. Andersson and C. Márquez Salazar. Methanol as a marine fuel report. Technical report, Methanol Institude, 2015.

ANWB. Alles over uitstoot, 2022. Retrieved 2022, from https://www.anwb.nl/auto/nieuws-en-tips/alles-over-uitstoot.

B. Bacalja, M. Krčum, and M. Slišković. A line ship emissions while manoeuvring and hotelling—a case study of port split. *Journal of Marine Science and Engineering*, 8(11), 2020. ISSN 2077-1312. doi: 10.3390/jmse8110953. URL https://www.mdpi.com/2077-1312/8/11/953.

Bertram and Volker. *Practical ship hydrodynamics*. Elsevier, 2012.

A. Bonte and A. Castelein. Strategy for shore power in the port of rotterdam. Technical report, Port of Rotterdam, 2020.

Mason J. Broderick J. Bullock, S. Shipping and the paris climate agreement: a focus on committed emissions. *BMC Energy 2*, 10 2020. doi: https://doi.org/10.1186/s42500-020-00015-2.

CBS. Emissions to air on dutch territory; mobile sources, 2021. Retrieved 2022, from https://opendata.cbs.nl/statline//CBS/en/dataset/84735ENG/table?ts=1640695601496.

J. Celic, S. Valcic, and M. Bistrović. Air pollution from cruise ships. *Proceedings Elmar - International Symposium Electronics in Marine*, pages 75–78, 10 2014. doi: 10.1109/ELMAR.2014.6923319.

J. Cofala, M. Amann, C. Heyes, F. Wagner, Z. Klimont, M. Posch, W. Schoepp, L. Tarasson, C. Whall, and A. Stavrakaki. Analysis of policy measures to reduce ship emissions in the context of the revision of the national emissions ceilings directive. Technical report, 2007. URL http://pure.iiasa.ac.at/id/eprint/8299/.

J J. Corbett, P.S. Fischbeck, and S.N. Pandis. Global nitrogen and sulfur emissions inventories for oceangoing ships. *Journal of Geophysical Research*, 104, 1999.

James Corbett, James Winebrake, Erin Green, Prasad Kasibhatla, Veronika Eyring, and Axel Lauer. Mortality from ship emissions: A global assessment. *Environmental Science & Technology*, 2007.

James J Corbett and Paul Fischbeck. Emissions from ships. *Science*, 278(5339):823–824, 1997.

Jurjen de Jong, Fedor Baart, and Migena Zagonjolli. Topological Network of the Dutch Fairway Information System, March 2021. URL https://doi.org/10.5281/zenodo.4578289.

Willem de Jong. Tribute to the diesel engine, but with which types of marine fuels? *SWZ|Maritime March 2020 special*, 2020.

Øyvind Endresen, Eirik Sørgård, Jostein K Sundet, Stig B Dalsøren, Ivar SA Isaksen, Tore F Berglen, and Gjermund Gravir. Emission from international sea transportation and environmental impact. *Journal of Geophysical Research: Atmospheres*, 108(D17), 2003.

Øyvind Endresen, Eirik Sørgård, Hanna Lee Behrens, Per Olaf Brett, and Ivar SA Isaksen. A historical reconstruction of ships' fuel consumption and emissions. *Journal of Geophysical Research: Atmospheres*, 112 (D12), 2007.

EPA, United States Environmental Protection Agency. Criteria air pollutants, August 16, 2021. Retrieved 2022, from https://www.epa.gov/criteria-air-pollutants.

European Commission. 2020 annual report from the european commission on co2 emissions from maritime transport. Technical report, European Commission, 2020.

European Technology and Innovation Platform. Marine biofuels. Fact Sheet, 2017.

JF Faber, Thomas Huigen, and Dagmar Nelissen. *Regulating speed: a short-term measure to reduce maritime GHG emissions*. CE Delft, 2017.

N. Florin, I. Roman, and A. Cotorcea. Air pollution from the maritime transport in the romanian black sea coast. 04 2018.

J. Fritt-Rasmussen, S. Wegeberg, K. Gustavson, K. Rist Sørheim, P. S. Daling, K. Jørgensen, O. Tonteri, and J. P. Holst-Andersen. Heavy fuel oil (hfo). Technical report, Nordic Council of Ministers, 2018.

M. Fu, H. Liu, X. Jin, and K. He. National-to port-level inventories of shipping emissions in china. *Environmental Research Letters*, 12(11):114024, 2017.

M. Ge, J. Friedrich, and L. Vigna. Four charts explain greenhouse gas emissions by countries and sectors, 2020. Retrieved 2022, from https://www.wri.org/insights/4-charts-explain-greenhouse-gas-emissions-countries-and-sectors.

S.L. Haga, A. Hagenbjörk, A.C. Olin, B. Forsberg, I. Liljelind, H.K. Carlsen, and L. Modig. Personal exposure levels to o3, nox and pm10 and the association to ambient levels in two swedish cities. *Environmental Monitoring and Assessment*, 193, 09 2021. doi: 10.1007/s10661-021-09447-7.

J Holtrop and GGJ Mennen. An approximate power prediction method. *International Shipbuilding Progress*, 29(335):166–170, 1982.

G. Horton, H. Finney, S. Fischer, I. Sikora, J. McQuillen, N. Ash, and H. Shakeel. Technological, pperational and energy pathways for maritime transport to reduce emissions towards 2050. Technical report, Ricardo, 2022.

C. C. Hsieh and C. Felby. Biofuels for the marine shipping sector - an overview and analysis of sector infrastructure, fuel technologies and regulations. Technical report, International Energy Agency Bioenergy, 2017.

J.H.J. Hulskotte. Kentallen zeeschepen ten behoeve van emissie- en verspreidingsberekingen in aerius, actualisatie 2018. Technical report, TNO, 2019.

International Maritime Organization. Nitrogen oxides (nox) – regulation 13, 2019a. Retrieved 2022, from https://www.imo.org/en/OurWork/Environment/Pages/Nitrogen-oxides-(NOx)-—Regulation-13.aspx.

International Maritime Organization. Sulphur oxides (sox) and particulate matter (pm) – regulation 14, 2019b. Retrieved 2022, from https://www.imo.org/en/OurWork/Environment/Pages/Sulphur-oxides-(SOx)-—Regulation-14.aspx.

International Maritime Organization. 2020 annual report from the european commission on co2 emissions from maritime transport. Technical report, International Maritime Organization, 2021.

International Transport Forum. Reducing shipping greenhouse gas emissions. Technical report, EOCD, 2018.

K. Johnson. Black carbon and other gaseous emissions from an ocean-going vessel auxiliary engine equipped with a scrubber. Technical report, California Air Resources Board Transportation and Toxics, 2013.

P. Jun, M. Gillenwater, and W. Barbour. Co2 , ch4 , and n2o emissions from transportation - waterborne navigation. Technical report, The Intergovernmental Panel on Climate Change, 2001.

R. Karimpour. Scrubber; is it the option to meet the shipping fuel sulphur cap on 2020, 2018. Retrieved 2022, from https://www.onthemosway.eu/18823-2/.

K.F. Kauffman and J. Hulskotte. Sea shipping emissions 2019: Netherlands continental shelf, 12-mile zone and port areas. Technical report, International Maritime Organization, 2021.

Sadaqat Khan, Young-Tade Chang, Suhyung Lee, and Kyoung-Suk Choi. Assessment of greenhouse gas emissions from ships operation at the port of incheon using ais. *Korea Port Economic Association*, 34(1):65–80, 2008.

J-H Kim and Y-H Kim. Motion control of a cruise ship by using active stabilizing fins. *Journal of Engineering for the Maritime Environment*, 225(Part M):311–324, 2011. doi: 10.1177/1475090211421268.

Niko Kommenda. How your flight emits as much CO2 as many people do in a year, 2019. Retrieved 2022, from https://www.theguardian.com/environment/ng-interactive/2019/jul/19/carbon-calculator-how-taking-one-flight-emits-as-much-as-many-people-do-in-a-year.

Norbert Kriedel, Laure Roux, Lucie Fahrner Athanasia Zarkou, and Sarah Meissner. Market insight inland navigation in europe. Technical report, Central Commission for the Navigation of the Rhine, 2021.

See Leong, Carol Hargreaves, Prateek Singhal, and Jun Yuan. Estimation of co2 emission from marine traffic in singapore straits using automatic identification systems data. *Taylor & Francis Group*, 06 2015. doi: 10.1201/b18559-31.

MAN Energy Solutions. *Basic principles of ship propulsion*. PrinfoTrekroner, 2018.

Olaf Merk. Shipping emissions in ports: overview, impact and prognosis. *International Transport Forum*, 11 2014.

Apollonia Miola and Biagio Ciuffo. Estimating air emissions from ships: Meta-analysis of modelling approaches and available data sources. *Atmospheric Environment*, 45(13):2242–2251, 2011. ISSN 1352-2310. doi: https://doi.org/10.1016/j.atmosenv.2011.01.046. URL https://www.sciencedirect.com/science/article/pii/S1352231011000872.

Juan Moreno-Gutiérrez, Fátima Calderay, Nieves Saborido, Maria Boile, Rafael Rodríguez Valero, and Vanesa Durán-Grados. Methodologies for estimating shipping emissions and energy consumption: A comparative analysis of current methods. *Energy*, 86:603–616, 2015. ISSN 0360-5442. doi: https://doi.org/10.1016/j.energy.2015.04.083. URL https://www.sciencedirect.com/science/article/pii/S0360544215005502.

NASA. The atmosphere: Getting a handle on carbon dioxide, 2022. Retrieved 2022, from https://edu.nl/p4vpc.

Hellenic Shipping News. Reefer ships now an “endagered species” ahead of IMO 2020 rules and a diminishing market share, 2019. Retrieved 2022, from https://www.hellenicshippingnews.com/reefer-ships-now-an-endagered-species-ahead-of-imo-2020-rules-and-a-diminishing-market-share/.

Simon K.W. Ng, Christine Loh, Chubin Lin, Veronica Booth, Jimmy W.M. Chan, Agnes C.K. Yip, Ying Li, and Alexis K.H. Lau. Policy change driven by an ais-assisted marine emission inventory in hong kong and the pearl river delta. *Atmospheric Environment*, 76:102–112, 2013. ISSN 1352-2310. doi: https://doi.org/10.1016/j.atmosenv.2012.07.070. Improving Regional Air Quality over the Pearl River Delta and Hong Kong: from Science to Policy.

H. Nilsson, J. Van Overloop, R.A. Mehdi, and J. Pålsson. Transnational maritime spatial planning in the north sea: The shipping context. report on work-package 4 of the northsee project. 2018.

Naya Olmer, Bryan Comer, Biswajoy Roy, Xiaoli Mao, and Dan Rutherford. Greenhouse gas emissions from global shipping, 2013-2015. Technical report, The International Council on clean Transportation, 2017.

OpenTNSim. Setup of a basic simulation, 2022. Retrieved 2022, from https://happy-bush-0c5d10603.1.azurestaticapps.net/examples/Example%2000%20-%20Basic%20simulation.html#3.-Create-graph.

Our World in Data. Greenhouse gas emissions by sector, romania, 2018, 2022a. Retrieved 2022, from https://ourworldindata.org/grapher/ghg-emissions-by-sector?time=latestcountry= ROU.

Our World in Data. Greenhouse gas emissions by sector, netherlands, 2018, 2022b. Retrieved 2022, from https://ourworldindata.org/grapher/ghg-emissions-by-sector?time=latestcountry= NLD.

Port of Antwerp Bruges. Hydrogen-powered tug is world first for port of antwerp, 2022. Retrieved 2022, from https://edu.nl/kvem4.

Port of Constanta. Port presentation, 2022. Retrieved 2022, from https://www.portofconstantza.com/pn/page/np_prezentare_port.

Port of Rotterdam. Port information guide. Technical report, Port of Rotterdam, 2021.

Port of Rotterdam. Uitdieping nieuwe waterweg en botlek voltooid, 2022a. Retrieved 2022, from https://www.portofrotterdam.com/nl/nieuws-en-persberichten/uitdieping-nieuwe-waterweg-en-botlek-voltooid.

Port of Rotterdam. Druk in nijlhaven, 2022b. Retrieved 2022, from https://www.portofrotterdam.com/nl/nieuws-en-persberichten/druk-in-nijlhaven.

Port of Rotterdam. Freight throughput in the port of rotterdam decreased by 1.5% in first quarter, 2022c. Retrieved 2022, from https://www.portofrotterdam.com/en/news-and-press-releases/freight-throughput-in-the-port-of-rotterdam-decreased-by-15-in-first.

PortSEurope. Port of constanta reports total cargo traffic down -9.3%, 2021. Retrieved 2022, from https://www.portseurope.com/port-of-constanta-reports-total-cargo-traffic-down-9-3/.

Reliawiki. The weibull distribution, 2018.

Rijksmuseum. Foto-opdrachten nederlandse geschiedenis. Photo subscribt, 2001.

Goutam Kumar Saha and Asim Kumar Sarker. Optimization of ship hull parameter of inland vessel with respect to regression based resistance analysis. In *Proceedings of The International Conference of Marine Technology*, pages 471–476, 2010.

E. Sarris. Naval ship propulsion and electric power systems selection for optimal fuel consumption. Master's thesis, Massachusetts Institute of Technology, 2011.

H. Schneekluth and V. Bertram. *Ship Design for Efficiency and Economy*. Butterworth-Heinemann, 1998. ISBN 0750641339.

L. J. M. Segers. Mapping inland shipping emissions in time and space for the benefit of emission policy development: a case study on the rotterdam-antwerp corridor. Master's thesis, Technische Universiteit Delft, 2020.

Seonguk Seo, Sunho Park, and BonYong Koo. Effect of wave periods on added resistance and motions of a ship in head sea simulations. *Ocean Engineering*, 137:309–327, 2017. ISSN 0029-8018. doi: https://doi.org/10.1016/j.oceaneng.2017.04.009. URL https://www.sciencedirect.com/science/article/pii/S0029801817301919.

Siemens Energy. Green methanol: The basis for a co2-neutral circular economy. Technical report, Siemens Energy, 2020.

KO Skjølsvik, AB Andersen, JJ Corbett, and JM Skjelvik. Study of greenhouse gas emissions from ships (report to international maritime organization on the outcome of the imo study on greenhouse gas emissions from ships), mepc 45/8, marintek sintef group. *Center for Economic Analysis/Det Norske Veritas, Trondheim, Norway*, 2000.

T. W. P. Smith, J.P. Jalkanen, B. A. Anderson, J.J. Corbett, J. Faber, S. Hanayama, E. OKeeffe, S. Parker, L. Johansson, L. Aldous, C. Raucci, M. Traut, S. Ettinger, D. Nelissen, D.S. Lee, S. Ng, A. Agrawal, J.J. Winebrake, M. Hoen, S. Chesworth, and A. Pandey. Third IMO greenhouse gas study 2014. Technical report, International Maritime Organization, 2015.

Starcrest consulting group LLC. Port of los angeles inventory of air emissions - 2020. Technical report, The Port of Los Angeles, 2020a.

Starcrest consulting group LLC. Port of long beach 2020 air emissions inventory. Technical report, The Port of Long Beach, 2020b.

T.J.C. Terwisga. *Weerstand en voortstuwing van bakken: een literatuurstudie*. Maritiem Research Instituut Nederland, 1989.

The Maritime Executive. Bimco expects world fleet will grow at slower pace in the next 5 years, 2022a. Retrieved 2022, from https://edu.nl/jvfdg.

The Maritime Executive. The zero-emissions tug, 2022b. Retrieved 2022, from https://www.maritime-executive.com/magazine/the-zero-emissions-tug.

Transport & Environment. Eu ports' climate perfomance - an analysis of maritime supply chain and at berth emissions. Technical report, European Federation for Transport and Environment, 2022.

United States environmental protection agency. Greenhouse gas inventory guidance - direct emissions from stationary combustion sources. Technical report, United States environmental protection agency, 2016.

S. Ushakov, D. Stenersen, and P.M. Einang. Methane slip from gas fuelled ships: a comprehensive summary based on measurement data. *Journal of Marine Science and Technology*, 24(2):1308–1325, 2019. doi: https://doi.org/10.1007/s00773-018-00622-z.

Gabrielle van Zwieteren. Analysing terminal performances using ais data: Ais tool development and data analysis to assess & compare observed nautical port processes with theoretical frameworks. Master's thesis, Technische Universiteit Delft, 2020.

M. B. Vermeire. Everything you need to know about marine fuels. Technical report, Chevron Marine Products, 2021.

Vopak. Vopak terminal vlaardingen, 2022. Retrieved 2022, from https://www.vopak.nl/locaties-nederland/vopak-terminal-vlaardingen?language_content_entity=nl.

Royal Wagenborg. Sulphur 2020: Everything you need to know about the upcoming regulations. 2020. URL https://www.wagenborg.com/cases/sulphur-2020-everything-you-need-to-know-about-the-upcoming-regulations.

David Watson. *Practical ship design*. Elsevier, 1998.

Tim Williamson, Jan Hulskotte (TNO), Richard German, and Kirsten May. Port of london emissions inventory. Technical report, Port of London Authority and Transport for London, 2016.

Hulda Winnes, Linda Styhre, and Erik Fridell. Reducing ghg emissions from ships in port areas. *Research in Transportation Business & Management*, 17:73–82, 2015.

Witkowski and Kazimierz. Research of the effectiveness of selected methods of reducing toxic exhaust emissions of marine diesel engines. *Journal of Marine Science and Engineering*, 8:452, 06 2020. doi: 10.3390/jmse8060452.

World Port Source. Port of rotterdam, 2022. Retrieved 2022, from http://www.worldportsource.com/ports/commerce/NLD_Port_of_Rotterdam_106.php.

Qingsong Zeng, Cornel Thill, Robert Hekkenberg, and Erik Rotteveel. A modification of the ittc57 correlation line for shallow water. *Journal of Marine Science and Technology*, 24, 07 2018. doi: 10.1007/s00773-018-0578-7.